INITIAL CHARACTERIZATION OF THE RIBOSOME-ASSOCIATED ATP BINDING CASSETTE (ABC) PROTEIN YHIH FROM *E. COLI*

JEFFREY JAMES FISCHER
B.Sc. University of Lethbridge, 2005

A Thesis
Submitted to the School of Graduate Studies
of the University of Lethbridge
in Partial Fulfillment of the
Requirements for the Degree

MASTER OF SCIENCE

Department of Chemistry and Biochemistry
University of Lethbridge
LETHBRIDGE, ALBERTA, CANADA

Abstract

Protein synthesis is a highly conserved process across all domains of life, both structurally and functionally. This cyclic process is catalyzed by numerous soluble protein factors that interact with the ribosome to facilitate efficient protein synthesis. Many canonical translation factors bind and hydrolyze GTP to induce conformational changes that facilitate translation. For example, GTP hydrolysis by EF-Tu is required for the release of aminoacyl-tRNA into the ribosomal A site; GTP hydrolysis by EF-G facilitates the movement of tRNA and mRNA from the A site to the P site of the ribosome. However, protein synthesis seems to also have a requirement for ATP; the essential yeast protein eEF-3 facilitates release of deacyl-tRNA from the ribosomal E site. In *Escherichia coli*, the protein product of the open reading frame *yhih* has been suggested to have a similar function. However, the role of this unique prokaryotic protein is not understood. Preliminary characterization of this protein suggests a nucleotide-dependent conformational change occurs in a truncated form of the protein, ΔP541 Yhih. Interestingly, this phenomenon is not observed in ΔL432 Yhih. Both ΔP541 Yhih, and to a lesser extent ΔL432 Yhih, exhibit a ribosome-dependent ATPase activity, suggesting the primary region for binding with the ribosome lies between Leu432 and Pro541.

Acknowledgements

To HJ, who gave me this opportunity.

To my family, always behind me.

To my friends, keeping me grounded.

Contents

List of Tables

List of Figures

List of Abbreviations

β-mEtOH	β-mercaptoethanol
ABC	ATP-binding cassette
ADP	Adenosine-5'- diphosphate
ADPNP	Adenosine-5'- (β,γ-imido)- triphosphate
ATP	Adenosine-5'- triphosphate
bp	base pair
DAB	3,3'-diaminobenzidine
DNA	Deoxyribonucleic acid
e	Eukaryotic
EDTA	Ethylenediamine tetraacetic acid
EF	Elongation factor
FRET	Fluorescence resonance energy transfer
IF	Initiation factor
IPTG	Isopropyl-β-D-thiogalactopyranoside
GBP	Guanine nucleotide binding protein
GDP	Guanosine-5'- diphosphate
GDPNP	Guanosine-5'- (β,γ-imido)- triphosphate
GTP	Guanosine-5'- triphosphate
GEF	Guanine nucleotide exchange factor
K_D	Dissociation constant
Mant	2'-(or 3')-O-(N-methylanthraniloyl)
NBD	Nucleotide binding domain
OD_{600}	Optical density at 600 nm
ORF	Open reading frame
PAGE	Polyacrylamide gel electrophoresis
PEP	Phosphoenolpyruvate
PK	Pyruvate kinase
PMT	Photomultiplier tube
Rb	Ribosome
RbbA	Ribosome-bound ATPase
RF	Release factor
RNA	Ribonucleic acid
RRF	Ribosome recycling factor
SAXS	Small-angle X-ray scattering
SDS	Sodium dodecyl sulfate
TMD	Transmembrane domain
X-GAL	5-bromo-4-chloro-3-indolyl-β-D-galactopyranoside

Chapter 1 - Introduction

Protein synthesis is a structurally and functionally conserved process in all living cells. Translation occurs in three stages: initiation, during which the ribosomal subunits are brought together with messenger RNA and an initiator tRNA (fMet-tRNA$_i^{fMet}$ in bacteria); elongation, during which mRNA is sequentially read codon by codon, and cognate amino acids are added to the growing nascent peptide chain; and termination, during which a stop codon is read by a release factor, signaling the release of the peptide, dissociation of the ribosome and associated factors, allowing the cycle to continue. All three stages of protein synthesis are mediated by numerous protein factors, several of which bind and hydrolyze GTP (Table 1). However, protein synthesis has a requirement not only for GTP, but also for ATP. The role of these ATPases during translation is only poorly understood.

Table 1: Protein factors associated with protein synthesis.

Description	Prokaryotic factor	Eukaryotic factor
Initiation Factors	IF-1	~ 12 eIFs
	IF-2 *	eIF-5B *
	IF-3	eIF-2 *
Elongation Factors	EF-Tu *	eEF-1α *
	EF-Ts	eEF-1β
	EF-G *	eEF-2 *
	RbbA (Yhih) [†]	eEF-3 (yeast) [†]
	lepA *	-
Termination Factors	RF-1	eRF-1
	RF-2	-
	RF-3 *	eRF-3 *

* GTPases
[†] ATPases

1

Current research in protein synthesis on the model organisms *Escherichia coli* and *Saccharomyces cerevisiae* focuses mainly on the canonical GTPases. However, recent research suggests that in both prokaryotes and eukaryotes, ATP hydrolysis plays a crucial role: notably, yeast eEF-3 is a protein essential for growth (Sandbaken M, 1990; Sandbaken et al., 1990; Triana-Alonso et al., 1995) that utilizes ribosome-dependent ATP hydrolysis to facilitate the release of deacyl-tRNA from the 80S ribosomal E-site (Andersen et al., 2006). In prokaryotes, a homologous ribosome-bound ATPase (RbbA, coded for by the open reading frame *yhih*) has been suggested to perform a similar function (for the purposes of this thesis, this protein will be referred to as Yhih). This 892 amino acid, 91 kDa protein is a homolog of eEF-3; it cross-reacts with anti-eEF-3 antibodies and exhibits a similar ribosome-dependent ATPase activity (Kiel et al., 1999; Kiel & Ganoza, 2001; Xu et al., 2006). This protein also protects rRNA located (A915, A937, and A949 of the 16S rRNA) near the ribosomal E-site from chemical modification (Xu et al., 2006).

In this study, we wanted to obtain a more detailed understanding of the biochemical properties of this protein, and how this protein functions during translation. The open reading frame *yhih* has been cloned; however, expression of the wild-type gene blocks bacterial. Constructed deletion mutants (ΔP541 and ΔL432) could be expressed as insoluble inclusion bodies that subsequently have been solubilized, purified by affinity chromatography, and refolded. Utilizing fluorescence techniques, the nucleotide binding properties of these proteins have been examined. The ability of these proteins to hydrolyze ATP has also been studied.

Chapter 2 - ATPases in Translation

2.1 Translation: a brief overview

2.1.1 Initiation

Prior to any actual ribosome-catalyzed protein synthesis, the ribosomal synthesis machinery must be initiated. During initiation in prokayotes, the 30S and 50S ribosomal subunits, initiator tRNA (fMet-tRNA$_i^{fMet}$, or tRNA$_i$) and initiation factors IF-1, IF-2, and IF-3 interact. In eukaryotes, this process is catalyzed by approximately 12 initiation factors, of which only eIF-5B and eIF-2 bind and hydrolyze GTP.

During initiation in prokaryotes (Figure 1), IF-2, mRNA, and tRNA$_i$ interact with the 30S ribosomal subunit (associated with IF-3). The Shine-Dalgarno sequence (consensus sequence of AGG AGG, located ~6-10 nucleotides upstream of the AUG start codon) then interacts with the 16S rRNA, positioning the AUG start codon in the 30S P site. This process is aided by IF-2, which interacts with the tRNA$_i$, and IF-3, which stabilizes tRNA$_i$ binding to the P site. IF-1 binds to the A site of the 30S ribosomal subunit, preventing the tRNA$_i$ from interacting with the A site and stabilizing the newly formed 30S preinitiation complex. The tRNA$_i$ interacts with the P site in a codon-independent manner, which is unstable and promotes a conformational change that causes a codon-anticodon interaction, forming a stable 30S initiation complex. At this point, IF-1 and IF-3 dissociate and IF-2 stimulates binding of the 50S ribosomal subunit. Upon GTP hydrolysis by IF-2, the initiation factor dissociates and the ribosome can then proceed to the elongation phase (Kozak, 1999; Laursen et al., 2005).

3
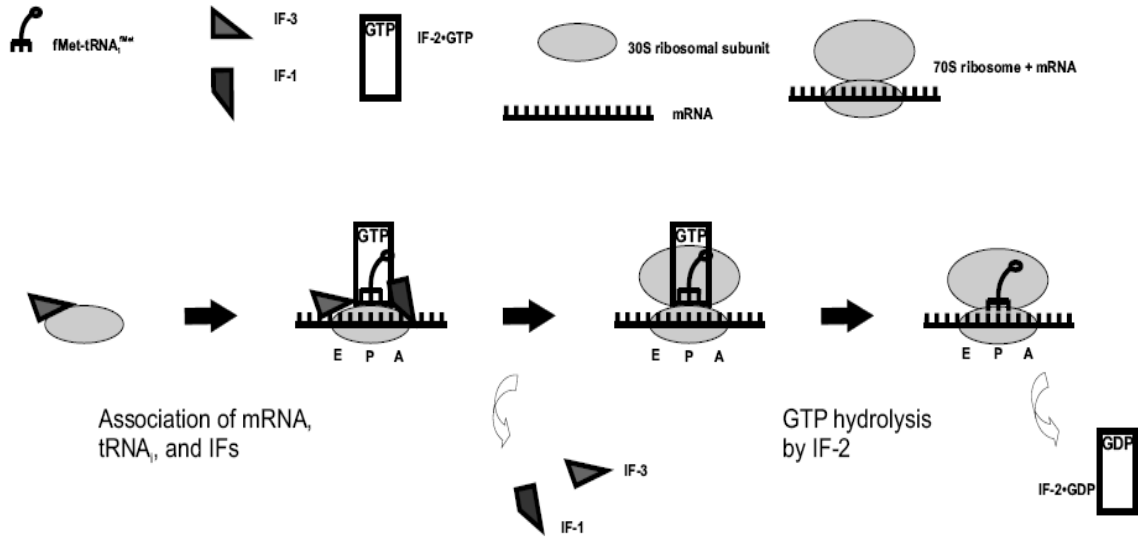
Figure 1: Initiation and 70S ribosomal assembly in prokaryotes.

The binary complex of the 30S ribosomal subunit and IF-3 associates with mRNA, tRNA$_i$, IF-1, and IF-2•GTP. Following dissociation of IF-1 and IF-3, the 50S ribosomal subunit associates. IF-2 hydrolyzes GTP, causing release of IF-2. Schematic representations of the involved factors are shown above the figure.

In eukaryotes, several key differences occur during initiation (Figure 2): interaction of eIF-4E with the 5' 7-methylguanosine (m^{7}G) cap is required for initiation. This m^{7}G cap is required for recognition of the mRNA rather than rRNA interaction. Upon binding of eIF-4E with the m^{7}G cap, the polyA-binding protein on the 3' polyA tail interacts with eIF-4G. eIF-4A (removes RNA secondary structure) and eIF-4B (a required RNA binding protein) then associates with the complex. eIF-2 binds Met-tRNA$_i$^{Met} (not fMet, as found in prokaryotes), and is joined in a complex with eIF-1, eIF-3, and eIF-5, followed by association with the 40S ribosomal subunit. The mRNA complex and the tRNA-40S complex then associate, and the AUG start codon is located in an ATP-dependent manner by which eIF-4A (an ATP-dependent RNA helicase) shifts

4

the mRNA with respect to the 40S subunit (scanning). GTP hydrolysis by eIF-2 then occurs, the 60S ribosomal subunit associates (aided by GTP hydrolysis by eIF-5B), and initiation factors dissociate; the 80S eukaryotic ribosome can then move into the elongation phase (Kozak, 1999).
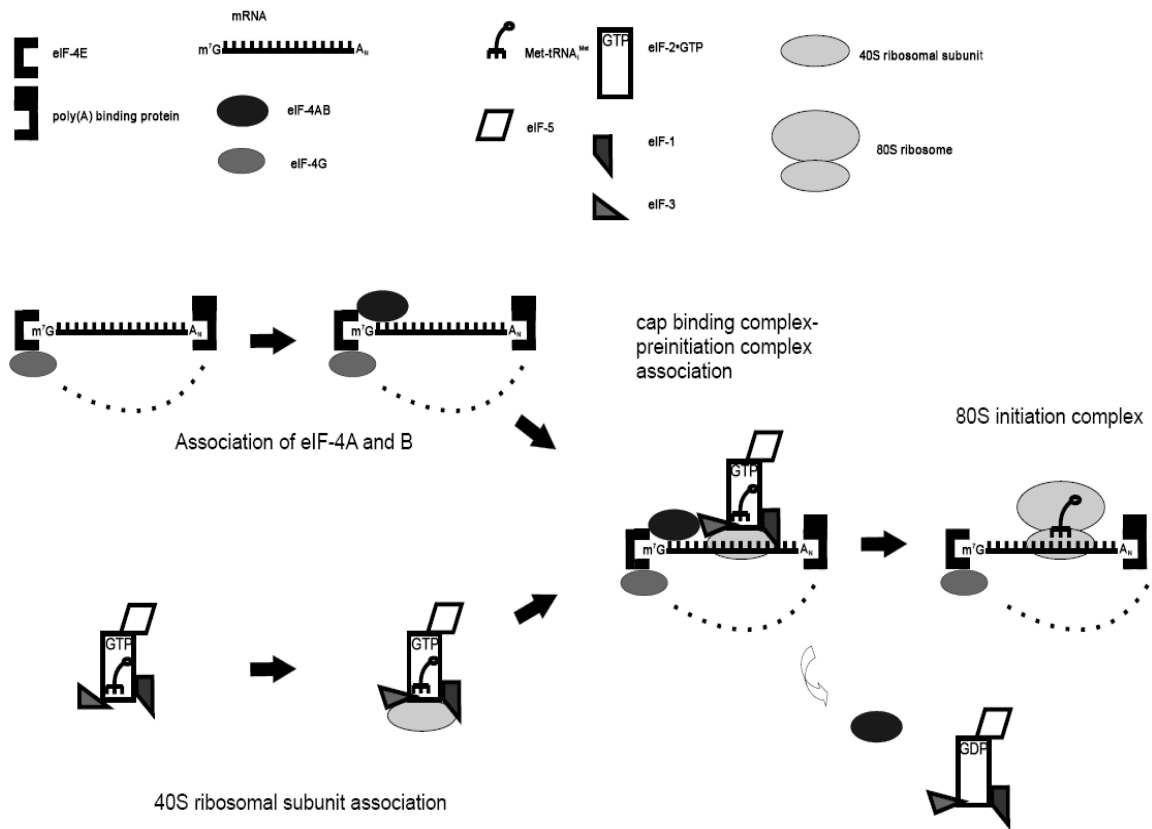
Figure 2: Scanning model of eukaryotic translation initiation.

The m^{7}G cap is recognized by eIF-4B and associates with the polyA binding protein (on the 3' region of mRNA), eIF-4G and eIF-4A. This complex associates with the 40S preinitiation complex. This complex "scans" for the AUG start codon, and upon locating it, GTP is hydrolyzed, and the initiation factors dissociate. The dashed line indicates eIF-4G is in complex with the polyA binding protein. Schematic representations of the involved factors are shown above the figure.

2.1.2 Elongation

The elongation phase of protein synthesis is characterized by addition of amino acids to the growing polypeptide in a sequential, codon dependent manner. This process is catalyzed by the essential GTPases EF-Tu and EF-G (eEF-1α and eEF-2 respectively in eukaryotes).

In prokaryotes, aminoacyl-tRNA (aa-tRNA) is delivered to the ribosome as a ternary complex of aa-tRNA•EF-Tu•GTP. The ternary complex binds to the ribosomal A site, and upon GTP hydrolysis, aa-tRNA is released into the A site and EF-Tu•GDP dissociates. The nucleotide exchange factor EF-Ts then catalyzes the exchange of GDP for GTP, allowing EF-Tu to rebind aa-tRNA and continue the cycle. A peptide bond is simultaneously formed between the A and P site tRNAs. Following peptide bond formation, EF-G mediated translocation occurs. After EF-Tu dissociates from the ribosome, EF-G binds and immediately hydrolyzes GTP. This is followed by a slower release of P_i and movement of tRNAs from the A and P sites to the P and E sites in parallel with the translocating mRNA (Rodnina et al., 2000; Stark et al., 2000; Peske et al., 2003). EF-G•GDP changes its conformation and dissociates from the ribosome (Rodnina et al., 2000; Stark et al., 2000). Dissociation of deacyl-tRNA from the ribosomal E-site occurs, though the mechanism of this is not yet clear in prokaryotes. The delivery of aa-tRNA to the ribosome by EF-Tu and translocation mediated by EF-G are the two key features of elongation and require GTP hydrolysis (Figure 3).

6
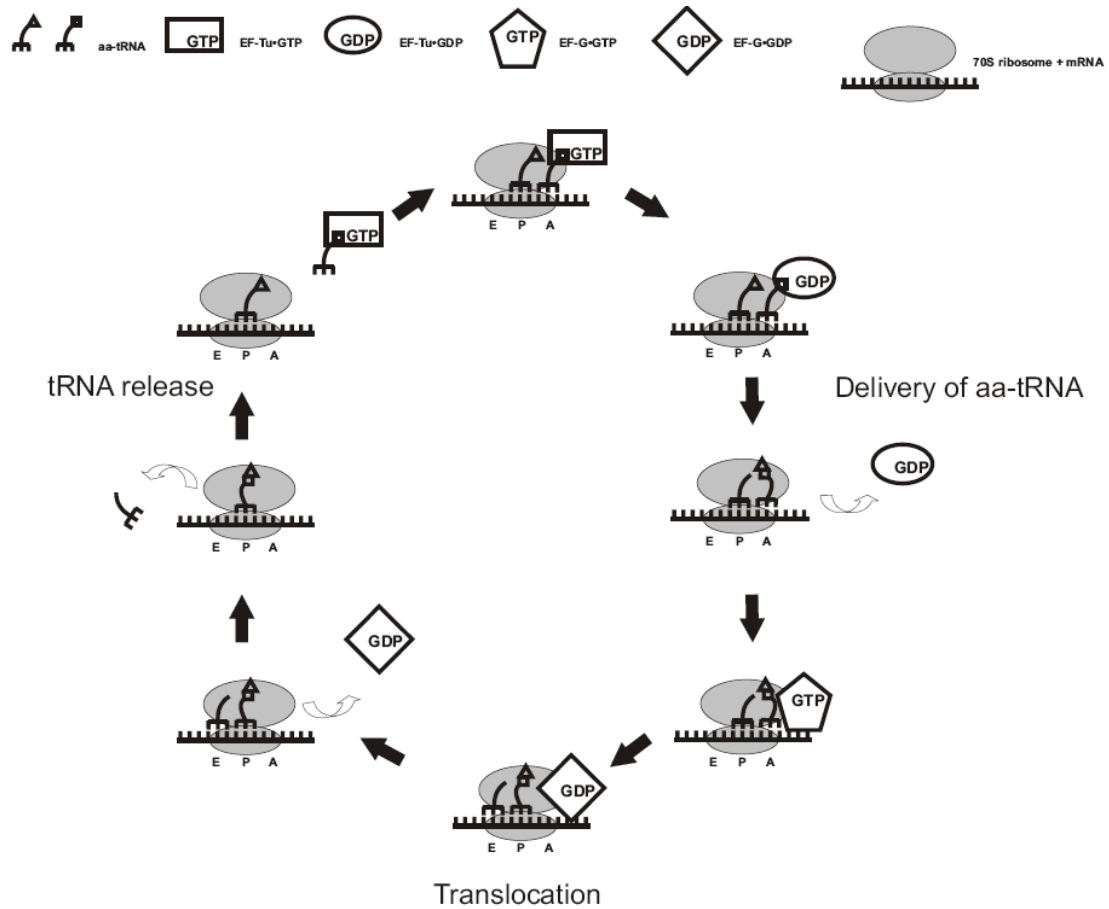
Figure 3: Summary of the prokaryotic elongation cycle.

With tRNA$_i$ in the P site, the aa-tRNA•EF-Tu•GTP ternary complex binds to the ribosome. EF-Tu hydrolyzes GTP, EF-Tu•GDP dissociates, aa-tRNA is released, and a peptide bond is formed. EF-G•GTP then binds, hydrolyzes GTP, and translocates the A and P site tRNA to the P and E site respectively. EF-Tu•GDP dissociates, E site tRNA is released, and the cycle continues. Schematic representations of the involved factors are shown above the figure.

The delivery of aa-tRNA by EF-Tu into the ribosomal A site involves numerous intermediates (Figure 4), and is well studied kinetically by monitoring GTP hydrolysis rates using rapid kinetic techniques (Rodnina et al., 2005) as well as single molecule

7

detection methods (Lee et al., 2007). This process of accommodation is a crucial step for maintaining the translational fidelity, as non-cognate aa-tRNA is rejected by the ribosome during delivery. Initial binding of the ternary complex is followed by codon recognition, both of which are reversible and dependent on a cognate tRNA codon-anticodon interaction. Binding to the ribosome activates GTP hydrolysis by EF-Tu and a very rapid subsequent release of inorganic phosphate from the complex. At this point, non-cognate aa-tRNA can be rejected, or the aa-tRNA can be fully accommodated into the ribosomal A site. Upon accommodation, a peptide bond is immediately formed, EF-Tu•GDP dissociates from the ribosome, and the elongating ribosome will continue through the elongation cycle (Kothe et al., 2004).
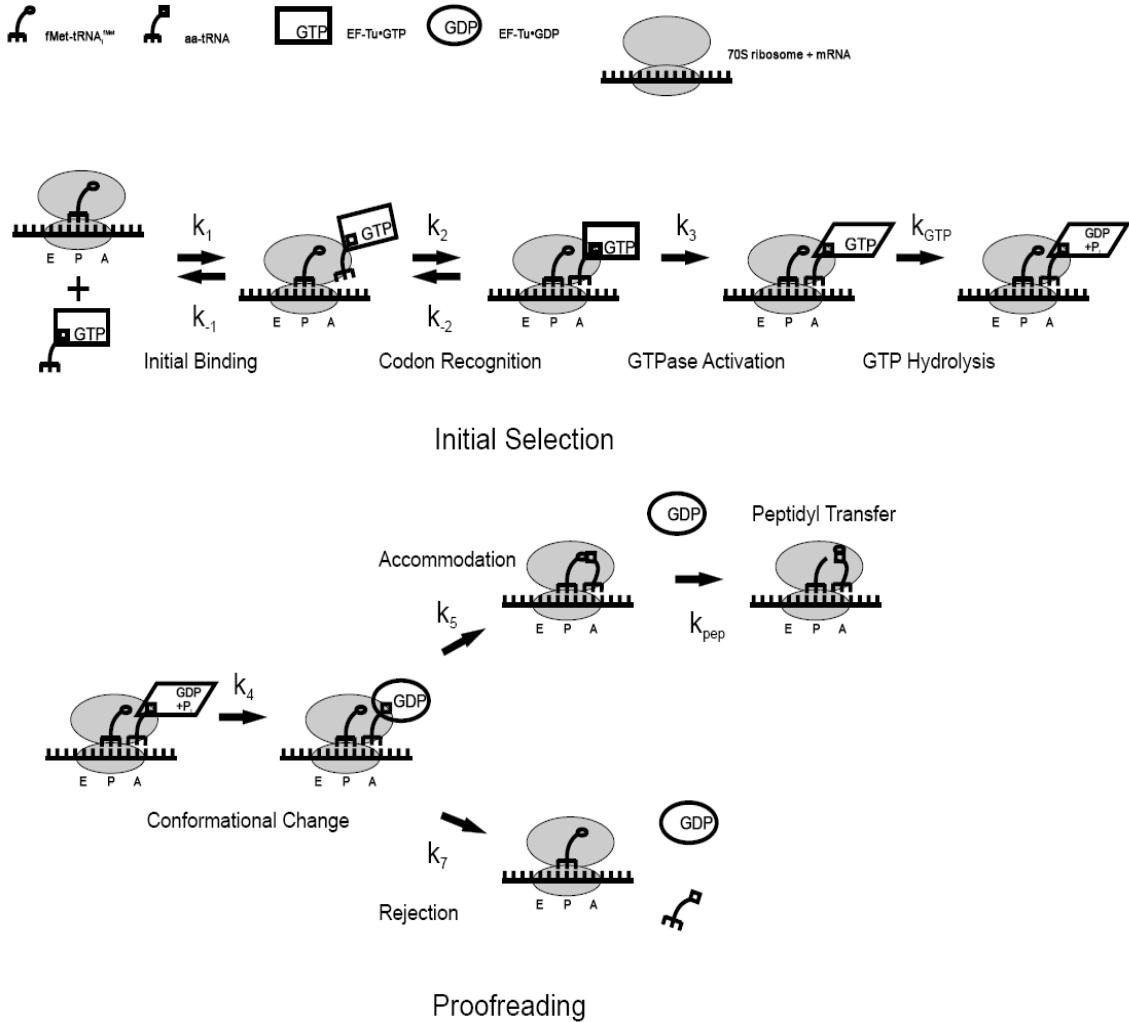
Figure 4: Kinetic mechanism of EF-Tu-dependent binding of aa-tRNA to the ribosome.

EF-Tu initially binds to the ribosome, in a codon-independent fashion (k_1/k_{-1}). Upon a cognate codon-anticodon interaction (recognition, k_2/k_{-2}), the GTPase activity of EF-Tu is activated (k_3). Following GTP hydrolysis (k_{GTP}), a conformation change in EF-Tu occurs (k_4), and P_i is released. Either cognate tRNA is accommodated into the A-site and a peptide bond is formed (k_5 and k_{pep} respectively), or a non-cognate interaction is rejected, and the ternary complex dissociates (k_7). Schematic representations of the involved factors are shown above the figure.

The elongation cycle in eukaryotes is similar and requires GTP hydrolysis by eEF-1α and eEF-2. In yeast however, another protein factor is involved: eEF-3, an ATP binding cassette (ABC) protein that is responsible for facilitating the release of deacyl-tRNA from the E-site. This action is accomplished by hydrolysis of ATP to drive a conformational change in the protein that causes the ribosomal L1 stalk to move from a locked, "closed" state to an "open" position where deacyl-tRNA dissociates (Andersen et al., 2006). A summary of eukaryotic elongation in yeast is presented (Figure 5).
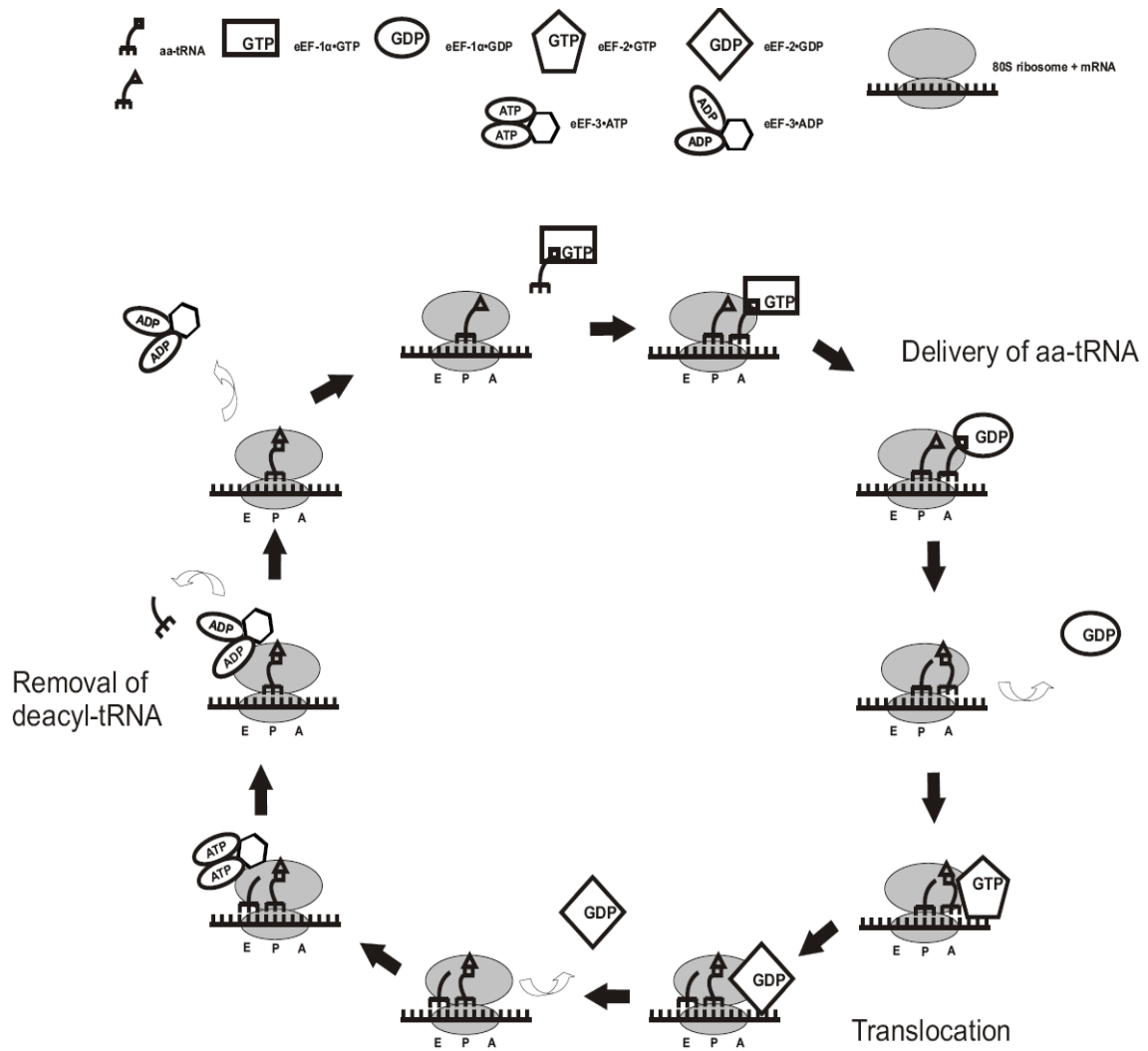
Figure 5: The yeast elongation cycle, including the proposed action of eEF-3.

The initial binding of aminoacyl-tRNA and translocation by eEF-1α and eEF-2 are analogous to that of prokaryotic factors EF-Tu and EF-G. In the E and P site tRNA bound state, eEF-3 binds near the L1 stalk and binds to ATP, causing eEF-3 to adopt a "closed" conformation that "unlocks" the L1 stalk. ATP is hydrolyzed, the E-site opens, and aminoacyl-tRNA is released. Schematic representations of the involved factors are shown above the figure.

11

2.1.3 Termination

Termination of translation (Figure 6) occurs when a stop codon is recognized by a release factor that binds to the ribosome and causes the release of the nascent polypeptide. In prokaryotes, RF-1 recognizes UAA and UAG stop codons, while RF-2 recognizes UAA and UGA codons; eukaryotic release factor eRF-1 recognizes all three stop codons and functions as a heterodimer with eRF-3 (Bertram et al., 2001; Kisselev et al., 2003). It has been suggested that the tRNA-mimicry by RF1 and eRF-1 allows direct interaction with the A-site stop codon, and this facilitates binding of the GTPase release factor (RF-3 and eRF-3) (Kisselev & Buckingham, 2000; Bertram et al., 2001; Kisselev et al., 2003). Recently, the crystal structure of RF-3 and the cryo-EM map of RF-3•GTP bound to the post-termination ribosome shows that binding of RF-3 causes a conformational change in the ribosome, and GTP hydrolysis causes a conformational change which disrupts the interaction of RF-1 or RF-2 with the decoding center. This in turn has been proposed to cause a nucleophilic attack on the C-terminus of the peptide by a water molecule, releasing the peptide (Gao et al., 2007).

After the nascent peptide is released, the complex of the 70S ribosome, mRNA, and deacyl-tRNA is disassembled (recycled) such that the individual components can be reused in another round of translation. This is catalyzed by the ribosome recycling factor (RRF), which binds to the post-termination complex with EF-G and GTP (Raj et al., 2005; Stagg & Harvey, 2005), and together release deacyl-tRNA and break apart the ribosomal subunits and mRNA with IF-3. However, the mechanism of RRF and EF-G

during ribosome recycling is still unclear. Upon dissociation of the subunits, the translation cycle can begin again.
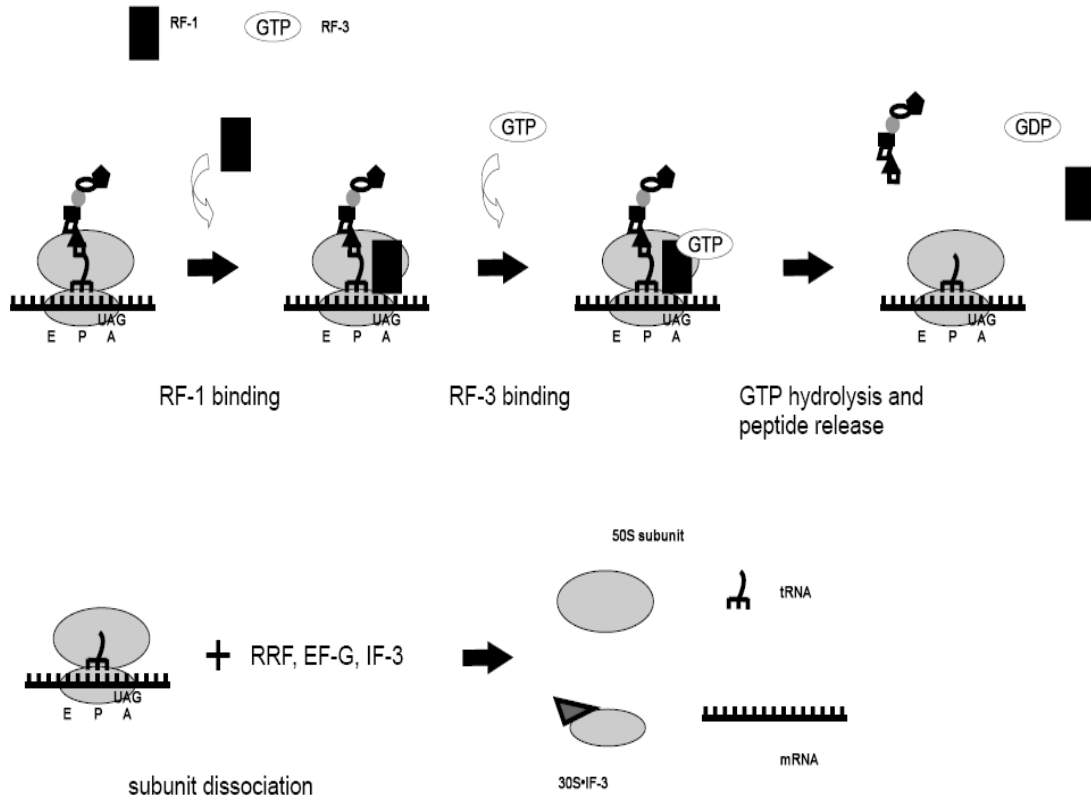
Figure 6: Prokaryotic termination and ribosomal subunit dissociation.

Upon recognition of a stop codon by RF-1, RF-3•GTP binds to the complex. GTP is hydrolyzed, the nascent peptide is released, and RF-1 and RF-3 dissociate. RRF, EF-G, and IF-3 cause the release of deacyl-tRNA and break apart the ribosomal subunits. The IF-3•30S subunit can now reenter the translation cycle, at the initiation phase. The scheme is analogous to eukaryotic termination, though different stop codons are read by different factors. Schematic representations of the involved factors are shown above the figure.

The nucleotide triphosphate binding proteins are one of the most abundant types of proteins within a living cell, and perform a variety of roles (Leipe et al., 2002). These proteins belong to several distinct protein folds (Figure 7): the Rossmann or dinucleotide binding fold and related tubulin/TtsZ fold, the protein kinase fold, the histidine kinase fold, the Hsp70/RNAse H fold, and the P-loop NTPases (Leipe et al., 2002).
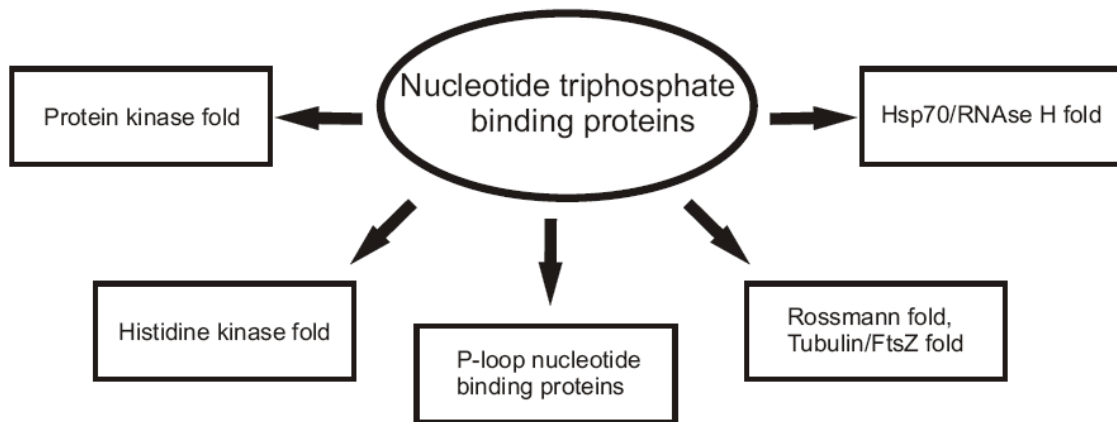
Figure 7: Nucleotide triphosphate binding protein folds.

The α/β P-loop NTPases are the most common fold and comprise 10-18% of all gene products, and are characterized by the Walker A motif, or P-loop, and a Walker B loop, which includes an aspartate residue that coordinates an essential Mg^{2+} ion (Leipe et al., 2002). This fold consists of seven lineages (Figure 8) as described by Leipe *et al*: the nucleotide kinases and GTPases, in which the P-loop and Walker B motif are direct neighbors; and the RecA related ATPases, nucleic acid-dependent ATPases, NACHT

NTPases, AAA+ ATPases, and ABC transporters, in which an additional strand is inserted between the Walker A and B motifs (Leipe et al., 2002).
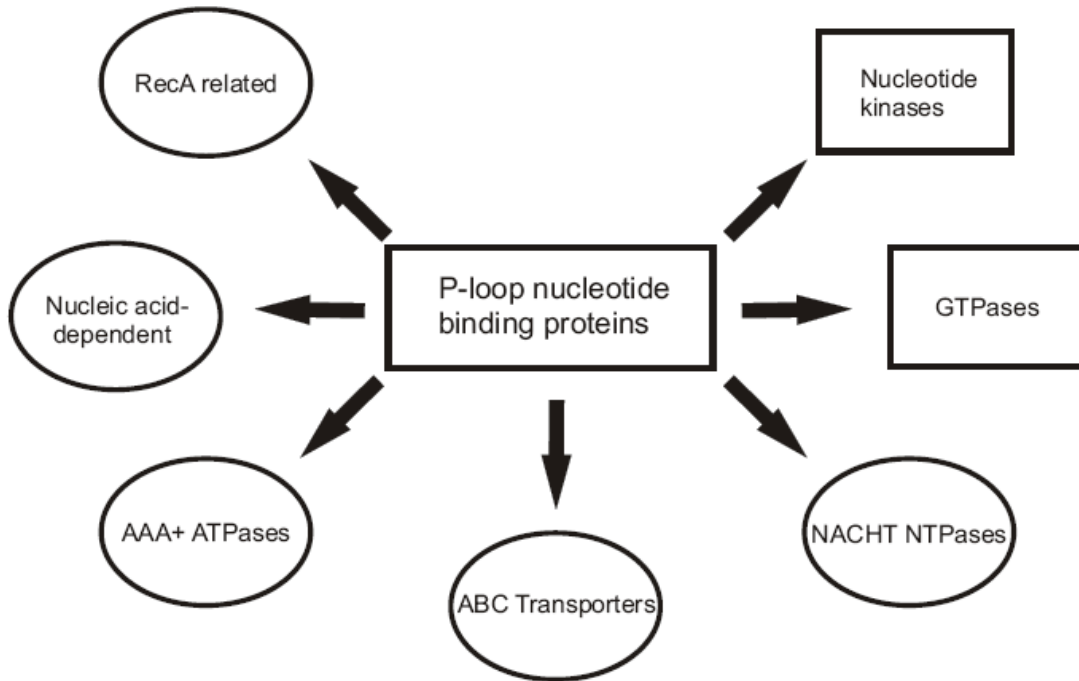
Figure 8: The phosphate-binding loop NTPase lineages.

2.2.1 GTP binding proteins: structure and function

GTP binding proteins fulfill numerous functions *in vivo* and are highly conserved across the domains of life. Often GTP binding acts as a switch mechanism between two conformations; for example, aa-tRNA•EF-Tu•GTP will hydrolyze GTP upon binding and accommodation of the ternary complex to the ribosome. This GTP hydrolysis triggers a conformational change that is required for release of the aa-tRNA into the ribosomal A-site (Rodnina et al., 2000; Rodnina et al., 2005). Other GTP binding proteins function as signaling messengers, where GTP hydrolysis is coupled to structural changes that affect their affinity for downstream regulators and effectors. Proteins of the *ras* gene family

cause a cascade of cellular reactions that can cause numerous downstream effects such as, for example, gene activation (Wittinghofer & Pai, 1991; Rak et al., 2003). Other GTPases are involved in secretion and transport, such as human Arf6 and Sec4 (vanderBliek et al., 1993; Stroupe & Brunger, 2000; Pasqualato et al., 2001), or signal recognition, such as the *E. coli* signal recognition particle Ffh (Buskiewicz et al., 2005). Several GTPases are universally conserved, such as the translation factors EF-Tu and EF-G (and their eukaryotic homologs). Several conserved GTPases, such as YchF, HflX, and EngA, fulfill unknown roles in the cell, though they have be suggested to be involved in regulating protein synthesis or ribosome biogenesis (Caldon et al., 2001; Teplyakov et al., 2003; Brown, 2005).

Table 2: Guanine nucleotide binding proteins with diverse functions.

Accession numbers given are from the EXPASY/Swiss-Prot database.

Protein	Organism	Role / Description	Reference(s)	Accession #
IF-2	*E. coli*	P-site tRNA$_i^{fMet}$ stabilization	(Kozak, 1999; Laursen et al., 2005)	P0A705
eEF-1α	*H. sapiens*	Delivery of aa-tRNA	(Brands et al., 1986)	P68104
LepA	*E. coli*	Reverse-translocase	(Qin et al., 2006; Youngman & Green, 2007)	P60785
RF-3	*E. coli*	Release factor	(Kisselev et al., 2003; Gao et al., 2007)	P0A7I4
Sec4	*S. cerevisiae*	Rab-related; exocytosis factor	(Stroupe & Brunger, 2000)	P07560
YPT1	*S. cerevisiae*	Ras-related; secretory protein	(Rak et al., 2003)	P01123
Arf6	*H. sapiens*	Intracellular transport	(Pasqualato et al., 2001)	P62330
Dynamin	*H. sapiens*	Endocytosis	(vanderBliek et al., 1993)	Q05193
Ffh	*E. coli*	Signal recognition particle	(Buskiewicz et al., 2005)	P0AGD7
Ychf	*E. coli*	Ribosome binding (?)	(Teplyakov et al., 2003)	A2UH87

Structurally, guanine nucleotide binding proteins are a member of the P-loop NTPase fold. These proteins share a mononucleotide binding fold that catalyzes the cleavage of the β-γ phosphoester bond of nucleotide triphosphates and are characterized by the presence of a phosphate-binding loop (or Walker A motif, Figures 9 and 10) with the consensus sequence GxxxxGK[ST], where x is a nonconserved amino acid (Moller & Amons, 1985; Brown, 2005). This P-loop consists of a hydrophobic β-strand followed by

a flexible loop linked to an α-helix that interacts directly with the phosphate moeity of the substrate (Moller & Amons, 1985; Koonin, 1993). The conserved lysine is essential for binding, and contacts the γ-phosphate. The glycine residues form flexible regions, and the main-chain amines contact and stabilize the β and γ phosphates. The conserved serine/threonine residues coordinate an essential Mg^{2+} ion located in close proximity to the β and γ phosphates (Wittinghofer & Pai, 1991). A coordinating water molecule is responsible for hydrolyzing the phosphoester bond, possibly through a nucleophilic attack (Wittinghofer & Pai, 1991; Maegley et al., 1996; Daviter et al., 2003). P-loop NTPases also contain a Walker B motif (consensus hhhhD, where h is a hydrophobic residue) in which the conserved aspartate aids in coordinating the Mg^{2+} ion (Brown, 2005).

IF-2	393	-	VVTIMGHVDHGKTSLLDYI	411
eEF-1α	9	-	NIVVIGHVDSGKSTTTGHL	27
lepA	6	-	NFSIIAHIDHGKSTISDRI	24
RF-3	15	-	TFAIISHPDAGKTTITEKV	33
Sec4	22	-	KILLIGDSGVGKSCLLVRF	40
YPT1	10	-	KLLLIGNSGVGKSCLLLRF	28
Arf6	15	-	RILMLGLDAAGKTTILYKL	33
Dynamin	33	-	QIAVVGGQSAGKSSVLENF	51
Ffh	102	-	VVLMAGLQGAGKTTSVGKL	120
Ychf	4	-	KCGIVGLPNVGKSTIFNAL	22

Figure 9: The phosphate-binding loop of GTP binding proteins.

Conserved residues are color coded: Black is conserved in 100% of sequences in the alignment, Blue in 70-90%, and Grey 60-70%.
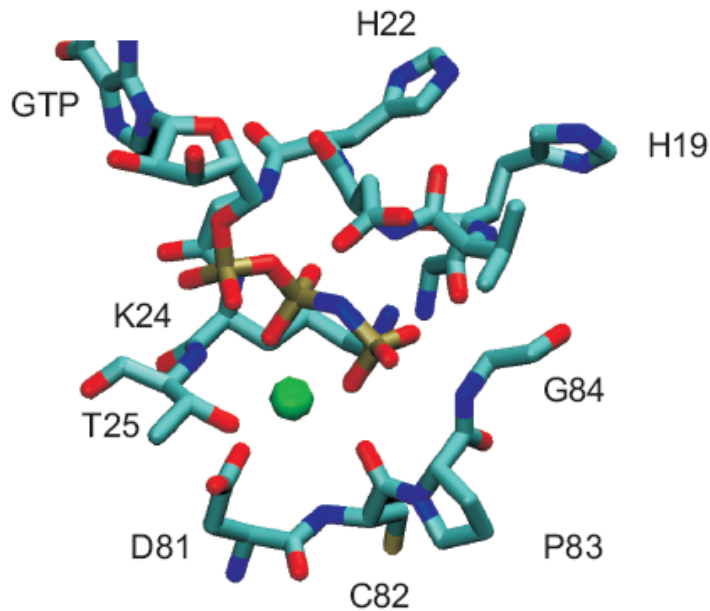
Figure 10: The Walker A motif and Walker B aspartate of *T. thermophilus* EF-Tu.

The Walker A motif (GHVDHGKT, residues 18-25) and conserved aspartate (D81) of the Walker B motif responsible for phosphate binding and Mg^{2+} (green sphere) coordination. The structure is of *Thermus thermophilus* EF-Tu in complex with GDPNP (PDB ID 1EXM).

In GTPases, a conserved NKxD motif (Figures 11 and 12) is also present that confers specificity to guanine over other nucleotides (Wittinghofer & Pai, 1991; Brown, 2005). The aliphatic chain of the conserved lysine of this motif stabilizes the guanine base in the binding pocket, while the carboxylic acid of the conserved aspartate interacts with hydrogen atoms attached to the endocyclic N1 and exocyclic amine attached to C2 of the guanine base (Wittinghofer & Pai, 1991). This aspartate is responsible for conveying guanine specificity (Soundararajan et al., 2007). The conserved aspartamine contacts the N7 position of the base (Scrima & Wittinghofer, 2006).

```
IF-2        490 - QVPVVAVNKIDKPEA    505
eEF-1α      145 - VKQLIVGVNKMDSTEP   160
lepA        123 - DLEVVPVLNKIDLPAA   138
RF-3        134 - DTPILTFMNKLDRDIR   149
Sec4        125 - EAQILLVGNKSDMETR   140
YPT1        113 - TVLKLLVGNKCDLKDK   128
Arf6        114 - DAILLIFANKQDLPDA   129
Dynamin     177 - GQRTIGVITKIDLMDE   192
Ffh         240 - LPLTGVVLTKVDGDAR   255
Ychf        171 - QLENAGMLRAIDLSAE   176
```

Figure 11: The conserved NKxD motif of GTP binding proteins.

Conserved residues are color coded: Black is conserved in 100% of sequences in the alignment, Blue in 70-90%, and Grey 60-70%.
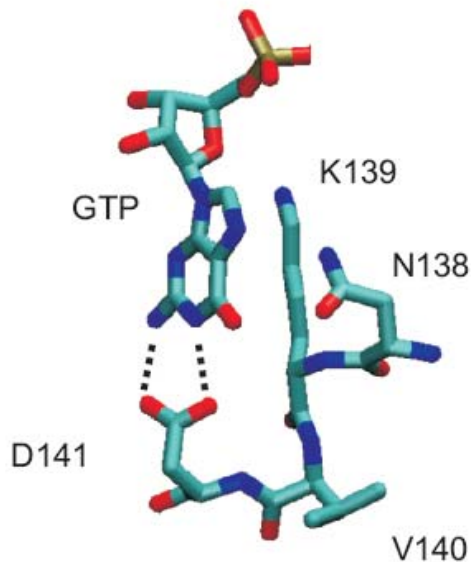
Figure 12: Structure of the conserved NKxD guanine specificity motif.

The hydrogen bonding interactions between D141 and the guanine ring are shown as dotted lines. The structure is of *Thermus thermophilus* EF-Tu in complex with GDPNP (PDB ID 1EXM).

The GTPase activity of the guanine nucleotide binding proteins is coupled directly to the action of the protein. In the GTP-bound "on" state, the protein is functional; in the GDP-bound or "off" state, the protein is inactive. These states influence the conformation of switch regions, which in turn influence protein function. Interestingly, G-proteins can interact with guanine-nucleotide exchange factors (GEFs) that facilitate the exchange of GDP for GTP, or GTPase-activating proteins (GAPs) that facilitate GTP hydrolysis (Figure 13). Most notably, the GEF EF-Ts stimulates GDP dissociation in EF-Tu by four orders of magnitude (Gromadski et al., 2002; Wieden et al., 2002). Other GEFs include Sos (GEF for Ras) (Boriack-Sjodin et al., 1998) and Sec7 (GEF for Arf1) (Goldberg, 1998).
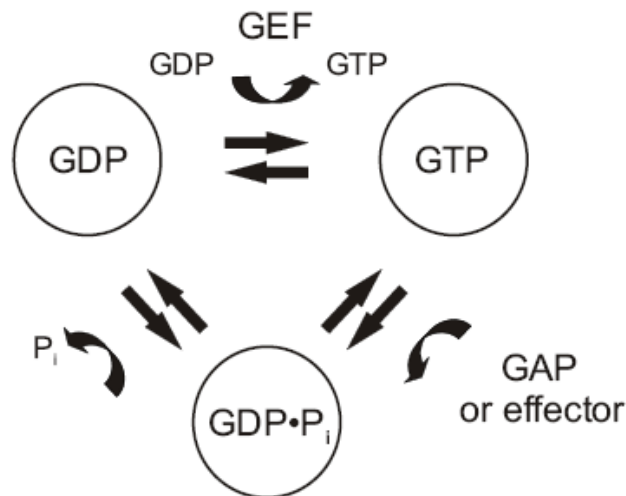
Figure 13: A model for interactions between GTPases, GEFs, and GAPs.

Guanine nucleotide exchange can be stimulated by guanine nucleotide exchange factors (GEFs); GTP hydrolysis can be stimulated by GTPase activating proteins (GAPs).

2.2.2 ATP binding proteins: structure and function

ATP binding proteins have different roles *in vivo*, and often have an essential role in maintaining cellular structure. Other roles include facilitating the release of deacyl-tRNA from the ribosomal E-site in yeast (by eEF-3 (Triana-Alonso et al., 1995; Chakraburtty, 2001; Anand et al., 2006; Andersen et al., 2006)), protein folding (by heat shock proteins such as Hsp90 (Garnier et al., 2006)), drug resistance through efflux mechanisms in eukaryotes (by human P-glycoprotein (Miyazaki et al., 1998; Qian et al., 2006)) homologous recombination DNA repair (by human RAD51 (Wiese et al., 2006)) and nucleotide base excision repair (by UvrA and UvrB in *E. coli* (Verhoeven et al., 2002; Truglio et al., 2004)).

Structurally, ATP binding proteins contain the Walker A motif (also known as the phosphate binding, or P-loop) that is shared with the guanine nucleotide binding proteins (Moller & Amons, 1985), and the Walker B motif (Moller & Amons, 1985; Koonin, 1993; Schneider & Hunke, 1998; Higgins, 2001). In addition to these two consensus motifs, an aromatic residue is often present ~25 amino acids upstream of the Walker A-loop that stabilizes the adenine moiety through π-π interactions (Ambudkar et al., 2006).

Table 3: Adenine nucleotide binding proteins with diverse functions.

Accession numbers given are from the EXPASY/Swiss-Prot database.

Protein	Organism	Role / Description	Reference(s)	Accession #
eEF-3	*S. cerevisiae*	deacyl-tRNA release	(Anand et al., 2006; Andersen et al., 2006)	P16521
Yhih	*E. coli*	Similar to eEF-3 (?)	(Kiel et al., 1999; Xu et al., 2006)	P37624
Hsp90	*G. gallus*	Chaperone; protein folding	(Garnier et al., 2006)	P11501
P-glycoprotein	*H. sapiens*	Multidrug resistance	(Qian et al., 2006)	P08183
RAD51	*H. sapiens*	Homologous recombination	(Wiese et al., 2006)	Q06609
ABCG2	*B. taurus*	Influences milk production	(Cohen-Zinder et al., 2005)	Q4GZT4
UvrB	*E. coli*	Nucleotide excision repair	(Verhoeven et al., 2002; Truglio et al., 2004)	P0A8F8
MalK	*E. coli*	Maltose import	(Walter et al., 1992)	P68187
CGR1	*C. glabrata*	Fluconazole resistance	(Miyazaki et al., 1998)	O74208
RecA	*E. coli*	DNA recombination	(Story & Steitz, 1992)	P0A7G6

The Walker A-motif differs slightly from that of the guanine binding proteins in that an additional conserved glycine is found within the P-loop (GXXGXGK[ST]). The

function of the Walker A motif is shared with all other P-loop NTPases. The conserved serine or threonine hydrogen-bonds to the aspartate of the Walker B motif (hhhhD). The Walker B motif again coordinates the crucial Mg^{2+} and also bonds to a water molecule that is essential for hydrolysis (Koonin, 1993). The NKxD motif that conveys specificity for GTP in guanine binding proteins is not present in ATP binding proteins.

```
eEF-3 ABC1      457 - RYGICGPNGCGKSTLMRAIANG   478
Yhih ABC1        50 - MVGLIGPDGVGKSSLLSLISGA    71
Hsp90           126 - DISMIGQFGVGSYSAYLVAEKV   147
P-glycoprotein  422 - TVALVGNSGCGKSTTVQIMQRL   443
RAD51           122 - ITEMFGEFRTGKTQICHTLAVT   143
ABCG2            74 - LNAILGPTGGGKSSLLDILAAR    95
UvrB             34 - HQTLIGVTGSGKTFTIANVIAD    55
MalK             31 - FVVFVGPSGCGKSTLLRMIAGL    52
CGR1            916 - LTAIMGASGAGKTTLLDCLAER   937
RecA             62 - IVEIYGPESSGKTTITLQVIAA    83
```

Figure 14: The Walker A motif of ATP binding proteins.

Conserved residues are color coded: Black is conserved in 100% of sequences in the alignment, Blue in 70-90%, and Grey 60-70%.

```
eEF-3 ABC1       571 - NADILLLDEPTN    582
Yhih ABC1        165 - DPELLILDEPTT    176
Hsp90            371 - VRRVFIMDNCEE    382
P-glycoprotein   548 - NPKILLLDEATS    559
RAD51            215 - RYALLIVDSATA    226
ABCG2            202 - DPSIIFLDEPTT    213
UvrB             161 - LTVGMIIDQRAI    172
MalK             151 - EPSVFLLDEPLS    162
CGR1            1044 - PKLLVFLDEPTS   1055
RecA             138 - AVDVIVVDSVAA    149
```

Figure 15: The Walker B motif of ATP binding proteins.

Conserved residues are color coded: Black is conserved in 100% of sequences in the alignment, Blue in 70-90%, and Grey 60-70%.

2.2.3 The ATP binding cassette (ABC) superfamily

The ATP binding cassette, or ABC, genes encode for an estimated 5% of the *E. coli* genome (Higgins & Linton, 2004). The ABC transporters can be identified by the conserved ABC signature, or Walker C, motif (consensus sequence LSGGQ(Q/R/K)QK) (Schneider & Hunke, 1998; Higgins, 2001; Kerr, 2002; Higgins & Linton, 2004) that is only found in this superfamily. These proteins are often associated with the coupling of ATP binding and hydrolysis to facilitate the translocation of molecules across biological membranes; however this is not the only role they fulfill: ABC transporters are involved in solute transport (*E. coli* MalK (Walter et al., 1992; Schneider et al., 1995)), signal transduction, drug and antibiotic resistance (*C. glabrata* PDH1 (Miyazaki et al., 1998)), ribosome biogenesis (Pixie in *D. melanogaster* (Andersen & Leevers, 2007)), and protein synthesis (eEF-3 in yeast (Andersen et al., 2006)). ABC transporters are of medical and economic importance; in humans, several inheritable diseases such as cystic fibrosis and Stargardt's disease are caused by the defective ABC transporters CFTR (cystic fibrosis conductance regulator) and ABCA4 (ABC transporter family A, protein 4) respectively (Schneider & Hunke, 1998). Tumour cells develop resistance to chemotherapeutic drugs through transport of drugs through P-glycoprotein (Qian et al., 2006). In cattle, mutations in the CGR2 ABC transporter influence both the quality and quantity of milk produced (Cohen-Zinder et al., 2005).

Figure 16: The ABC signature motif of ABC proteins.

Conserved residues are color coded: Black is conserved in 100% of sequences in the alignment, Blue in 70-90%, and Grey 60-70%.

Structurally, ABC transporters typically consist of two nucleotide binding domains (NBDs) and two transmembrane domains (TMDs) (Kerr, 2002; Higgins & Linton, 2004), though some ABC proteins are instead expressed in the same operon as a transmembrane domain. The NBDs exhibit positive cooperativity, which suggests the two domains interact tightly during ATP hydrolysis (Davidson et al., 1996). Some proteins, such as yeast eEF-3, have helical domains that do not appear to interact with cellular membranes, though they are structurally similar to transmembrane domains (Andersen et al., 2006). The Walker A and B motifs are responsible for coordinating the Mg^{2+} and nucleophillic water molecule responsible for ATP hydrolysis (similar to GTPases). However, unlike GTPases, the nucleotide binding pocket can be formed using the Walker A and B motifs from the same NBD, as in MalK, or using the Walker A motif from one domain and the Walker B from the other, as in the case of Rad50 (Nikaido, 2002). The flexible Walker C motif (Figure 17) is crucial in transport proteins for ligand movement and ATP hydrolysis; the conserved serine interacts with the γ phosphate and signals a conformational change when this interaction is not present (Schneider & Hunke, 1998;

Nikaido, 2002). In human multidrug resistance protein 1 (MDR1), ATP hydrolysis and subsequent release of the γ phosphate causes this flexible loop to be displaced (Ren et al., 2004). This has been postulated to cause a conformational change in the transmembrane domain, which in turn facilitates transport of the drug (Ren et al., 2004). Interestingly, ATP binding appears to be influenced more by hydrophobic interaction with the aromatic, or A-loop, (Figure 18) rather than a specificity motif, as in the case of the NKxD motif of GTP binding proteins. This conserved A-loop, is upstream of the Walker A motif and essential for binding to the adenine nucleotide (Ambudkar et al., 2006). As a result, ATP binding proteins such as eEF-3 can also bind guanine nucleotides under physiological conditions (Dasmahapatra & Chakrabartty, 1981; Kamath & Chakrabartty, 1989)
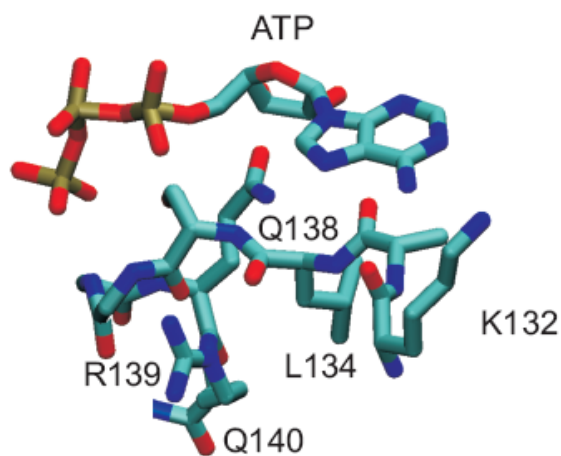
Figure 17: The Walker C motif of MalK.

The interaction between the Walker C motif (LSGGQRQ, residues 134-140) and ATP is shown. The structure is of *Escherichia coli* MalK in complex with ATP (PDB ID 1Q12).
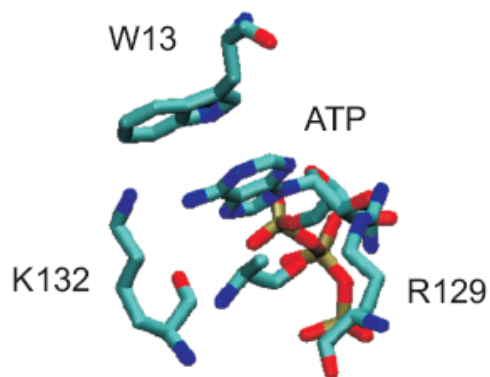
Figure 18: Hydrophobic interaction between the A-loop and ATP.

The interaction between W13 and the adenine residue of ATP is shown in the ATP binding pocket. The structure is of MalK from *E. coli* (PDB ID 1Q12).

2.3 ATP and Translation

2.3.1 ATPases and Translation

The requirement for ATP in a crude rat liver homogenate system was first described in 1950 by the Greenberg group (Winnick, 1950) and confirmed in 1952 by Siekevitz (Siekevitz, 1952). These early experiments monitored the incorporation of radioactive alanine into newly synthesized protein; Siekevitz studied the incorporation of [^{14}C]-DL-alanine into synthesized proteins; these were precipitated with trichloroacetic acid, and the incorporated [^{14}C]-DL-alanine was quantified (Siekevitz, 1952). It was concluded from this experiment that the microsome-containing fraction of the liver

homogenate contained the greatest amount of incorporated radiolabeled amino acid. In this same series of experiments, it was found that the addition of both ATP and MgCl$_2$ resulted in a 2 to 5-fold increase in uptake of radioactive alanine into synthesized proteins (Winnick, 1950; Siekevitz, 1952). Similar experiments were performed by the Greenberg group, confirming the dependence of the translation machinery on both ATP and Mg^{2+} (Kit & Greenberg, 1952; Peterson & Greenberg, 1952).

Siekevitz' research was carried on by the Keller group in collaboration with Siekevitz. In 1954, Keller and Zamecnik demonstrated that the presence of ATP was required for incorporation of [^{14}C] labeled leucine when adenylic compounds were removed from homogenates by dialysis (Zamecnik & Keller, 1954). In addition, the requirement for ATP was concentration-dependent (Zamecnik & Keller, 1954). Later in 1956, Keller and Zamecnik showed that the presence of GTP and GDP was also required for the efficient incorporation of [^{14}C]-L-leucine (Keller & Zamecnik, 1956). This was initially attributed to an amino acid transfer factor by Nathans and Lipmann (Nathans & Lipmann, 1961), and is now accounted for by the activities of G-proteins such as the canonical translation factors eIF-2, eEF-1α, eEF-2, and eRF-3 (and their respective prokaryotic counterparts).

In 1964, the requirement for ATP during protein synthesis was localized upon both the 50S and 30S ribosomal subunits in *E. coli,* based on the ability of isolated subunits to hydrolyze ATP (Schlessinger, 1964). ATPase activity has also been found linked to the 5S rRNA-protein complex (rRNA in complex with 50S proteins L5 and L22) in *B. stearothermophilus*, which was inhibited by GTP (Horne & Erdmann, 1973),

and rat liver ribosomes (Friedrich Grummt, 1974; Grummt & Grummt, 1974). In yeast, a ribosome-dependent GTPase, distinct from eEF-2, was found to be required for polyphenylalanine synthesis by Skogerson and Wakatama in 1976 (Skogerson & Wakatama, 1976), though this factor was later shown to also exhibit a strong ribosome-dependent ATPase activity by Uritani and Miyazaki (Uritani & Miyazaki, 1988) as well.

2.3.2 Yeast Elongation Factor 3

Yeast eEF-3 was identified in 1976 by Skogerson and Wakatama as a ribosome-dependent GTPase that is essential for polyphenylalanine synthesis (Skogerson & Wakatama, 1976). Initial attempts to purify translation factors were done prior to the advent of molecular cloning techniques, thus, numerous purification techniques were used to purify factors from crude cell extracts (polyethylene glycol extraction, NH_4Cl washes, ammonium sulfate precipitation, hydroxylapatite chromatography, DEAE-sephadex chromatography, and phosphocellulose chromatography; (Skogerson & Wakatama, 1976)). While purifying eEF-1 and eEF-2 on a DEAE-sephadex column, Skogerson and Wakatama observed a number of protein fractions that contained a ribosome-dependent GTPase activity that could not be attributed to either eEF-1 or eEF-2. This new GTPase could be separated from eEF-2 using phosphocellulose chromatography, leading to the identification of a new factor involved in protein synthesis in yeast (Skogerson & Wakatama, 1976). This 117 kDa factor , now known as eEF-3, has also been identified in *Candia albicans* (Myers et al., 1992), *Neurospora, Aspergillus,* and *Mucor* genera (Miyazaki & Kagiyama, 1990), and *Pneumocystis carinii,*

30

as well as other species (Belfield & Tuite, 1993). Despite higher eukaryotic ribosomes also possessing an intrinsic ATPase activity, this appears to be different from the prokaryotic ribosomal ATPase: the ATPase of higher eukaryotes cannot be purified (Kamath & Chakraburtty, 1989; Rodnina et al., 1994; El'skaya et al., 1997).

Yeast elongation factor 3 is essential, suggested by inhibition experiments with monoclonal anti-eEF-3 antibodies (Hutchison et al., 1984) and the isolation of temperature-sensitive mutants of eEF-3 that do not grow at non-permissive temperatures (Kamath & Chakraburtty, 1986). This was confirmed by gene disruption (Qin et al., 1990) and is consistent with *in vitro* experiments where eEF-3 is required for the efficient synthesis of proteins in reconstituted systems (Triana-Alonso et al., 1995). Studies *in vitro* using rabbit liver ribosomes show that in addition to eEF-1α and eEF-2, the intrinsic ATPase on 80S ribosomes is required for the efficient poly(U)-directed synthesis of polyphenylalanine (Rodnina et al., 1994; El'skaya et al., 1997). This intrinsic eukaryotic ATPase has been suggested to have a role similar to eEF-3; however, this protein has not yet been isolated.

Further experiments on eEF-3 revealed that it binds and hydrolyzes GTP, but also a broad range of other substrates (GTP, ATP, UTP, CTP), though it appears to have a preference for ATP (ATP: K_M = 0.12 mM and k_{cat} = 610 mol (mol protein^{-1}) min^{-1}; GTP: K_M = 0.20 mM and k_{cat} = 390 mol (mol protein^{-1}) min^{-1} (Uritani & Miyazaki, 1988)). ATP was determined to be required for the efficient synthesis of polyphenylalanine, though to a lesser extent, GTP was sufficient when in high concentration (Uritani & Miyazaki, 1988). ATP binding (and presumably hydrolysis) is absolutely required for the

activity of eEF-3: mutations introduced into the Walker A motifs of eEF-3 (G to V, K to R in the sequence G*xxGxGK*[ST], where * indicates the mutated residue) disrupt yeast growth through interrupting ATP binding when introduced into an eEF-3 knockout mutant strain (Yang et al., 1996). Recombinant proteins containing these mutations are also inactive in stimulating polyphenylalanine synthesis (Yang et al., 1996).

Increasing evidence suggests a role for eEF-3 during the release of deacyl-tRNA from the 80S yeast ribosomal E site (Triana-Alonso et al., 1995). However, the mechanism by which this is accomplished remained mysterious until the solving of the crystal structure of eEF-3 and the localization of the protein on the 80S ribosome (via cryo-EM) by the Andersen group in 2006 (Andersen et al., 2006). The crystal structure of eEF-3 shows that the protein is divided into several domains: a 16 helix HEAT domain (Huntington, Elongation Factor 3, PR65/A, TOR; also found in eIF-4G (Marcotrigiano et al., 2001)) connected through a 4-helix bundle (4HB) to the 2 ABC nucleotide binding domains. ABC domain 2 is interrupted by a chromatin remodeling domain (chromodomain), which is then followed by a C-terminus rich in basic residues (Andersen et al., 2006) (not visible in the crystal structure). Surprisingly the crystal structures of the apo, ADP, and ADPNP bound states show very little change in conformation (Andersen et al., 2006). However, small-angle X-ray scattering experiments suggest that a large conformational change occurs upon ribosome binding and ATP hydrolysis (Andersen et al., 2006).

Andersen and colleagues discovered that the most stable 80S ribosome•eEF3 complex was formed in the presence of ADPNP, suggesting that ATP hydrolysis occurs

after binding to the ribosome. The cryo-EM map of this complex reveals that eEF-3 binds to proteins and rRNA in both the 40S and 60S subunits; eEF-3 interacts with the ribosome through the chromodomain, which is located near the L1 stalk of the ribosome, and the HEAT domain, which contacts the 40S subunit via loops that connect the helices of the HEAT domain (Andersen et al., 2006). The chromodomain is positioned such that upon a conformational change in eEF-3 (presumably induced by hydrolysis of ATP), the L1 stalk may also undergo a conformational change, "opening" the E site and allowing deacyl-tRNA to dissociate.

Based on this data, Andersen and coworkers have suggested a model of eEF-3 mediated release of deacyl-tRNA from the E site where the ribosome containing deacyl-tRNA in the E site and peptidyl-tRNA in the P site (post-state) interacts with eEF-3. eEF-3 then binds ATP, causing a conformational change to occur. Upon ATP hydrolysis, eEF-3 dissociates and E site deacyl-tRNA is released, allowing for a new elongation cycle to occur (Andersen et al., 2006).

2.3.3 Factor "W" and the Ribosome Bound ATPase, RbbA

The protein synthesis machinery in *E. coli* has been well characterized, with the exception of the role of ATP during prokaryotic translation. Initially, the role of facilitating the release of deacyl-tRNA from the ribosomal E-site was attributed to a factor identified in 1985 by the Ganoza group (Ganoza et al., 1985; Green et al., 1985; Ganoza et al., 1995). The so-called factor "W" was isolated from the high-salt (1.0 M

NH$_4$Cl) washes of *E. coli* ribosomes and had an approximate molecular mass of 60 kDa (Green et al., 1985). Factor "W", when added to a crude *in vitro* translation system with the proposed EF-P and rescue protein, enabled the successful synthesis of a hexapeptide (fMet-Ala-Ser-Asp-Phe-Thr, encoded for by f2am3 bacteriophage RNA) whereas the system lacking these components did not synthesize the polypeptide (Green et al., 1985). A similar result was obtained when the system was programmed with MS2 RNA. "W" was also proposed to prevent binding of deacyl-tRNA to the ribosome, thus facilitating polypeptide synthesis (Ganoza et al., 1985).

In 1999, the Ganoza group first reported the identification of a ribosome-bound ATPase, RbbA (Kiel et al., 1999). Utilizing the same salt washes (1.0 M NH$_4$Cl) used to isolate "W", a 91 kDa protein was purified and found to cross-react with polyclonal antibodies raised against eEF-3 from yeast (Kiel et al., 1999). This protein was found to possess a ribosome-stimulated ATPase activity that could be inhibited by vanadate ions and anti-eEF-3 antibodies, and could be cross-linked to [α-^{32}P]-ATP (Kiel et al., 1999). This same group also demonstrated that this ribosome-bound ATPase, or RbbA, stimulated polyphenylalanine synthesis in an *in vitro* system programmed with poly(U) and containing the canonical factors EF-Tu and EF-G (Kiel et al., 1999). Based on mass spectrometry data, the open reading frame *yhih* was confirmed as the gene coding for RbbA, which they subsequently cloned and purified. This recombinant, 6X-His-tagged RbbA exhibited similar properties to the native purified RbbA (Kiel et al., 1999). The sequence alignment of RbbA and the C-terminus of eEF-3 from both *S. cerevisiae* and *C. albicans* shows that the proteins share 22% identity and 40% similarity (Kiel et al., 1999).

Further experiments on both native and recombinant, His-tagged RbbA demonstrated that the antibiotic hygromycin B, and to a lesser extent streptomycin, inhibited both the ribosome-stimulated ATPase activity of native RbbA as well as the ability of RbbA to simulate polyphenylalanine synthesis (Ganoza & Kiel, 2001; Kiel & Ganoza, 2001). RbbA was found to bind to EF-Tu based on pull-down assays, which was suggested to provide a regulatory mechanism for the delivery of amino-acyl tRNA (Kiel & Ganoza, 2001); eEF-3 fulfills a similar role and has been shown to bind eEF-1α (Anand et al., 2006). Interestingly, factor "W" was deemed to be a truncated version of RbbA, despite lacking ribosome-dependent ATPase activity, and no cross-reactivity experiments with anti-eEF-3 antibodies were performed (Ganoza et al., 2002).

Recently the purification of a truncated form of RbbA of approximately 61 kDa has been reported by the same group. It was derived from *E. coli* overexpressing recombinant RbbA (Xu et al., 2006). Based on mass spectrometry data, this protein was found to be truncated at proline 541, possibly due to a proteolytic cleavage (Xu et al., 2006). This truncated RbbA (RbbAtrc) was found to be more readily expressed and more stable. Interestingly, this truncation also possessed the same ribosome-stimulated ATPase activity as the wild-type and recombinant full-length protein. In addition, the truncated RbbA was able to stimulate poly(U)-directed polyphenylalanine synthesis, as well as the release of deacyl-tRNA from the ribosomal E-site (Xu et al., 2006). Based on a chemical protection mapping of rRNA on 70S *E. coli* ribosomes in the presence of RbbA, it was shown that this protein protects 16S rRNA residues A915, A937, and A949 located near the ribosomal E-site, on the 30S subunit (Xu et al., 2006).

35

2.3.4 Emerging Roles for ATP in Translation

While ATP has been known to have a role in protein synthesis since the 1950s, research in the role of ATP and ATP binding proteins has not proceeded as studies on the essential translation GTPases have. Aside from eIF-4A, an ATP-dependent RNA helicase responsible for removing secondary structure from mRNA during initiation, and eEF-3, very little is known about the role of ATP-dependent processes during translation. However, recent research has shown that these factors may play a larger role in protein synthesis than expected. For example, the GTPase eEF-2 is known to be responsible for translocation of mRNA and tRNA within the ribosome. In addition, eEF-2 has a role during termination, where RRF and eEF-2 break apart the 80S ribosome (See section 2.1.3). Interestingly, Demeshkina and colleagues recently reported that in the presence of ATP, eEF-2 can break apart 80S eukaryotic ribosomes (Demeshkina et al., 2007).

Additional ribosome-associated ATPases of various classes have been identified, including NVL2, a mammalian nucleolar AAA+ ATPase that interacts with the ribosomal protein L5 (Nagahama et al., 2004) and Prp43p, a DEAH box helicase that functions in ribosome biogenesis (Leeds et al., 2006). Based on sucrose-density gradient centrifugation experiments, Andersen and Leevers have recently shown that in *Drosophila*, the ABC transporter Pixie binds to 40S ribosomes in an ATP-dependent manner (Andersen & Leevers, 2007). This protein is the fly ortholog of human RNase L inhibitor, which plays a role in initiation and in ribosome biogenesis (Andersen & Leevers, 2007). Pixie can also be purified in complex with eIF-3 components, binds to

ribosomal proteins RpS17 and RpS25, and when depleted by dsRNAi, causes a decrease

in production of several eIF-3 components.

Chapter 3 – Materials and Methods

3.1 Materials

All chemicals were obtained from VWR, Sigma, or Invitrogen, unless otherwise specified. Restriction enzymes were from Fermentas (except *Bsa*I from New England Biolabs); all other enzymes were purchased as described in the following sections. PCR primers, nucleotides, and fluorescent nucleotide derivatives were purchased from Invitrogen. Radiochemicals were purchased from Perkin-Elmer. Small-scale plasmid preparations were performed by kit preparation (EZ spin column plasmid DNA kit, BioBasic).

3.2 Molecular Biology

3.2.1 Cloning of ORF yhih

Genomic DNA was isolated from a 25 mL overnight culture of *E. coli* strain DH5α. Cells collected by centrifugation at 4 ℃ for 5 min at 5000 xg and resuspended in 8 mL buffer TES (50 mM Tris-Cl pH 7.5, 10 mM NaCl, 10 mM EDTA) and opened by incubation at 37 ℃ for 1 h with 5 mg lysozyme (EMD BioSciences) and proteinase K (Invitrogen). 4 mL of 4M ammonium acetate was added to the solution, which was then incubated at room temperature for 10 min. Following the addition of 4 mL of 1:1 phenol:chloroform, the mixture was centrifuged at 4 ℃ for 2 min at 5000 xg. Two more phenol:chloroform extractions were performed and an equal volume of isopropanol was added, followed by incubation at -20 ℃ for 10 min. Precipitated DNA was separated by centrifugation for 5 min at 5000 xg at 4 ℃. The resulting DNA pellet was air dried at

room temperature and resuspended in 1 mL of 0.1 M ammonium acetate. 1 mL of 70 % ethanol was added to reprecipitate DNA followed by incubation at -20 ºC. Precipitated DNA was collected by centrifugation for 5 min at 5000 xg at 4 ºC, resuspended in 200 μL buffer TES, and stored at -20 ºC.

Open reading frame *yhih* was PCR amplified from *E. coli* genomic DNA using the *yhih* cloning primers (Table 4) reported by Ganoza and colleagues (Kiel et al., 1999). The PCR reaction was catalyzed by Phusion polymerase (Finnzymes). PCR components are listed in Table 5; cycle conditions are listed in Table 6. The resulting 2.7 kbp PCR product was subsequently purified by agarose gel electrophoresis, excised from low-melting point agarose (Fermentas) followed by gel extraction (MinElute PCR Purification Kit, Qiagen).

Purified PCR product was ligated (T4 DNA ligase, Invitrogen) into *Sma*I digested pUC19 in the presence of the restriction endonuclease. The ligation mixture was transformed into sub-cloning efficiency chemically competent *E. coli* DH5α (Invitrogen) by heat shock: 10% (v/v) ligation mixture was added to competent cells. Transformation mixtures were incubated on ice for 30 min, followed by a 45 s heat shock at 42 ºC and 2 min incubation on ice. 500 μL LB media was added and cells were incubated at 37 ºC for 1 h prior to plating cells on LB-agar plates supplemented with 50 μg/mL ampicillin (BioBasic) and 50 μg/mL X-GAL (Rose Scientific). Recombinant plasmids, designated pUC*yhih*, were confirmed by agarose gel electrophoresis, restriction analysis, and DNA sequencing (University of Calgary DNA Services).

Larger quantities of plasmid DNA for further cloning procedures were isolated by growing *E. coli* strain DH5α containing the desired plasmid in LB containing 50 μg/mL

ampicillin for pUC19 plasmids and derivatives and 25 μg/mL kanamycin for pET28a plasmids and derivatives. 200 mL of overnight culture were pelleted by centrifugation for 10 min at 5000 xg at 4 ºC and resuspended in 3 mL alkaline lysis solution I (25 mM Tris-Cl pH 8.0, 50 mM glucose, 10 mM EDTA, 10 μg RNAse A). Cells were lysed with 5 mg lysozyme at room temperature for 10 min, followed by addition of 6 mL alkaline lysis solution II (0.2 M NaOH, 1 % SDS). The lysed cell solution was incubated at room temperature for 10 min and neutralized by addition of alkaline lysis solution III (2 M acetic acid, 3 M potassium acetate). Following incubation on ice for 10 min, cell debris was pelleted by centrifugation (see above). Three 1:1 phenol/chloroform extractions (4 mL each) were performed on the aqueous supernatant; 60 % volume of isopropanol was added and the mixture was incubated at -20 ºC for 15 min. Precipitated DNA was centrifuged, washed with 1 mL 70 % ethanol, dried, and resuspended in 200 μL water. Isolated pDNA was characterized by agarose gel electrophoresis and stored at -20 ºC. If contaminated with RNA, plasmid samples were digested at 37 ºC with RNAse A for 2 h.

ORF *yhih* was excised from pUC*yhih* by restriction digestion with *Bam*HI *Hind*III*,* and *Bsa*I (*Bsa*I further digested pUC19 background vector), and, followed by gel purification. The *yhih* open reading frame was then ligated into *Bam*HI and *Hind*III digested pET28a, transformed into *E. coli* DH5α and plated on LB-agar-kanamycin plates. Sequence, gene orientation, and reading frame were confirmed by DNA sequencing (University of Calgary DNA Services).

3.2.2 Mutagenesis

Site-directed mutagenesis was performed by the Quik-change mutagenesis protocol (Stratagene) using the respective primers listed in Table 4. PCR components and cycle conditions are given in Tables 5 and 6 respectively. After digestion of template DNA with *Dpn*I at 37 ºC for 2 h, reactions were heat inactivated at 80 ºC for 15 min. 10% (v/v) mutagenesis reactions were then transformed into *E. coli* strain NEB5α (New England Biolabs) or DH10B (Invitrogen). Mutations were confirmed by restriction analysis where possible and DNA sequencing.

Table 4: Primers used for cloning and mutagenesis of *yhih*

Primer name	Sequence (5' - 3')	Description	T_M (ºC)
yhih **cloning sense**	gc**g gat cc**c agc att atg gaa aaa ccg ttg	Cloning primer, *Bam*HI site introduced	90.0*
yhih **cloning antisense**	cg**a agc tt**g taa atg gcg cat cat ccc tcc	Cloning primer, *Hind*III site introduced	92.0*
yhih **sequencing forward**	ttc gac tgg ctg gta gcg atg at	Sequencing primer	68.0*
yhih **sequencing reverse**	cgt cga tcc aga cgc cga g	Sequencing primer	66.0*
yhih **K299L sense**	tcg aac ggc tgc **ggt ctc** tcc acc acc atg aaa	K to L mutation, *Bsa*I site introduced	75.8†
yhih **K299L antisense**	ttt cat ggt ggt gga **gag acc** gca gcc gtt cga	K to L mutation, *Bsa*I site introduced	75.8†
yhih **P541opal sense**	gaa ctg cga cgc gat tga gta cg**g tcg ac**g ctg	Nonsense mutation, *Sal*I site introduced	80.0†
yhih **P541opal antisense**	cag c**gt cga c**cg tac tca atc gcg tcg cag ttc	Nonsense mutation, *Sal*I site introduced	80.0†
yhih **L432amber sense**	gcg cga gag **gtc gac** cat cta ctg cct gaa cat atc	Nonsense mutation, *Sal*I site introduced	78.4†
yhih **L432amber antisense**	gat atg ttc agg cag tcg atg **gtc gac** ctc tcg cgc	Nonsense mutation, *Sal*I site introduced	78.4†

Bold, underlined bases represent restriction sites
* Calculated by $T_M = 4(G+C) + 2(A+T)$
† Calculated by $T_M = 81.5 + 0.41(\%GC) - 675/N - (\%\ mismatch)$; N = number of bases

Table 5: PCR components

Component	*yhih* PCR amplification	pET*yhih* mutagenesis
Template*	500 ng	200 ng
Primers	25 pmol	25 pmol
10X buffer	1 X Phusion GC	1 X *Pfu* buffer
dNTPs	10 pmol	7.5 pmol
Polymerase	0.5 units Phusion	7.5 units *Pfu*
Distilled water	To 50 µL	To 25 µL

* Amplification template was *E. coli* genomic DNA; mutagenesis template was plasmid pET*yhih*.

Table 6: PCR cycling conditions

Description	*yhih* PCR amplification	pET*yhih* mutagenesis
Initial Denaturation	95 ºC, 1 min	95 ºC, 5 min
Denaturation	95 ºC, 20 s	95 ºC, 1 min
Annealing	60 ºC, 30 s	72 ºC, 1 min
Extension	72 ºC, 3 min	68 ºC, 20 min
Final extension	None	68 ºC, 20 min
Number of cycles	30	18

3.3 Expression and Detection

3.3.1 Expression

Plasmids pET*yhih*, pET*yhih* K315L, pET*yhih* ΔP541opal, pET*yhih* ΔL432amber, and pET*yhih* ΔL665ochre were transformed into *E. coli* strain BL21-DE3 (Invitrogen). Selected colonies were grown overnight in LB medium (10 % bacto-tryptone, 5 % yeast extract, 10 % NaCl) supplemented with 25 μg/mL kanamycin (phosphate supplemented media contained LB media with 0.2 % Na_2HPO_4 and 0.1 % KH_2PO_4). Cultures were used to inoculate fresh LB-kanamycin media with cells to an OD_{600} ~ 0.1. Cultures were grown at 37 ºC and induced at an OD_{600} ~ 0.6 with 1 mM isopropyl-β-D-thiogalactopyranoside (ITPG). After induction, cultures were grown at 30 ºC until the late logarithmic growth phase was reached and subsequently harvested by centrifugation (5000 xg, 10 min). 1 OD samples were taken every 30 minutes to monitor protein expression by SDS-PAGE and Western blot analysis. Cell pellets were flash frozen and stored at -80 ºC until use.

3.3.2 SDS-PAGE

Cells from the 1 OD expression samples were collected by centrifugation at 15800 xg for 1 min. The resulting cell pellets were then lysed in 100 μL lysis buffer (50 mM Tris-Cl pH 7.5 at 4 ºC, 30 mM KCl, 70 mM NH_4Cl, 7 mM $MgCl_2$, 8 M urea) for 1 h and subsequently centrifuged at 15800 xg for 5 min. 10 μL samples were analyzed on discontinuous SDS-PAGE gels consisting of a 5% stacking gels and 10 – 15% resolving gels, depending on the size of the expressed protein. Gels were run at 200 V for 1 h (Mini

PROTEAN 3 system, BioRad) and stained with Coomassie blue. All further SDS-PAGE gels run during purification procedures were run in a similar fashion.

3.3.3 Western blotting

Proteins were separated on a 12% SDS-PAGE gel and transferred onto a nitrocellulose membrane (BioTrace NT pure nitrocellulose transfer membrane, Pall Corporation) at 150 mA for 2 h at 4 ℃ in transfer buffer (48 mM Tris-Cl pH9.2, 39 mM glycine, 0.037% SDS). Transfer was confirmed by staining with Ponceau S. Membranes were then washed with TBS (10 mM Tris-Cl pH 7.5, 150 mM NaCl) to remove Ponceau S. The nitrocellulose membrane was blocked for 1 h at room temperature (blocking buffer: TBS with 3% (w/v) fat free dried milk powder), followed by incubation with a 1:100 dilution (in blocking buffer) of mouse monoclonal His-probe antibody (Santa Cruz Biotechnology) for 2.5 h at 4 ℃. Samples were washed with TTBS (20 mM Tris-Cl pH 7.5, 500 mM NaCl, 0.05% Tween-20, 0.2% Triton X-100) twice and once with TBS. A 1:1000 dilution (in blocking buffer) of goat anti-mouse horseradish peroxidase conjugate antibody (Santa Cruz Biotechnology) was used to detect the primary antibody for 1 h at 22℃. The nitrocellulose membrane was washed twice with TTBS and once with TBS. Staining was performed by incubating the membrane with 0.05% 3,3'-diaminobenzidine (DAB) with 0.03% $NiSO_4$, 0.03% $CoCl_2$, and 0.1% H_2O_2 in TBS.

3.4 Purification and Refolding

Previously frozen cells were thawed on ice and lysed in 7 mL lysis buffer (50 mM Tris-Cl pH 7.5 at 4 ℃, 30 mM KCl, 70 mM NH_4Cl, 7 mM $MgCl_2$, 7 mM β-mEtOH, 8 M urea) per gram of cells. The obtained lysate was centrifuged at 20000 xg for 45 min at

4ºC. The resulting cleared lysate was applied to a 5 mL Ni^{2+} sepharose column (XK-16 column, Amersham; Ni^{2+} Sepharose, Amersham) using LKB p-500 pumps (Pharmacia) and washed with lysis buffer until a baseline OD_{280} was reached. The column was then washed with 5 column volumes (25 mL) lysis buffer containing 10 mM imidazole and similarly with lysis buffer containing 20 mM imidazole. 6X-His tagged proteins were eluted from the Ni^{2+} sepharose column using a 200 mL imidazole gradient (final concentration of 250 mM). Fractions were collected using a LKB FRAC-100 fraction collector (Pharmacia). The FPLC was controlled by FPLC director v1.0 (Pharmacia). Collected fractions were analyzed by SDS-PAGE.

Fractions containing the respective protein were pooled and diluted to a concentration of 0.5 μM with elution buffer and refolded overnight at room temperature by dialyzing with refolding buffer (50 mM Tris-Cl pH 7.5 at 4 ºC, 30 mM KCl, 70 mM NH_4Cl, 7 mM $MgCl_2$, 7 mM β-mEtOH, 50 mM L-Arg, 20% v/v glycerol, 50 μM ADP). The refolded protein was then concentrated using a Vivaspin 20 mL concentrator (10000 MWCO, Sartorius) centrifuged at 5000 xg followed by size exclusion chromatography (XK-10/300 GL superdex-75 column, Pharmacia) equilibrated in refolding buffer. Fractions containing protein were identified by UV absorbance at 280 nm and SDS-PAGE. Fractions containing ΔP541 Yhih or ΔL432 Yhih were pooled and concentrated to 17.5 μM and 32.1 μM respectively. Aliquots of purified protein were flash frozen in liquid nitrogen and stored at -80 ºC prior to use. Protein concentrations were determined photometrically at 280 nm using a molar extinction coefficient of 46785 $M^{-1}cm^{-1}$ and 38180 $M^{-1}cm^{-1}$ for mutants ΔP541 Yhih and ΔL432 Yhih respectively (calculated based on amino acid sequences using the software ProtParam (Gasteiger et al., 2005)).

3.5 Fluorescence techniques

3.5.1 Direct tryptophan fluorescence titrations

Relative fluorescence measurements were performed on a Varian Cary Eclipse Fluorescence Spectrophotometer. The intrinsic tryptophan fluorescence (six Trp residues in ΔP541 Yhih, five in ΔL432 Yhih) was excited at 295 nm, to minimize nucleotide absorption ($\lambda_{max,\ Adenosine}$ = 259 nm), in 0.3 cm x 0.3 cm quartz cells (Starna) at room temperature. Fluorescence measurements were carried out with 10 μM protein in refolding buffer lacking ADP. The fluorescence was monitored from 305-405 nm through 5 nm slits. The change in fluorescence (ΔFl) at 343 nm upon addition of nucleotide was determined by subtracting background fluorescence of Yhih (Fl_{Yhih}) and nucleotide (Fl_{nt}) from the fluorescence of the Yhih-nucleotide complex, $Fl_{complex}$ (Equation 1). Fluorescence values were adjusted with respect to changes in protein concentration upon substrate addition. Fluorescence change (ΔFl) was then plotted against nucleotide concentration ([nt]) and fitted to a hyperbolic function (Equation 2), with respect to the initial (ΔFl_0) and maximum fluorescence (ΔFl_{max}), to determine the dissociation constant (K_D) for each nucleotide using the software TableCurve (Jandel Scientific). Titrations were performed with GDP, GTP, ADP, ATP, and 2'- (or 3')-O-(N-methylanthraniloyl)-adenosine derivatives (mant-ADP and mant-ATP).

$$\Delta Fl = Fl_{complex} - Fl_{Yhih} - Fl_{nt} \qquad\qquad (1)$$

$$\Delta Fl = \Delta Fl_0 + (\Delta Fl_{max} * [nt]) / (K_D + [nt]) \qquad\qquad (2)$$
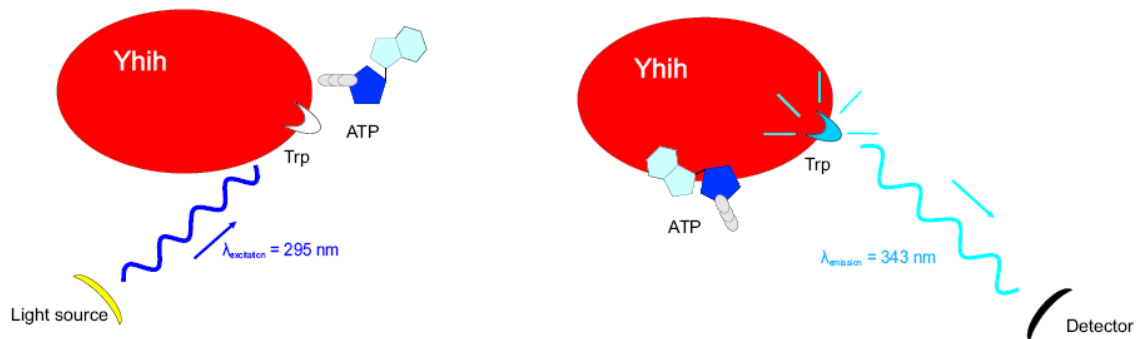
Figure 19: Direct tryptophan fluorescence titration assay with ATP.

Tryptophan residues in ΔP541 and ΔL432 Yhih were excited at 295 nm in the presence of nucleotide. Upon binding to one (or both) of the putative ATP binding sites, the Trp emission was monitored from 305 to 405 nm (λ_{max} = 343 nm). The location of the ATP binding sites is relative to tryptophan residues is not known, as no structural information is currently available.

3.5.2 Fluorescence resonance energy transfer (FRET)

Fluorescence resonance energy transfer from tryptophan residues to the mant group of mant-ATP or mant-ADP was monitored by nucleotide titration as described in section 3.4.1, except fluorescence was monitored from 305-605 nm. The observed concentration dependence in the FRET signals were analyzed using equation 2.
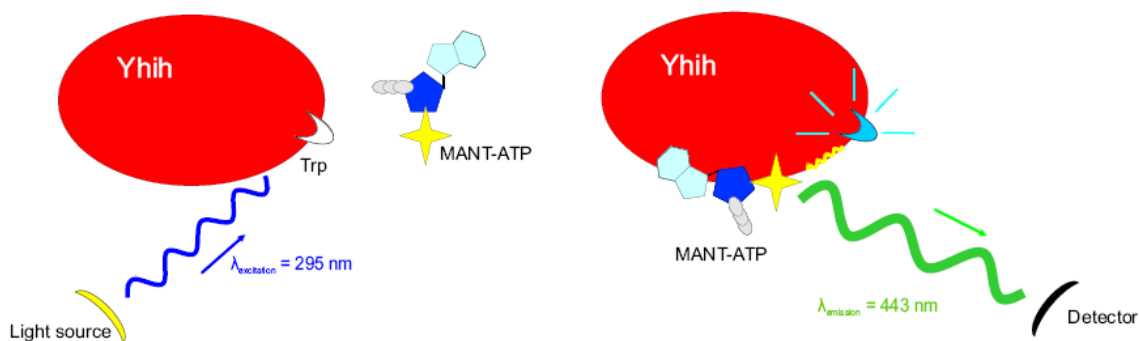
Figure 20: FRET titration assay with mant-ATP.

Tryptophan residues in ΔP541 and ΔL432 Yhih were excited at 295 nm in the presence of mant-nucleotide. Upon binding to one (or both) of the putative ATP binding sites, the Trp emission was monitored from 305 to 600 nm (λ_{max} = 443 nm). The location of the ATP binding sites is relative to tryptophan residues is not known, as no structural information is currently available.

3.6 ATPase assays

Hydrolysis of ATP by Yhih was monitored by observing the liberation of [^{32}P$_i$] from γ-[^{32}P]-ATP. ATP charging solution (960 μM γ-[^{32}-P]-ATP at ~100 dpm/pmol, 0.25 μg/μL pyruvate kinase (PK), 3 mM phosphoenolpyruvate (PEP)) and Yhih charging solution (16.8 μM protein, 0.25 μg/μL PK, 3 mM PEP) were incubated at 37 ºC for 15 minutes to catalyze ATP formation from ADP. ATPase assays were carried out in buffer TAKM$_7$ (50 mM Tris-Cl pH7.5 at 4 ºC, 30 mM KCl, 70 mM NH$_4$Cl, 7 mM MgCl$_2$). Reaction volumes were 60 μL. Reactions contained 7500 pmol γ-[^{32}-P]-ATP, 60 pmol Yhih, and varying amounts of 70S ribosomes, 50S and 30S ribosomal subunits. 5 μL samples were removed and quenched in 50 μL 1M HClO$_4$ with 3 mM K$_2$HPO$_4$.

Following the addition of 300 μL 20 mM Na$_2$MoO$_4$ and 400 μL isopropyl acetate, samples were mixed for ~30 s and centrifuged at 15800 xg for 5 min. [^{32}P$_i$] was extracted

49

as a phosphate-molybdate complex in the organic phase, added to 2 mL of EcoLite scintillation cocktail (EcoLite, MP Biomedical), and counted in a Perkin-Elmer Tri-Carb 2800TR liquid scintillation analyzer. Background radioactivity was subtracted. Background hydrolyzed ATP by 30S ribosomal subunits was subtracted in reactions containing 30S ribosomal subunits.

3.7 Stopped-flow kinetics

The dissociation rate of mant-ATP from ΔP541 Yhih was determined using a KinTek SF-2004 Stopped-flow apparatus. Prior to experiments, ΔP541 Yhih was charged with mant-ATP (1 μM Yhih was incubated with 10 μM mant-ATP, 0.01 μg/μL PK and 3 mM PEP at 37 ºC for 15 min). Tryptophan residues were excited at 295 nm; fluorescence emission from the mant group was monitored after passing through 400 nm cut off filters. Experiments were performed at 20 ºC by rapidly mixing 25 μL from syringes loaded with A) Yhih•mant-ATP and B) ATP (100 μM, incubated with PK and PEP). The change in fluorescence was monitored over time and fitted according to an one exponential function (Equation 3; k_{app} is the apparent rate of nucleotide exchange, A is signal amplitude, F is fluorescence at time t, and F_∞ is the final fluorescence signal).

$$F = F_\infty + A \exp(-k_{app}t) \qquad\qquad (3)$$

Chapter 4 – Results

4.1 Yhih is a homolog of eEF-3

The *E. coli* protein Yhih has been suggested by Kiel and Ganoza to be a homolog of the yeast factor eEF-3 based on the cross-reactivity of RbbA with polyclonal anti-eEF-3 antibodies and a generated sequence alignment between the open reading frames of *E. coli* Yhih and eEF-3 from *S. cerevisiae* (Kiel et al., 1999). Both proteins exhibit a ribosome-dependent ATPase activity (also observed in the presence of 30S ribosomal subunits) (Kiel et al., 1999; Kiel & Ganoza, 2001; Xu et al., 2006). The sequence alignment proposed in 1999 shows that the N-terminus of Yhih (603 of 894 amino acids) and the C-terminus of eEF-3 (736 of 1044 amino acids) are 22% identical (40% similar) and share the Walker A and B motifs (responsible for ATP binding), as well as the ABC signature motif (Kiel et al., 1999). Accounting for the ATP binding motifs, the proteins are 19 % identical and 37% similar. With the crystal structure and domain assignment of eEF-3 available (Andersen et al., 2006), a more in depth analysis is now possible. According to the domain alignment given by Andersen and colleagues (Andersen et al., 2006), the ABC domain 2 of eEF-3 is interrupted by a chromodomain. A new domain alignment needed to be generated that takes into account the presence of the chromodomain, which is not a homolog to any region in Yhih (Figure 22).

```
            440           *         460          *        480          *         500        *
RbbA : -----MSQHYGKTVALNNITIDIPARCMVGLIGPIGVGKSSLISLISGARVIEQGNVMVIGGDMRDEKHRRDVGPRIAWMPQGIGK :  81
EF-3 : LCNCEFSLAYGAKIILNKTQIRIKRARRYGICGPNGGGKSTLM------RAIANG--QVDG----FET--QEBG-RTVYVEHDI-- : 498
          S   YG  6 LN    L 6        G6 GP1G GKS3L6          R I G     V G        P     C R  56   6

          520          *          540         *         560          *         580         *         600
RbbA : NLYHILSVYENVDF-EARLFGHDKAEFEVRINELILTSTGIAPFRDREAGKLSGGMKCKIGICCALIHIPEILILDEPTIGVDPISR : 166
EF-3 : LGTHSDISV--LDFVEESGVGTKEAIRDKLIEFGFIDEMIA----MEISALSGGWKMKIALARAVIRNADILILLDEPTNHIDTYNV : 578
         1  H3 3     6DF F     G   A 4   I  T    6A      P   LSGG K KL L   A66 1    6L6LDEPT   6D 6

            *        620          *        640          *        660          *         680
RbbA : SQFWDIIDSIRQRQSNMSVLVAIAYMEEAERGDWLVAMNAGEVLATGSAEBLRQQTQSATLEEAFINILIPQAQRCAHQAVVIPPYC : 252
EF-3 : A--WLVNYLNTCGIISITISHDGSVFLDNVCEYIINYEGLKLRKYKGNFTDFVKKCPAAKAYEELSNTDIEFKFPEPGYLEGVKTKC : 662
          W  6         3 636   3 56     5           E  64        EE   L    2        6  Q

          *        700          *         720          *         740          *        760          *
RbbA : PENAEIAIEARDLTMRFGSFVAYDHVNERIPRGEIFGFLGSNGGGKSTTYKMLTG-LLPASBGEAYLFGQPVIPKDIDTRRRVGYM : 337
EF-3 : KAIVKVTNMEFQYPG--TSKPQITDINFQCSLSSRIAVIGPNGAGKSTLLNVLTGBLLPTS-GEVYT---HEN-------QRIAYI : 735
          6            S    6  6NF          6G NG GKST 6 6LTG LLP S  GE 5        1         R6 Y6

          780          *        800          *         820          *        840          *        860
RbbA : SG-ABSLYNELTVRQNIELHARLEH--------------------------------------------------------------- : 361
EF-3 : KQHABAHIESHLDKTPSEYIQWREQTGEDRETMDRANRQINENDAEAMNKIFKIEGTPRRIAGIHSRRKFKNTYEYECSFLLGENI : 821
         Q AF        4   E       F

              *        880          *        900          *         920          *         940
RbbA : ----------------------------------------IPEAEIPARVAEMSERFKINDVEDILPES----LPIGIRQRISIA : 402
EF-3 : GMKSERWVPMMSVDNAWIPRGELVESHSKMVAEVDMKEALASGGFRPLTRKEIEEHCSMI--GLIDPEIVSHSRIRGISGGQKVKIV : 905
                                                 2       R         L   D   S      L    Q46 L

            *        960          *         980          *        1000          *        1020         *
RbbA : VA--VIHRPEMLILDEPTSGVDPVARDMFWQLKVDLSRQDKVTIFISTHFMNEAERCDRISLMHAGKVIASGTPQEIVEKRGAASI : 486
EF-3 : LAAGTWQRPHLIVLDEPTNYLIRDSLGALSKAIKEFEGG--VIII-I-THSAEFTKNLTEEVWAVKDGRMTPSGHNWVSGQGAGPRI : 987
         6A      RP 666LDEPT  6D       6         V II  TH        6      6       6          6

          1040          *         1060         *        1080          *        1100          *       11
RbbA : EEAFIAYLQEAAGQSNEAEAPPVVHDITIHAPRQGFSIRRLFSYSRREALELRRDPVRSTLALMGTVILMLIMGYGISMDVENLRFA : 572
EF-3 : EKKEDEEDKFDAMGNKIAGGKKKKKLSSAELRKKKKBRMKKKKELGDAYVSSDEEF----------------------------- : 1043
         E         A    A      33     R    R        A
```

Figure 21: Alignment between the N-terminus of Yhih (RbbA) and eEF-3.

E. coli Yhih (RbbA) was aligned with *S. cerevisiae* eEF-3 (EF-3) using ClustalW. Identical amino acids are colored black; similar amino acids in grey. The numbers below similar amino acids are as follows: 1 (D, N); 2 (E, Q); 3 (S, T); 4 (R, K); 5 (F, Y, W) and 6 (L, I, V, M). The C-terminus of Yhih is not shown.
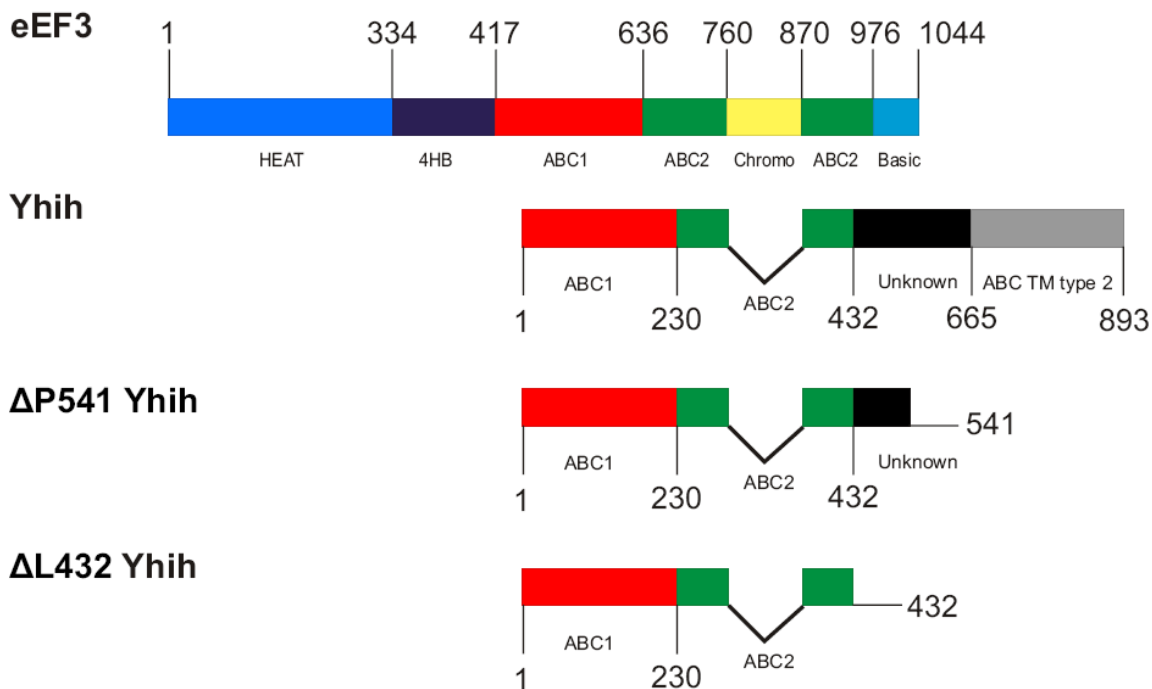
Figure 22: Graphical domain alignment of eEF-3, Yhih, and Yhih mutants.

The putative domains of Yhih and Yhih mutants were aligned based on their sequence similarity. The Huntington, Elongation factor 3, PR65/A, TOR (HEAT) domain is shown in light blue next to the 4-helical bundle domain (dark blue). ATP binding cassette domains (ABC) are shown in red and green. The chromatin remodeling domain (chromo) is shown in yellow, followed by the basic N-terminus. Unknown domains in Yhih and truncated Yhih are shown in black, and the putative transmembrane domain (based on sequence similarity to known transmembrane regions) is shown in grey. Residue numbers based on the *E. coli* numbering are indicated.

The homologous ABC1 domains of both eEF-3 and Yhih are 229 and 230 residues respectively. The unknown domain in Yhih is not homologous to any region of eEF-3. When this unknown domain is compared to known protein sequences using the Basic Local Alignment and Search Tool (BLAST) in a non-redundant *E. coli* database, only putative ABC transporter domains are identified. Interestingly, both the chromodomain in eEF-3 and unknown domain have no significant sequence similarity,

although they both contain regions of basic amino acids interspersed between hydrophobic residues, which in chromatin remodeling domains interact with RNA. Kiel and Ganoza noted that these regions share an ELVE motif (Kiel et al., 1999), which is also found in helix D of EF-Tu and interacts with the nucleotide exchange factor EF-Ts as well as ribosomal factors L7/L12 (Kawashima et al., 1996; Wieden et al., 2002). This motif may have a similar role in interacting with ribosomal proteins; thus, the unknown domain of Yhih may have a similar role to the eEF-3 chromodomain in binding to the ribosome. The putative ABC transmembrane domain, was identified based on amino acids similarity to other α-helical ABC transmembrane domains in the ABC-2 integral membrane protein family. Structurally, this region consists of numerous α-helices inserted into the membrane of bacteria; it may be similar to the helical HEAT domain and interact with the ribosome.

4.2 Identification of a homolog of Yhih

BLAST searches within protein databases using Yhih as a query protein have identified a homolog of *yhih*, encoded by the hypothetical open reading frame *ybhf* in *E. coli*. The predicted protein product of this ORF is 578 amino acids long (67 kDa), possesses similar features to Yhih (Figure 23), including two putative ABC domains, a 73 residue subdomain that interrupts the two ABC domains and that is 17% identical (31% similar) to the chromodomain of eEF-3 (Figure 24), followed by an unknown domain that is 34% identical and 53% similar to the unknown domain of Yhih. Overall, the two proteins share about 34% identity and 46% similar amino acids. Ybhf lacks a putative transmembrane domain, or any potential α-helical regions that are present in eEF-3 or

Yhih. This gene does exist within the putative ybhGFSR operon, in which the ORFs *ybhs* and *ybhr* encode putative ABC transmembrane domain similar to that found in the C-terminus of *yhih*; thus Ybhf may be expressed in tandem with these helical proteins. Based on sequence similarity to Yhih, it is possible that Ybhf also has some similar role during translation. Therefore, this protein makes an ideal target for future research. The study of the *ybhs* and *ybhr* -encoded proteins may determine some role for the homologous structure in Yhih.
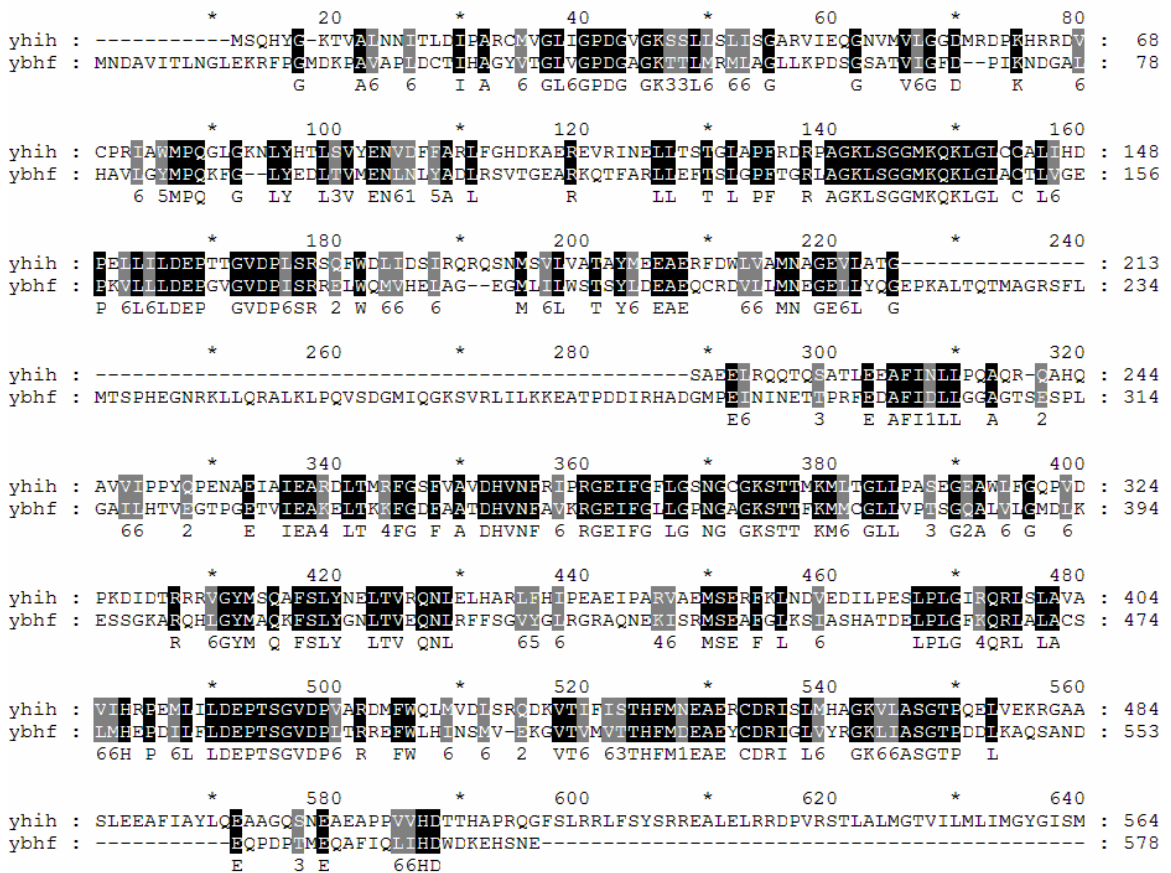

Figure 23: Sequence alignment of Yhih with Ybhf.

The sequence of *E. coli* Yhih was aligned with the predicted amino acid sequence of *E. coli* open reading frame Ybhf using ClustalW. Identical amino acids are colored black;

similar amino acids in grey. The numbers below similar amino acids follow the scheme in figure 21.


```
                    *         20         *         40         *         60
ybhf    : ----------------PKALTCTMAGRSFIMTSP------HEGNRKLLQRALKLPQVSDGMIQGKSVR :  46
chrcmo  : QTGEDRETMDRANRQINENDABAMNKIFKIEGTPRRIAGIHSRRKFKNTYEYECSFLLGENIGMKSER :  68
                            2 M       6   3P        H   4              6     I  KS R

              *         80         *         100        *
ybhf    : LILLKKEATPDDIFR-----HADGMPEININET--------- :  72
chrcmo  : WVPMMSVDNAWIPRGELVESHSKMVAEVDMKEALASGQFRPL : 110
              6           I R      H    6 E616 E
```

Figure 24: Alignment of the putative chromodomain of Ybhf with eEF-3.

The putative chromodomain of Ybhf was aligned with the chromodomain (residues 760-870) of eEF-3 (chromo). Identical amino acids are colored black; similar amino acids in grey. The numbers below similar amino acids follow the scheme in figure 21.
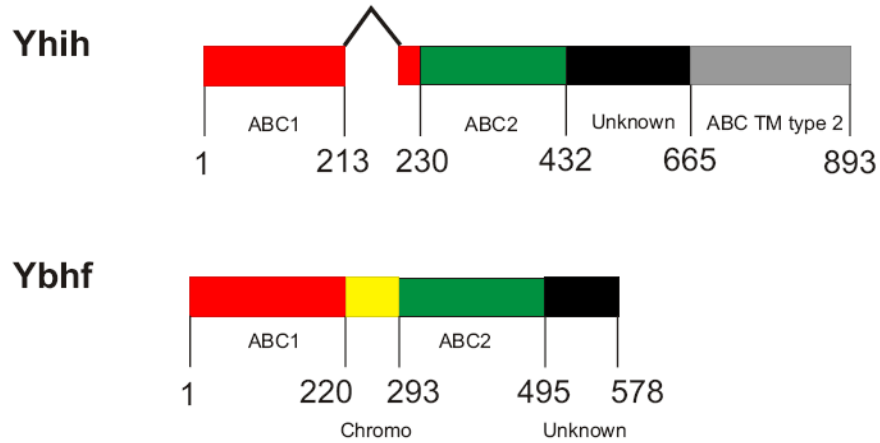

Figure 25: Proposed domain alignment between Yhih and Ybhf.

Putative domains of *E. coli* Yhih and Ybhf were aligned based on the sequence alignments in figures 23 and 24. The color scheme is the same as those in Figure 21. Residue numbers are indicated.

56

4.3 Overexpression of Yhih and Yhih mutants

The effect of expression of recombinant proteins in *E. coli* can initially be monitored by observing the effect expression has on bacterial growth. Expression of toxic proteins often suppresses growth, and this is often a complication with expressing mammalian factors in a bacterial system, particularly those with transmembrane domains (Inoue et al., 2000). Thus it is important to monitor the growth of cells expressing transmembrane proteins. Figure 26 shows that *E. coli* BL21-DE3 harboring no plasmid showed a typical bacterial growth curve with distinct lag, logarithmic growth, and stationary phases with a final $OD_{600} \sim 4.3$. BL21-DE3 containing pET*yhih* followed a similar pattern, though cells reached the stationary phase earlier and at a lower cell density ($OD_{600} \sim 3.5$). BL21-DE3 pET*yhih*, upon induction with 1 mM IPTG, reached the stationary phase within 1 h and growth ceased at an $OD_{600} \sim 1.0$. After diluting cultures 10 fold upon reaching the stationary phase, both BL21-DE3 and the uninduced culture containing the plasmid resumed growth, while the induced culture did not. Overnight growth revealed that the induced culture resumed growth; though the maximum optical density ($OD_{600} \sim 2.3$) was significantly lower than either BL21-DE3 or the uninduced culture with pET*yhih*. Therefore, expression of wild-type pET*yhih* blocked bacterial growth upon induction with IPTG.
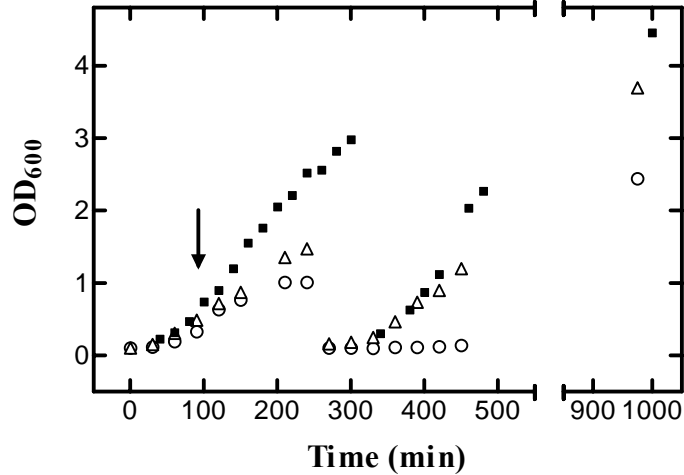
Figure 26: Growth curve of *E. coli* BL21-DE3 containing pET*yhih*.

The growth of *E. coli* BL21-DE3 (squares) or BL21-DE3 containing plasmid pET*yhih* (open triangles, uninduced; or open diamonds, IPTG induced) was monitored by measuring optical density at 600 nm. Cultures were diluted 10 fold upon reaching the stationary phase. Induction is indicated (↓).

In addition to blocking bacterial growth, no protein overexpression was detected by either SDS-PAGE or Western blot. In response to this, several mutants were constructed in an effort to reduce cellular toxicity. Inoue et al (2002) have reported that in addition to proteins containing transmembrane domains, those containing ATP binding domains can also suppress growth in *E. coli* (Inoue et al., 2000). The mutant pET*yhih* K299L was generated in response to the possibility that expression of the ATPase activity may influence cellular processes; lysine 299 is part of the conserved Walker A motif that is involved in phosphate binding and Mg^{2+} coordination. Mutations to this conserved lysine in eEF-3 have been shown to disturb growth in yeast and disrupt ATP binding and hydrolysis by eEF-3 (Yang et al., 1996). Nonsense mutants pET*yhih* P541opal and L432amber were constructed in order to delete regions of the C-terminus of Yhih in an

58

effort to reduce both the size of the protein and remove the putative transmembrane domain.

Cells containing the pET*yhih* K299L plasmid, when induced, exhibit a similar growth compared to that of cells induced to express the wild-type protein (Figure 27). Cells expressing the truncated forms of Yhih, ΔP541 and ΔL432 Yhih, exhibited a growth pattern comparable to *E. coli* BL21-DE3 lacking plasmid (Figure 27). Cells expressing these truncated proteins, however, show an indistinct logarithmic growth phase. The final optical densities reached comparable levels (OD_{600} ~ 4 and 4.3 for mutant-expressing strains and BL21-DE3 lacking plasmid respectively).
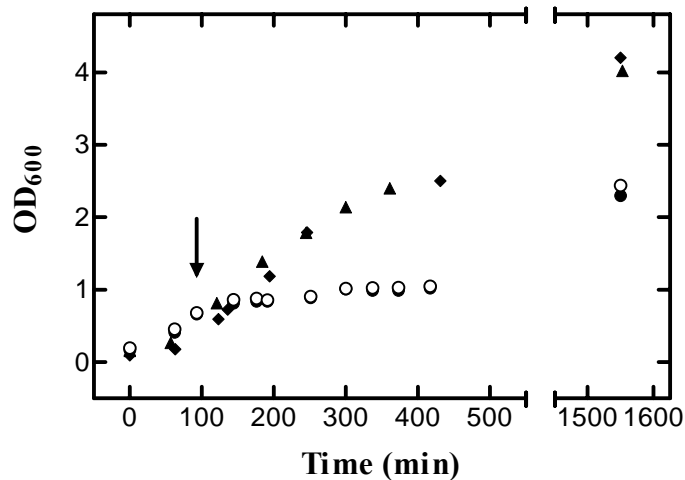

Figure 27: Growth curve of *E. coli* BL21-DE3 containing pET*yhih* mutants.

The growth of *E. coli* BL21-DE3 containing plasmid pET*yhih* (open circles), pET*yhih* K299L (closed circles), pET*yhih* P541opal (closed triangles), and pET*yhih* L432amber (closed diamonds) was monitored by measuring optical density at 600 nm. Induction is indicated (↓).

SDS-PAGE and Western blot analysis of samples taken from BL21-DE3 cells containing pET*yhih* and pET*yhih* K299L prior to and post induction revealed no differential protein expression. Expression samples of pET*yhih* P541opal and L432amber show the differential expression of 65 and 51 kDa proteins respectively (Figure 28 A and B) when lysed under denaturing conditions with 8M urea; these proteins were not present when cells were opened under non-denaturing conditions with 10 mg/mL lysozyme. Expression of ΔP541 Yhih from cells containing the pET*yhih* P541opal plasmid was confirmed by western blot using antibodies specific for the 6x His tag epitope. Figure 29 shows the expression of a single 6x His-tagged protein occurs post induction, with no detectable expression in cell lysate prior to addition of IPTG.

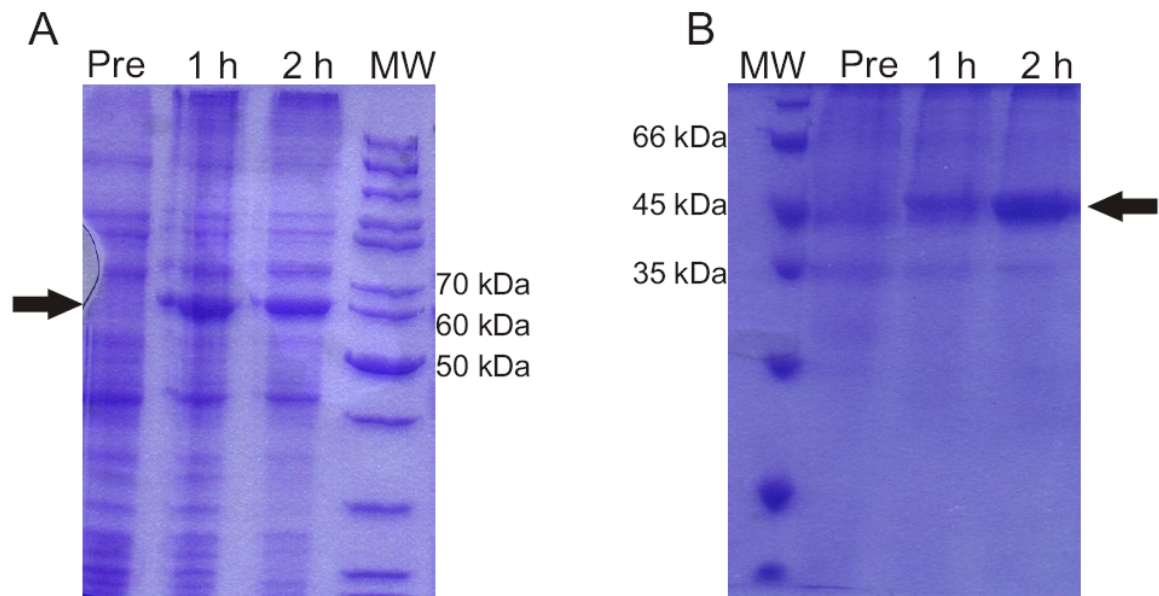**Figure 28: Overexpression of ΔP541 Yhih and ΔL432 Yhih.**

Overexpression of (A) ΔP541 Yhih and (B) ΔL432 Yhih. Equal amounts of urea cell lysate before (Pre) and post induction were loaded on 12 and 15% SDS-PAGE gels. Molecular weights (MW) are indicated.
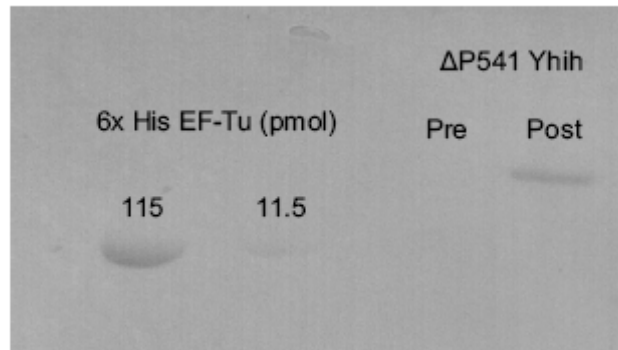
Figure 29: Western blot detection of 6x His-tagged ΔP541 Yhih.

ΔP541 Yhih from urea cell lysates was detected pre- and post-IPTG induction. 6x His-tagged EF-Tu was used as a control.

As *E. coli* harboring the pET*yhih* P541opal and L432amber plasmids express ΔP541 and ΔL432 Yhih as insoluble inclusion bodies, expression conditions were optimized by altering induction conditions (IPTG concentration, cell density at induction, growth temperature, media composition, presence of the pLysS plasmid for regulation of expression). The addition of phosphate to bacterial growth media has previously been shown to aid in the production of soluble *E. coli* MalK, a maltose transporter (Schneider et al., 1995). Interestingly, growth of cells expressing ΔP541 and ΔL432 Yhih in a phosphate-supplemented media resulted in increased cell density (Figure 30); however, despite optimizing expression, none of the explored conditions reduced the toxicity of wild-type Yhih nor resulted in the production of soluble protein for any of the mutants.
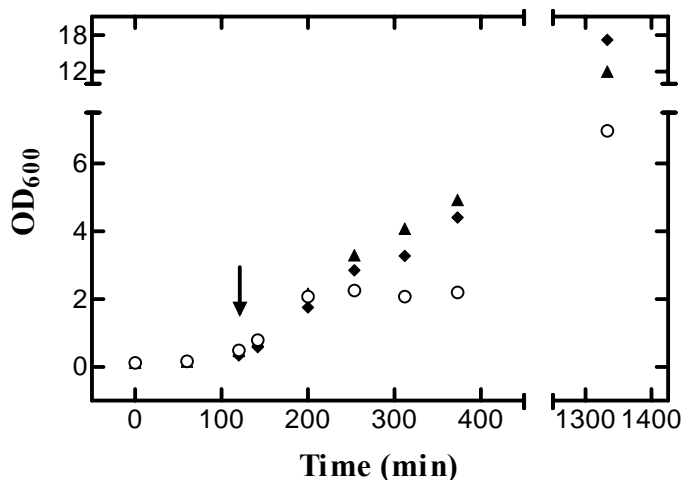
Figure 30: Growth of *yhih*-expressing cells in phosphate-supplemented LB.

The growth of *E. coli* BL21-DE3 containing plasmid pET*yhih* (open circles), pET*yhih* P541opal (closed triangles), and pET*yhih* L432amber (closed diamonds) in phosphate-supplemented LB media was monitored by measuring optical density at 600 nm. Induction is indicated ($\downarrow$).

4.2 Purification and Refolding of ΔP541 and ΔL432 Yhih

To study the structure and function of the proteins expressed by pET*yhih* P541opal and L432amber, these proteins were purified by affinity chromatography. The pET28a plasmid used as an expression system adds a 6x His tag on the N-terminus of recombinant proteins, making an Ni^{2+} affinity resin an ideal matrix for purifying these proteins. These proteins were bound to a 5 mL Ni^{2+} sepharose column under denaturing conditions and eluted by increasing concentration of imidazole. The elution profiles (determined by absorbance at 280 nm) of ΔP541 Yhih and ΔL432 Yhih from the affinity column are shown in figures 31 and 32 respectively. SDS-PAGE analysis of the elution fractions shows that the majority of His-tagged proteins remain bound to the column after washing with lysis buffer. Elution occurred for both proteins at an imidazole

62

concentration of approximately 25 mM. Fractions containing eluted ΔP541 Yhih were contaminated by low molecular mass proteins that were removed by size exclusion chromatography. ΔL432 Yhih was pooled and refolded without further purification.
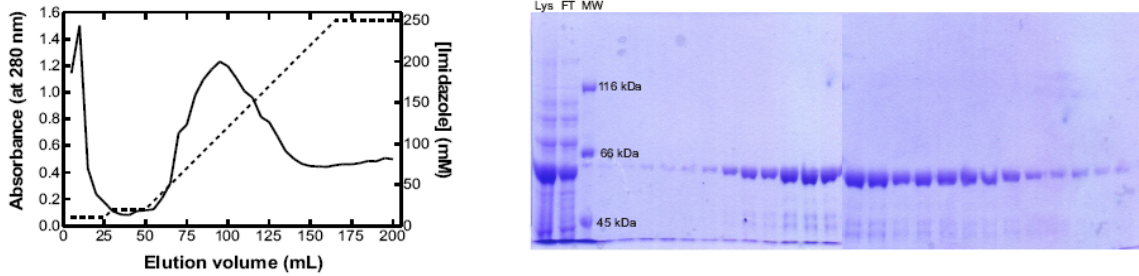
Figure 31: Purification of ΔP541 Yhih by Ni^{2+} sepharose affinity chromatography.

Left: A$_{280}$ elution profile of ΔP541 Yhih. Right: SDS-PAGE analysis of fractions ΔP541 Yhih, starting at fractions containing 25 mM imidazole. Lys, lysate bound to the Ni^{2+} sepharose column; FT, flow through after baseline wash with lysis buffer. Molecular masses (MW) are indicated.
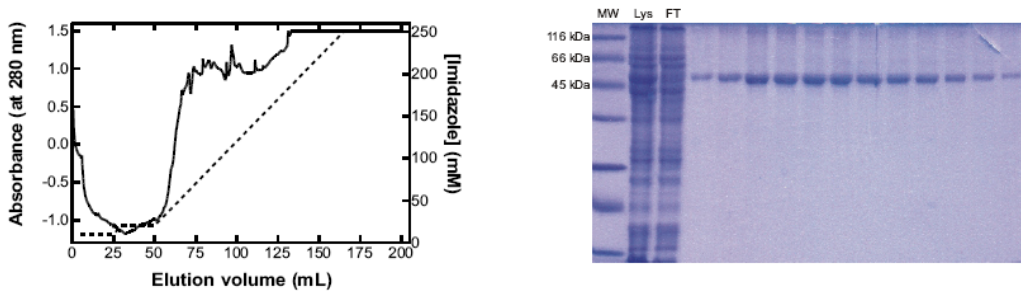
Figure 32: Purification of ΔL432 Yhih by Ni^{2+} sepharose affinity chromatography.

Left: A$_{280}$ elution profile of ΔL432 Yhih. Right: SDS-PAGE analysis of fractions ΔL432 Yhih, starting at fractions containing 25 mM imidazole. Lys, lysate bound to the Ni^{2+} sepharose column; FT, flow through after baseline wash with lysis buffer. Molecular masses (MW) are indicated. A maximum A$_{280}$ was observed due to an improper baseline setting.

As the truncated Yhih proteins were purified under denaturing conditions, they must be refolded into a functional conformation prior to any subsequent study. Numerous

protein refolding methods have been reported in the literature, such as simple dilution and pulse dilution into a non-denaturing buffer (Vallejo & Rinas, 2004; Swietnicki, 2006), dialysis (Vallejo & Rinas, 2004; Swietnicki, 2006), chaperone-mediated refolding (Vallejo & Rinas, 2004; Ario de Marco, 2007), and chromatographic techniques (Vallejo & Rinas, 2004; Swietnicki, 2006). Of these, chaperone-mediated refolding is the most expensive and thus impractical; pulse dilution and simple dilution are rapid techniques that do not allow proteins to refold more slowly through finding the most stable (and presumably correct) conformation.

The ABC transporter MalK from *Salmonella typhimurium* has been successfully refolded using chromatography by binding the denatured protein to a red agarose column, removing the urea present in the cell lysis buffer, and eluting the refolded protein (Walter et al., 1992). Therefore, a similar experiment was attempted with ΔP541 Yhih using the Ni^{2+} sepharose affinity column as a support, providing a "scaffold" (the column bound 6x His tag) to facilitate correct refolding. However, upon removal of urea through a gradient wash (8M to no urea) and subsequent elution by addition of imidazole, no protein could be eluted from the column, possibly due to the precipitation of the protein. Addition of imidazole under denaturing conditions caused ΔP541 Yhih to elute.

Dialysis of ΔP541 Yhih against refolding buffer, while resulting in aggregation of significant amounts of protein (61% of protein aggregated), yielded some soluble protein. The components of the refolding buffer (50 mM Tris-Cl pH 7.5 at 4 °C, 30 mM KCl, 70 mM NH_4Cl, 7 mM $MgCl_2$, 7 mM β-mEtOH, 50 mM L-Arg, 20% v/v glycerol, 50 μM ADP) were chosen based on several considerations: ΔP541 Yhih was found to be more

soluble in low salt conditions, as determined by small-scale dialysis experiments altering salt concentrations. The presence of 50 mM L-Arg and glycerol have been shown to improve protein solubility and stability, and facilitate protein refolding (Rariy & Klibanov, 1997; Golovanov et al., 2004; Vallejo & Rinas, 2004; Arakawa et al., 2007a; Arakawa et al., 2007b). L-Arginine in particular has been used as an inexpensive aid in protein refolding as the amino acids acts as a chaotropic agent (similar to guanidine hydrochloride, though L-Arg does not denature the protein) (Arakawa et al., 2007a; Arakawa et al., 2007b). Most recently, L-Arg has been used to suppress aggregation of recombinant mink and porcine growth hormones (Bajorunaite E., 2007). β-mEtOH was added as a disulfide reducing agent; the crystal structure of eEF-3 from *S. cerevisiae* shows that no disulifide bridges are present in the protein (Andersen et al., 2006), suggesting Yhih may not have essential disulfide bridges. Mg^{2+} is a required cofactor for ATP binding proteins that is essential for ATP hydrolysis and nucleotide binding; ADP was added in the dialysis buffer at 100 fold excess over the amount of protein refolded (0.5 μM) in an effort to facilitate refolding in a substrate-dependent manner.

Protein samples were dialyzed at room temperature over two days to encourage refolding proteins to reach the global energy minimum. Final urea concentrations were approximately 30 mM. SDS-PAGE analysis of the refolded protein showed no change in molecular mass, suggesting no degradation occurred during the refolding process. During the refolding process, significant amounts of both ΔP541 and ΔL432 Yhih precipitated. Refolding yields for the dialysis experiment were 39% (ΔP541 Yhih) and 27% (ΔL432 Yhih) (Table 7). Proteins were concentrated until precipitate formation was observed;

maximum solubility was 17.5 μM and 32.1 μM for ΔP541 Yhih and ΔL432 Yhih respectively (Table 7).

Table 7: Summary of Yhih purification.

Protein	Yield	Solubility
ΔP541 Yhih	39 %	17.5 μM
ΔL342 Yhih	27 %	32.1 μM

4.3 Fluorescence studies on Yhih

Refolding of recombinant proteins is a poorly understood process. As such, the activity of refolded proteins must be examined. If ΔP541 and ΔL432 Yhih are active and the refolding process yielded functional protein, it should bind ADP and/or ATP. Fluorescence techniques such as direct tryptophan excitation and FRET have been successfully used previously to characterize the adenine nucleotide binding properties of other ABC transporters, such as the oleandomycin transporter OleB from *Streptomyces antibiotics* (Buche et al., 1997) and the *E. coli* protein YjeE (Allali-Hassani et al., 2004).

4.3.1 Direct tryptophan fluorescence

Initial characterization of ΔP541 and ΔL432 Yhih was performed using the intrinsic tryptophan fluorescence to determine the affinity of the proteins for ADP, ATP, GDP, and GTP. The addition of ATP to ΔP541 Yhih resulted in an increase in tryptophan fluorescence, that was dependent on the concentration of the respective nucleotide (Figure 33, panel A); titration of the protein with ADP caused a decrease of the tryptophan fluorescence signal (Figure 33, panel C). Concentration-dependent fluorescence changes at 343 nm and calculated dissociation constants are shown in panels B and D for ATP and ADP respectively. The affinity of ΔP541 Yhih for ATP (K_D = 150 μM) is approximately 7.5 fold greater than the affinity for ADP (K_D = 21 μM).

Figure 33: Titration of ΔP541 Yhih with ATP and ADP.

ΔP541 Yhih was titrated with increasing amounts of ATP (A) and ADP (C). The changes in relative fluorescence at 343 nm were plotted as a function of nucleotide concentration, from which dissociation constants (K_D) were calculated (panels B and D for ATP and ADP respectively). Nucleotide concentrations are shown on a color scale (bottom, center).

Addition of ATP and ADP to ΔL432 Yhih caused a decrease of the tryptophan fluorescence signal (Figure 34, panels A and C for ATP and ADP respectively). Calculated affinities were similar for both nucleotides (151 μM and 127 μM for ADP and ATP respectively). Interestingly, addition of ATP caused an initial fluorescence increase, after which the addition of increasing amount of nucleotide caused a quenching of the signal. Neither ΔL432 Yhih nor ΔP541 Yhih showed a change in tryptophan fluorescence upon addition of GTP and GDP, suggesting truncated Yhih proteins do not bind guanine nucleotides (data not shown). That Yhih does not bind guanine nucleotide cannot be confirmed, since at higher concentrations of guanine nucleotide, binding may occur. The fluorescence titration of other guanine nucleotide binding proteins with GDP or GTP is usually not performed, as the affinity of GTPases for guanine nucleotides is often too great to use this technique to measure dissociation constants (Ahmadian et al., 2002). Dissociation constants for ADP and ATP are summarized in Table 8 at the end of this chapter.
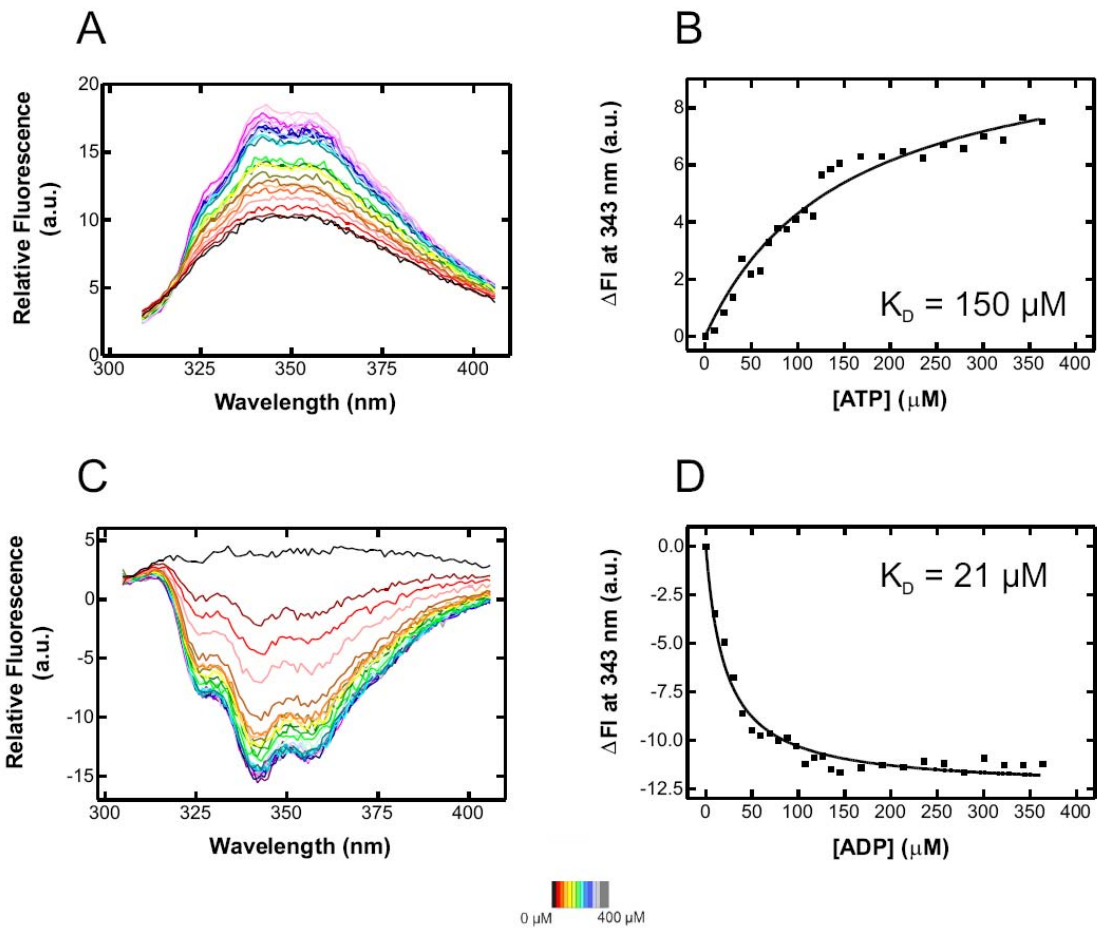
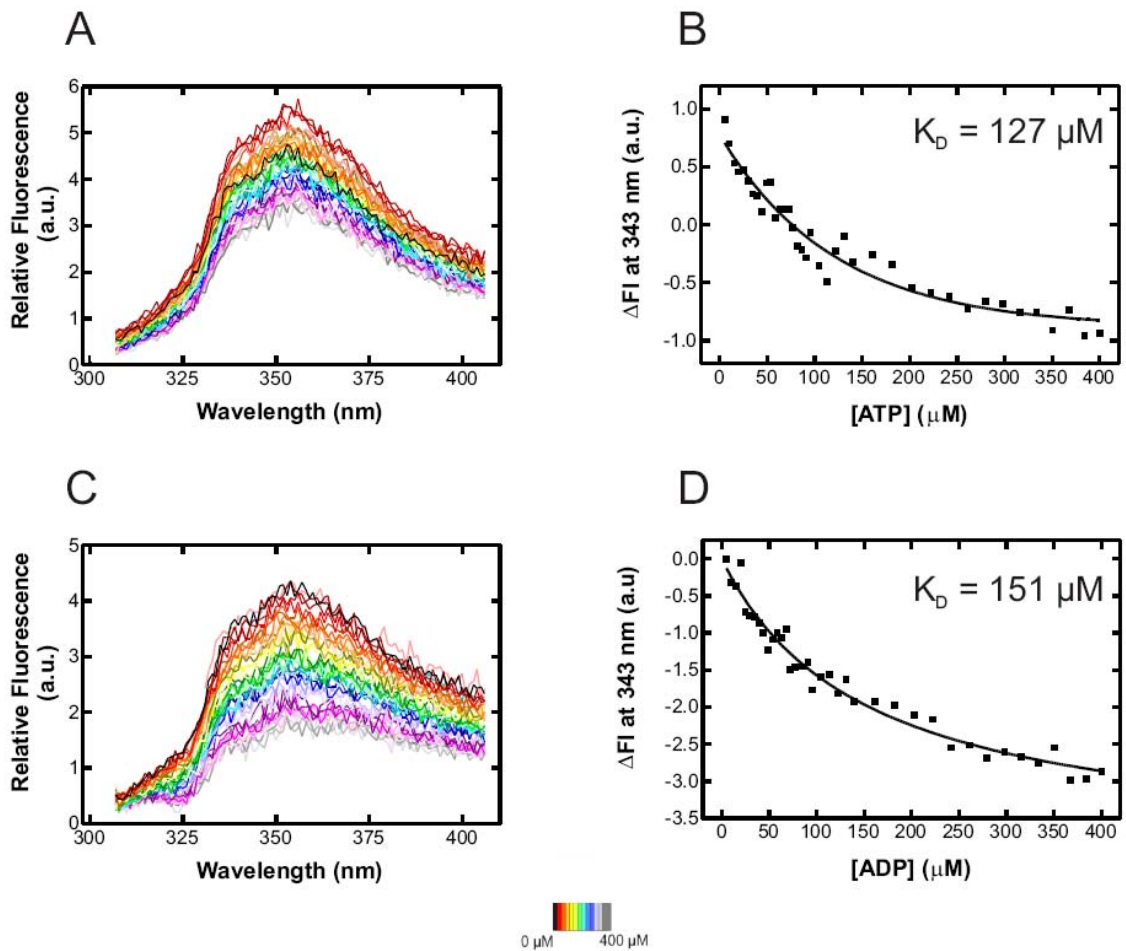**Figure 34: Titration of ΔL432 Yhih with ATP and ADP.**

ΔL432 Yhih was titrated with increasing amounts of ATP (A) and ADP (C). The changes in relative fluorescence at 343 nm were plotted as a function of nucleotide concentration, from which dissociation constants (K_D) were calculated (panels B and D for ATP and ADP respectively). Nucleotide concentrations are shown on a color scale (bottom, center).

4.3.2 Titration of Yhih with mant-nucleotides

Previous studies have successfully used FRET between an endogenous tryptophan residue and the mant group of mant-nucleotides to study nucleotide binding properties (K_D, $k_{association}$, $k_{dissociation}$) (Gromadski et al., 2002; Wieden et al., 2002). This approach would provide a better fluorescence signal/noise ratio, and confirm nucleotide binding if FRET is observed. The tryptophan fluorescence emission (λ_{max} = 343 nm) is suitable to excite the mant group ($\lambda_{excitation, max}$ = 356 nm; $\lambda_{emission}$ = 448 nm), while the emission signals of tryptophan and the mant group do not overlap.

Upon addition of both mant-ATP and mant-ADP to ΔP541 Yhih (Figures 35 and 36), a decrease in the tryptophan fluorescence signal (region I, panel B) and an increase in the mant fluorescence signal (region II, panel C) was observed. The decrease in the tryptophan signal was approximately 4 fold with respect to the initial fluorescence of the system. Interestingly, the dissociation constants for ATP and mant-ATP were comparable (150 μM and 208 μM respectively), while the dissociation constants for ADP and mant-ADP differed by ~8 fold (21 μM and 171 μM respectively). Since the proteins did bind guanine nucleotides, mant-GDP and mant-GTP titrations were not performed.
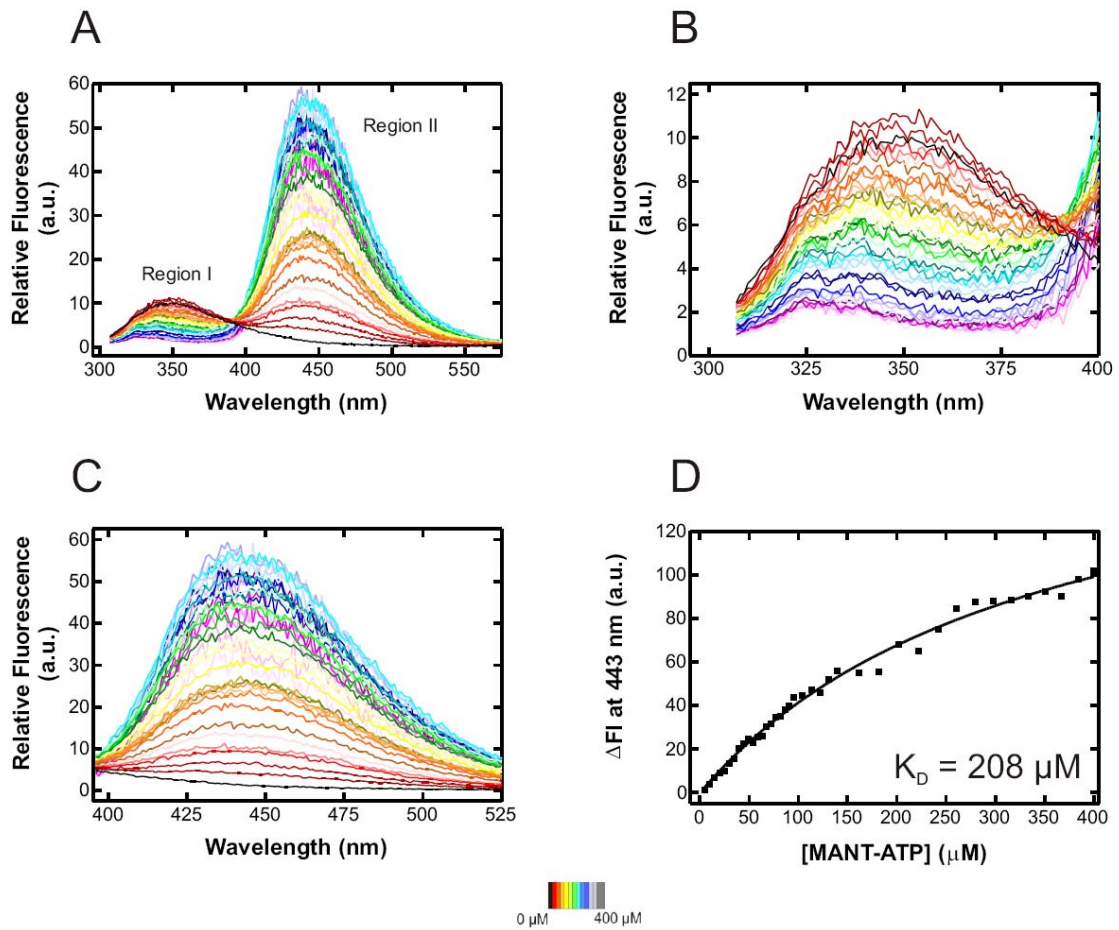
Figure 35: Titration of ΔP541 Yhih with mant-ATP.

(A) Fluorescence signal of ΔP541 Yhih upon addition of mant-ATP. The fluorescence signal from region I (tryptophan fluorescence) and region II (mant fluorescence) are shown in greater detail in panels B and C respectively. The change in mant fluorescence at 443 nm was plotted as a function of nucleotide concentration, from which dissociation constants (K_D) were calculated (panel D). Concentrations are indicated by the color scheme provided.
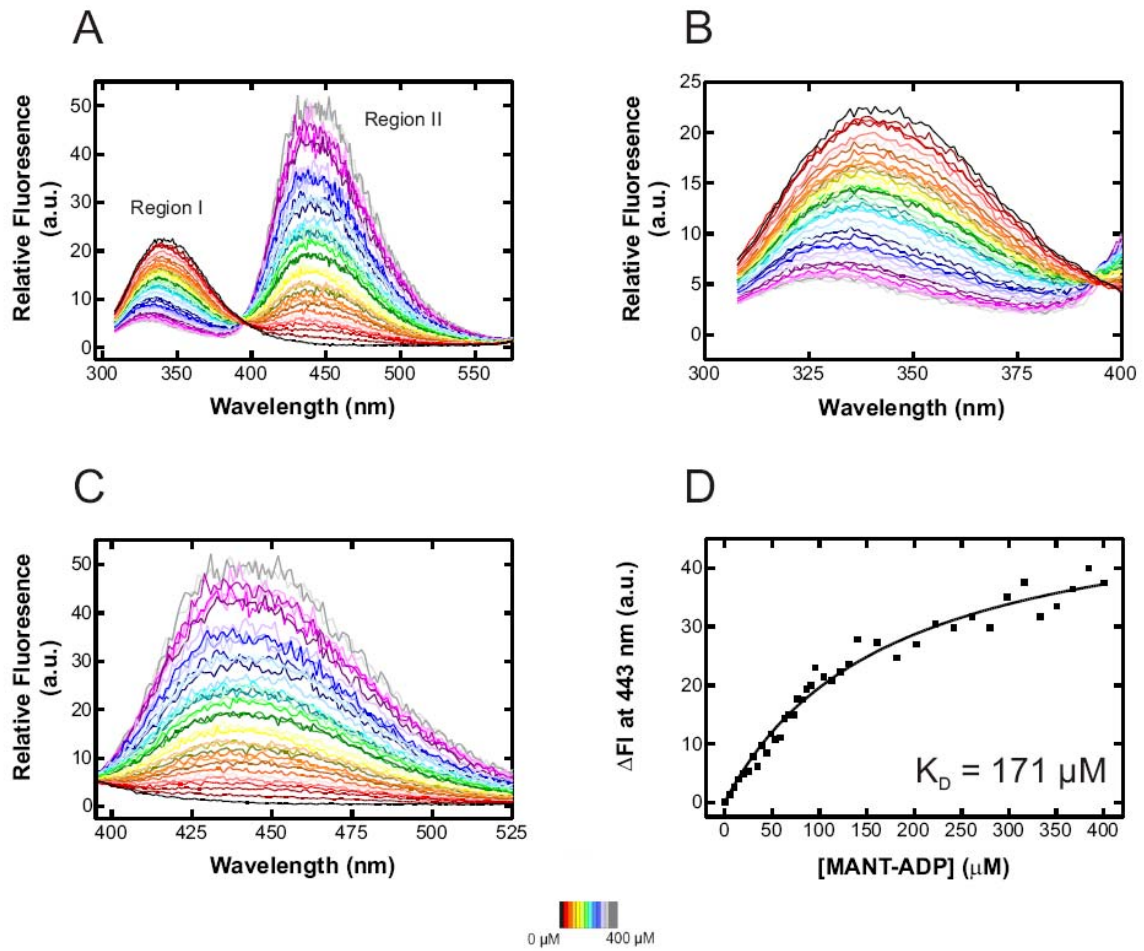
Figure 36: Titration of ΔP541 Yhih with mant-ADP.

(A) Fluorescence signal of ΔP541 Yhih upon addition of mant-ADP. The fluorescence signal from region I (tryptophan fluorescence) and region II (mant fluorescence) are shown in greater detail in panels B and C respectively. The change in mant fluorescence at 443 nm was plotted as a function of nucleotide concentration, from which dissociation constants (K_D) were calculated (panel D). Concentrations are indicated by the color scheme provided.

Interestingly, upon titration of ΔL432 Yhih with mant-ATP (Figure 37), no FRET was observed: the tryptophan fluorescence signal (Figure 37 A, region I) did not change upon addition of nucleotide. In fact, a quenching of the mant fluorescence signal (Figure 37, panel B) was observed. No FRET was observed; therefore, the dissociation constant for the binding of mant-ATP to ΔL432 Yhih cannot be calculated. However, FRET was observed upon addition of mant-ADP (Figure 38, panel A); the tryptophan fluorescence signal decreased (panel B) and the mant fluorescence signal increased (panel C). Based on this experiment, the dissociation constant was calculated as described above (panel D) as 157 μM, comparable to that of ΔP541 Yhih (171 μM).
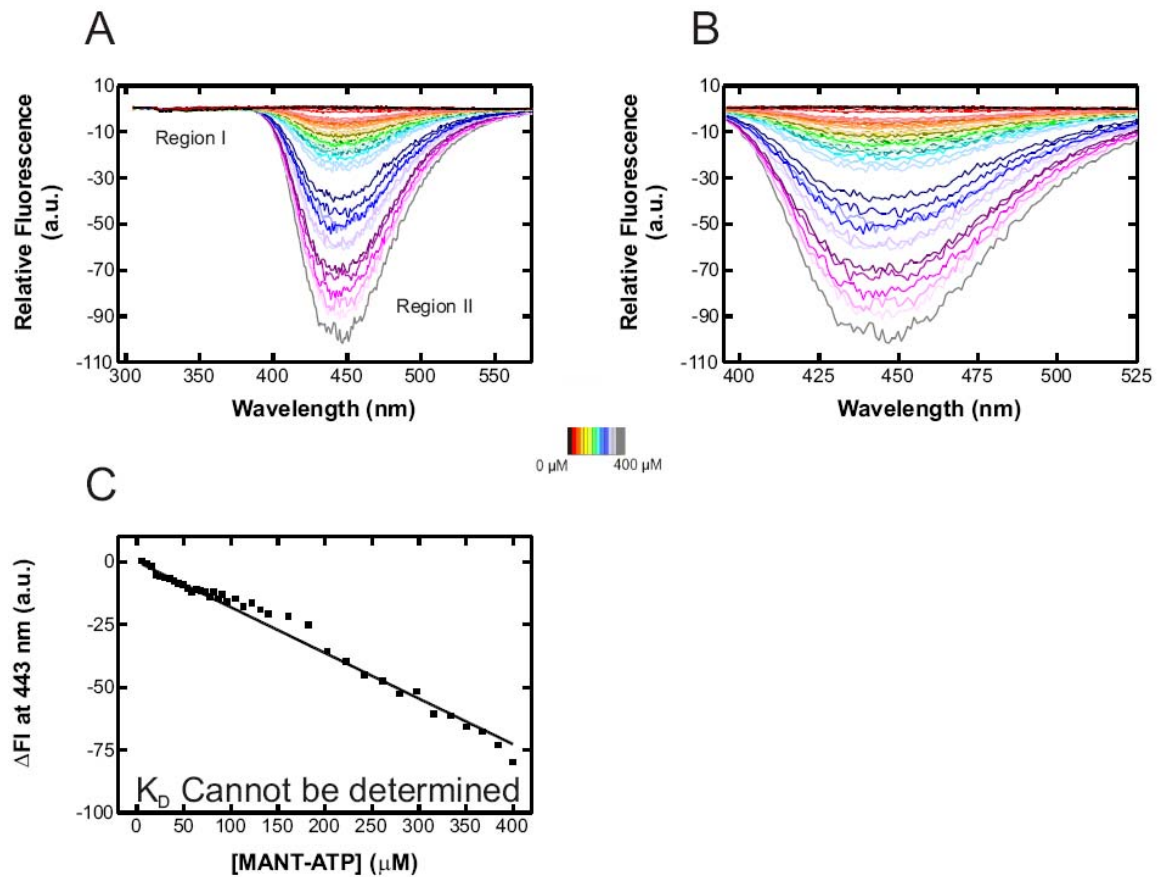
Figure 37: Titration of ΔL432 Yhih with mant-ATP.

(A) Fluorescence signal of ΔL432 Yhih upon addition of mant-ATP. No fluorescence change was observed in region I; region II (mant fluorescence) is shown in greater detail in panel B. The change in mant fluorescence at 443 nm was plotted as a function of nucleotide concentration (panel C). Concentrations are indicated by the color scheme provided.
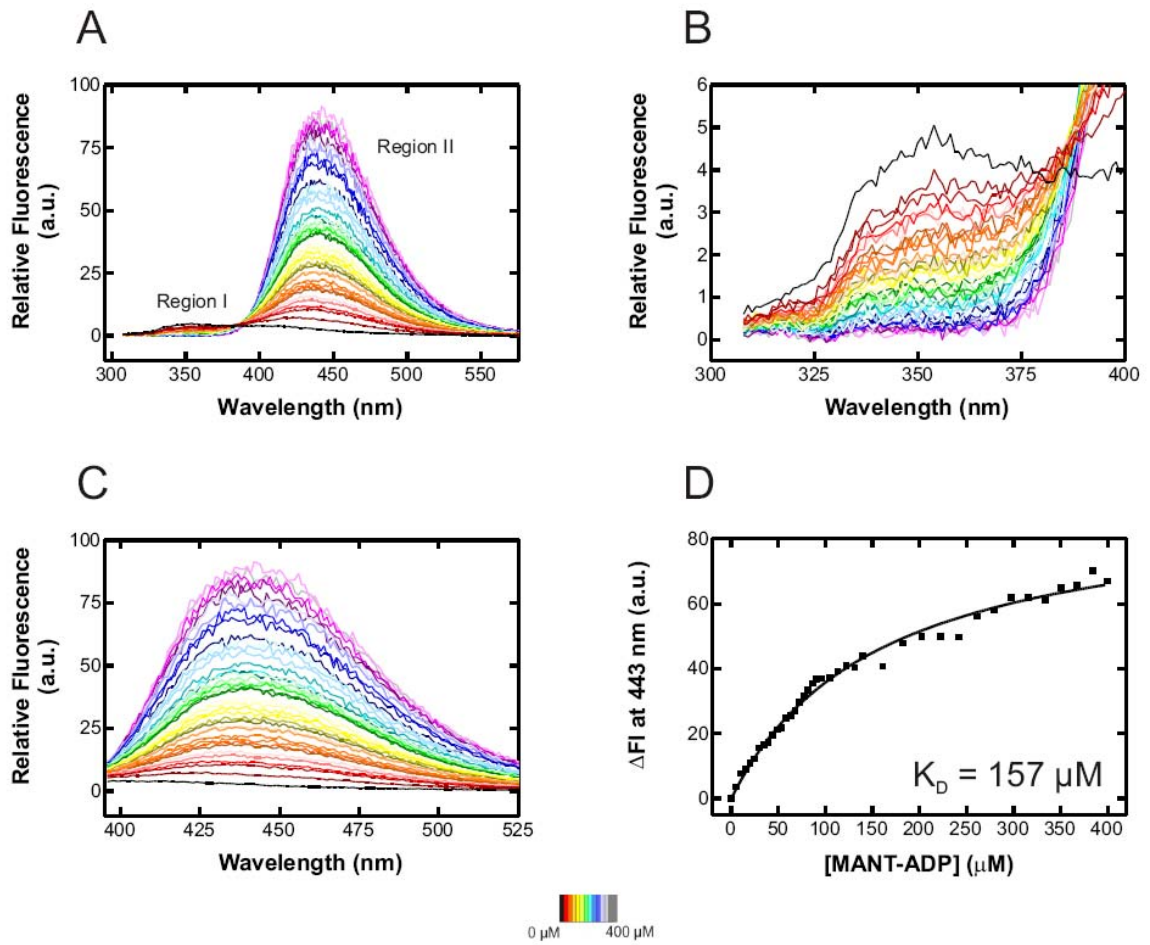
Figure 38: Titration of ΔL432 Yhih with mant-ADP.

(A) Fluorescence signal of ΔL432 Yhih upon addition of mant-ADP. The fluorescence signal from region I (tryptophan fluorescence) and region II (mant fluorescence) are shown in greater detail in panels B and C respectively. The change in mant fluorescence at 443 nm was plotted as a function of nucleotide concentration, from which dissociation constants (K_D) were calculated (panel D). Concentrations are indicated by the color scheme provided.

Based on the steady state FRET experiments using mant-nucleotides, it was determined that the mant group makes a suitable fluorescent tag for studying the pre-steady state kinetics of ΔP541 Yhih. However, the dissociation constant for mant-ADP, which is ~ 10 fold greater than ADP, suggests a different fluorescent analog of ADP may be required to study the kinetics of the Yhih – ADP interaction. A summary of the obtained dissociation constants, which includes data obtained from at least two trials for each experiment, is shown in Table 8 below:

Table 8: Summary of dissociation constants.

The number of experiments performed is indicated (n)

Nucleotide	Experiment	ΔP541 Yhih	ΔL432 Yhih
ADP	Direct trp fluorescence	17.9 ± 2.1 μM (n = 4)	155 ± 14.1 μM (n = 2)
ATP	Direct trp fluorescence	136 ± 12.3 μM (n = 3)	116 ± 13.9 μM (n = 2)
mant-ADP	FRET	168 ± 15.3 μM (n = 2)	156 ± 8.9 μM (n = 2)
mant-ATP	FRET	192 ± 12.1 μM (n = 2)	No FRET observed

4.4 Ribosome-stimulated hydrolysis of ATP by Yhih

During their initial characterization of RbbA, Kiel and Ganoza demonstrated that RbbA hydrolyzes ATP, and this hydrolysis is greatly stimulated by 70S ribosomes and 30S ribosomal subunits (Kiel et al., 1999; Xu et al., 2006). The ATPase activity of eEF-3, by contrast, has been shown to be stimulated by 50S ribosomal subunits in addition to 30S subunits and 70S ribosomes (Gontarek et al., 1998; Kovalchuke et al., 1998). Therefore, the ability of refolded, nucleotide-binding ΔP541 and ΔL432 Yhih to hydrolyze ATP in the presence and absence of ribosomes and ribosomal subunits was examined. Figure 39 A shows that under the assay conditions described in materials and methods, the S100 extract from *E. coli* hydrolyzes ATP and was used as a reference. 70S ribosomes and 50S ribosomal subunits showed no intrinsic ability to hydrolyze ATP; interestingly, the 30S ribosomal subunit preparation showed some ability to hydrolyze ATP (Figure 39 B).
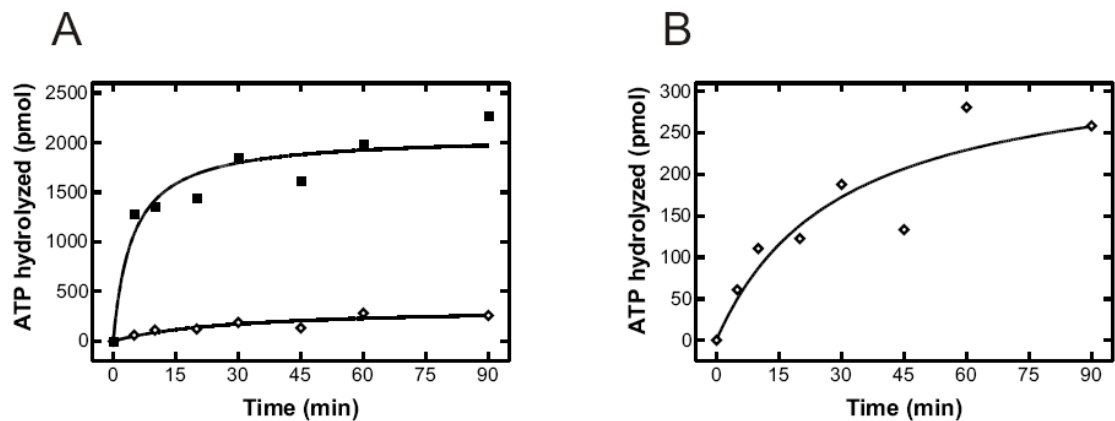
Figure 39: ATP hydrolysis by S100 extract and 30S ribosomal subunits.

(A) Ability of the S100 extract (closed squares) and 30S ribosomal subunits (open diamonds) to hydrolyze ATP. (B) The intrinsic ATPase activity of 30S ribosomal subunits.

The ATP hydrolyzing ability of both ΔP541 and ΔL432 Yhih was investigated in the presence of 70S ribosomes, as well as 50S and 30S ribosomal subunits (Figure 40). The intrinsic ATPase of the proteins is extremely slow, and could not be detected under current conditions. Interestingly, in the presence of equimolar amounts of ribosomes or subunits (Figure 40 A), the ATPase activity of ΔP541 Yhih was strongly stimulated by 30S subunits (~1200 pmol ATP hydrolyzed), followed by 50S subunits (~500 pmol ATP hydrolyzed) and 70S ribosomes (~50 pmol ATP hydrolyzed). This ATPase activity was increased in the presence of 3 fold excess 50S subunits (~2 times more ATP hydrolyzed compared to the experiment with equimolar amounts of ΔP541 Yhih and 50S ribosomal subunits) and 70S ribosomes (~8 times more ATP hydrolyzed) ΔL432 Yhih only hydrolyzed ATP in the presence of 3 fold excess 50S ribosomal subunits, though 2.5 times less ATP was hydrolyzed compared to the same experiment with ΔP541 Yhih.

79
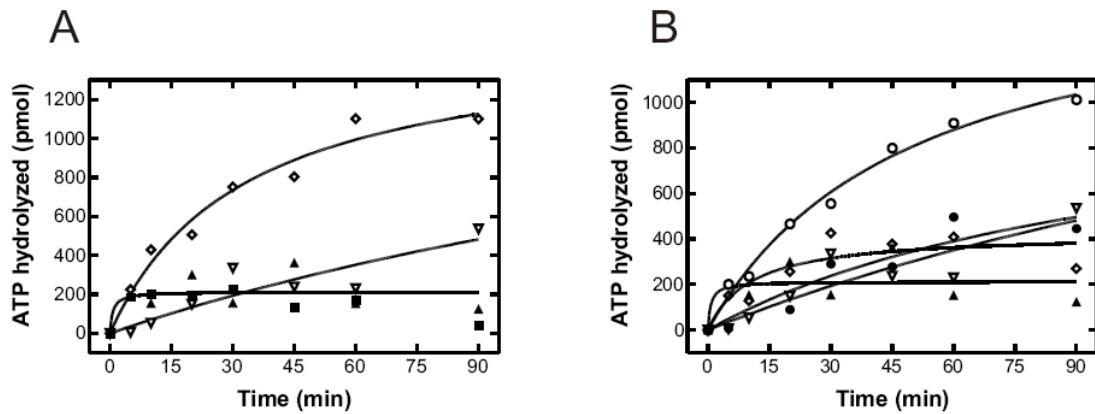
Figure 40: Ribosome-stimulated ATPase activity of ΔP541 and ΔL432 Yhih.

(A): The ATPase activity of ΔP541 Yhih (closed squares) in the presence of equimolar amounts of 30S (open diamonds) and 50S ribosomal subunits (open triangles), as well as 70S ribosomes (closed triangles). (B): In the presence of 3 fold excess 70S ribosomes (closed circles) and 50S subunits (open circles), the ATPase activity of ΔP541 Yhih was stimulated compared to equimolar amounts (also shown, same scheme as panel A). In the presence of 3 fold excess 50S ribosomal subunits, the ATPase activity of ΔL432 was detectable (closed circles).

The concentration dependence of the ribosome-stimulated ATPase activity of ΔP541 Yhih was further examined in the presence of 70S ribosomes (Figure 41 A) and 50S ribosomal subunits (Figure 41 B). 30S ribosome concentrations were too low to further examine their effect on the ATPase activity of Yhih. The concentration dependence on 70S ribosomes saturates at 5 μM, while the ATP hydrolysis signal does not appear to saturate in the presences of 50S ribosomal subunits. An estimated dissociation constant of 3.3 ± 1.7 μM was calculated for the interaction between ΔP541 Yhih and 70S ribosomes; a dissociation constant could not be estimated for 50S ribosomal subunits, though the affinity for 50S ribosomal subunits appears to be lower

despite stimulating ATP hydrolysis to a greater extent. However, since these experimental conditions give multiple-turnover ATP hydrolysis, this is only an estimate.
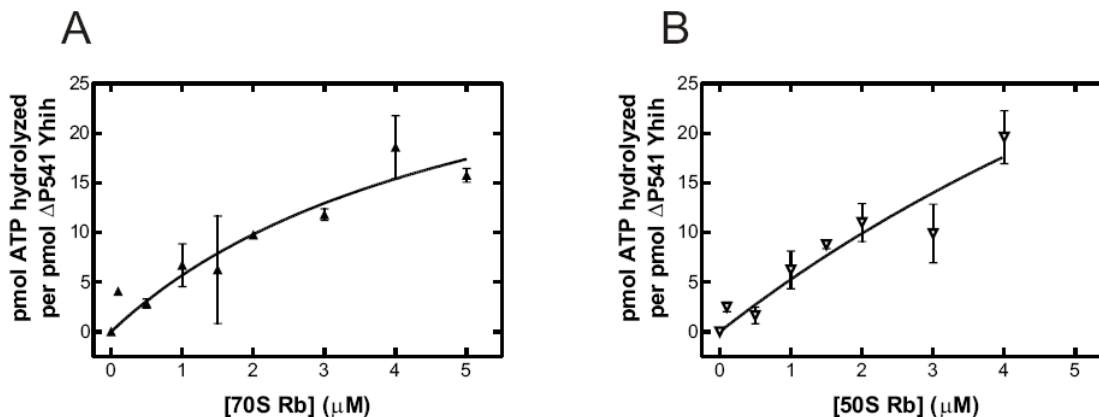
Figure 41: Ribosome concentration dependent ATPase activity of ΔP541 Yhih.

(A): ATP hydrolysis by ΔP541 Yhih after 90 min in the presence of increasing concentrations of 70S ribosomes. (B): ATP hydrolysis after 90 min in the presence of 50S ribosomal subunits.

4.5 The rate of ATP dissociation from ΔP541 Yhih

The rate constant for ATP dissociation from ΔP541 Yhih was determined by FRET measurements from the tryptophan residues of ΔP541 Yhih to the mant group of mant-ATP. This complex dissociated in the presence of excess ATP, causing a decrease in fluorescence signal that when fitted with an exponential decay function (equation 3), yielding a pseudo-first order rate constant: as the bound mant-ATP is exchanged with ATP, rather than dissociation occurring where the binding site for ATP is empty. Interestingly, the presence of pyruvate kinase in a control experiment (no mant-ATP) caused a decrease in the fluorescence signal (Figure 42 A) that was subtracted from the

FRET signal during the actual dissociation experiment (Figure 42 B). A dissociation rate

constant of 0.0037 s^{-1} was obtained for the dissociation of ATP from ΔP541 Yhih.
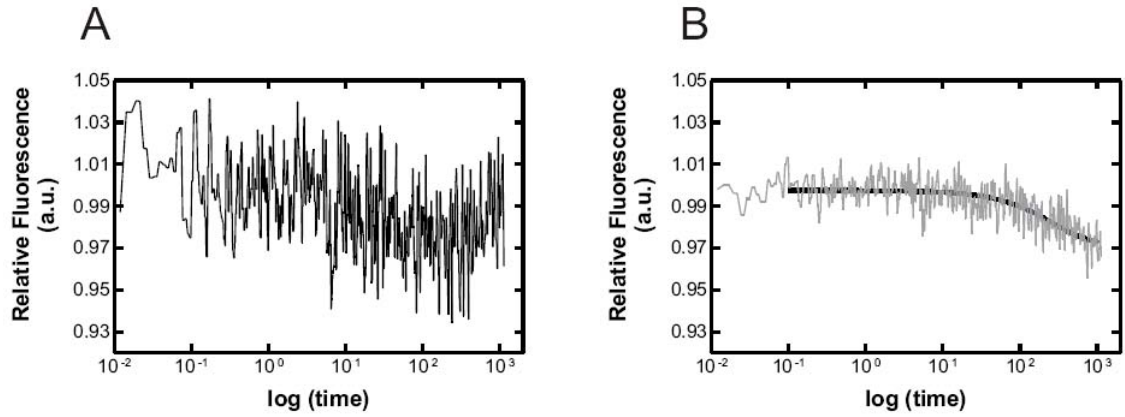
Figure 42: Dissociation of mant-ATP from the ΔP541 Yhih•mant-ATP complex.

(A) Fluorescence change due to pyruvate kinase (no mant-ATP present). (B) Fluorescence change due to the dissociation of mant-ATP from the ΔP541 Yhih•mant-ATP complex. The data fit is shown in black.

Chapter 5 – Discussion

5.1 Expression of yhih

Interestingly, the overexpression of the wild-type *yhih* gene blocked bacterial growth. However, cell cultures continue to grow after incubation over longer periods of time, likely due to the utilization of all IPTG, thus effectively "switching off" the T7 promoter, and thereby reducing the amount of Yhih present in bacterial cells. This phenomenon has been observed in other ABC transporters, notably the *P falciparum* chloroquine resistance transporter PfCRT (Amoah et al., 2007). It has been suggested that the large protein size (Amoah et al., 2007), the presence of ATP binding domains or transmembrane domains (Inoue et al., 2000), high A/T gene content, and frequent lysine and arginine rich repeats (Flick et al., 2004; Amoah et al., 2007) may cause inhibition of bacterial growth in recombinant expression systems. Despite altering numerous expression conditions such as IPTG concentration, cell density at induction, temperature, and regulation of the T7 promoter by T7 lysozyme (produced by the pLysS plasmid), the expression of wild-type Yhih blocked bacterial growth.

In order to reduce toxicity and express the wild-type protein, the mutant K299L Yhih was created that disrupted the Walker A motif in the ABC1 domain, which in turn should inhibit ATP binding. Presumably, overexpression of an ATP binding protein could disrupt essential cellular processes requiring ATP. In an effort to supplement the ATP supply of recombinant cells, bacteria were grown in phosphate-supplemented

media. Cellular growth was not affected by the additional phosphate present, though phosphate-supplemented media has previously been shown to aid in the production of soluble *E. coli* MalK, a maltose transporter (Schneider et al., 1995).

The C-terminal deletion mutant pET*yhih* P541opal was generated as this mutant removed the putative transmembrane domain, and significantly reduced the size of the protein. A truncated form of RbbA has been reported previously to result from a proteolytic cleavage at P541 based on mass spectrometry data (Xu et al., 2006). This protein was shown to have the same properties as the full-length protein. Ganoza and coworkers have alluded to the fact that the wild-type RbbA is unstable and difficult to overexpress (Xu et al., 2006); however the truncated form of the protein possessed the same ribosome-stimulated ATPase activity as the wild-type gene, and stimulated polyphenylalanine synthesis *in vitro.* In addition, the truncated protein was found to be stable. Expression of ΔP541 Yhih no longer blocked bacterial growth, and 6x His-tagged protein is readily overexpressed, though as insoluble protein aggregates (inclusion bodies). The C-terminal deletion mutant pET*yhih* L432amber was also generated to determine the role of the region between L432 and P541, which is within the unknown domain of Yhih. This mutant was found to readily express, though again as inclusion bodies. Purification attempts under nondenaturing conditions yield no soluble protein, despite again optimizing growth conditions; it is possible that these proteins aggregate due to high concentration (vandenBerg et al., 2000). Even under conditions resulting in lowered protein expression, these proteins could only be identified in urea cell lysates, suggesting that these proteins may be difficult to fold *in vivo,* or disturb essential processes.

5.2 Nucleotide-bound states of Yhih

The observation that ΔP541 Yhih tryptophan fluorescence signal increased in the presence of ATP, whereas ADP caused tryptophan fluorescence decrease, suggests that two different conformations occur in solution, depending on the nucleotide bound to the protein. Interestingly, the tryptophan fluorescence signal of ΔL432 Yhih increases in the presence of both ATP and ADP, which indicates the ADP-bound conformation is not detected by this technique. It is likely that upon ATP hydrolysis by the protein, a conformational change occurs in the unknown domain, between L432 and P541. Although the crystal structures of eEF-3 in the apo, ADP-bound and ATP-bound states showed few structural changes, small-angle X-ray scattering experiments demonstrated that a large conformational change can occur in solution (Andersen et al., 2006), dependent on both pH and the bound nucleotide. Based on the Andersen's model of eEF-3 in the ATP bound and ATP•ribosome bound state of eEF-3, another large conformational change occurs upon binding to the 80S yeast ribosome (Andersen et al., 2006). Conformational changes in the apo, ADP, and ATP-bound states have also been observed in the crystal structures of the MalK maltose transporter from *E. coli* (Chen et al., 2003; Lu et al., 2005).

The dissociation constants for ΔP541 Yhih binding to ADP and ATP are 17.9 ± 2.1 μM and 136 ± 12.3 μM respectively, indicating a stronger affinity for ADP. Estimates for *in vivo* ATP and ADP concentrations vary depending on growth conditions, ranging from ratios of 2:1 ATP:ADP (~ 1 mM : ~ 0.5 mM; (Yang et al., 2003)) to 19:1

(Michelsen, 1992), suggesting that despite an ~8 fold difference in affinity, ADP dissociation and subsequent binding of ATP is likely accomplished without need for a nucleotide exchange factor. The affinities for ΔL432 Yhih binding to ADP and ATP are 155 ± 14.1 μM and 116 ± 13.9 μM respectively; it is possible that the presence of the unknown domain influences or regulates the proteins' affinity for ADP. Another possibility is that the affinity of ΔL432 Yhih (five trp residues) for ADP is in fact closer to that of ΔP541 Yhih (six trp residues), since the removal of one tryptophan would influence the fluorescence signal depending on its location with respect to the ATP binding motifs. The affinities of these proteins for ATP are comparable to that of refolded MalK (~ 150 μM, (Walter et al., 1992)).

Upon titration of ΔP541 Yhih with mant-ATP and mant-ADP, the tryptophan fluorescence signal decreases while the mant fluorescence signal increases, indicating that FRET between the two dyes occurs upon binding to these nucleotides. The affinity of this protein for mant-ATP is comparable to that of ATP (136 ± 12.3 μM and 192 ± 12.1 μM respectively), indicating that mant-ATP is a suitable analog for studying the interaction between ΔP541 Yhih and ATP. The K_D for mant-ADP, however, is ~ 9 fold higher than for ADP (168 ± 15.3 μM and 17.9 ± 2.1 μM respectively) and as such may not be suitable for use in future experiments. No FRET was observed for mant-ATP binding to ΔL432 Yhih. Interestingly, the mant fluorescence signal was quenched, perhaps due to decreased shielding of the mant group by the protein, thus preventing mant fluorescence detection. Andersen and colleagues proposed that the ATP-bound state of eEF-3 represents a "closed" state that opens upon ribosome-dependent hydrolysis of ATP (Andersen et al., 2006). If a similar "closed" conformation occurs in ΔP541 Yhih,

86

the extra tryptophan residue in ΔP541 Yhih must be responsible for FRET to the mant group of mant-ATP (but not to mant-ADP, since FRET still occurs between ΔL432 Yhih and mant-ADP). The affinity of ΔL432 Yhih for mant-ADP was comparable to that of ADP.

The combined nucleotide-dependent intrinsic tryptophan fluorescence data and FRET data suggest that two different conformations occur that influence the movement of the region between L432 and P541. This is consistent with the "ATP-switch" model that describes the function of ABC transporters, in which an ABC transporter forms a "closed" dimer in the presence of ATP, which then dissociates into the "open' form upon ATP hydrolysis and subsequent ADP release (Linton & Higgins, 2007). This switch from "closed" to "open" form induces a conformational change in the transmembrane domains in many transporters that facilitates transport or some other relevant function (Linton & Higgins, 2007). In the case of truncated Yhih mutants, the observed conformational change in the unknown domain could signal a conformational change in the putative transmembrane domain (in the wild-type protein). In eEF-3, based on this model, the ADP-bound "open" state likely causes a conformational change in the HEAT domain, which allows dissociation from the 80S ribosome and is consistent with Andersen's model (Andersen et al., 2006).

5.3 Ribosome-stimulated ATP hydrolysis

Neither ΔP541 Yhih nor ΔL432 Yhih show any intrinsic ATPase activity under the used experimental conditions. Only 30S ribosomal subunits exhibit a slow intrinsic ATPase activity, possibly due to ribosome-associated protein contaminants or inadequate

separation from other cellular proteins. Interestingly, 70S ribosomes and both ribosomal subunits stimulate ATP hydrolysis, though only 70S ribosomes and 30S ribosomal subunits have previously been shown to have ribosome-stimulated ATPase activity (Kiel et al., 1999; Xu et al., 2006). According to this study, ATP hydrolysis by refolded ΔP541 is stimulated to the greatest degree by 30S ribosomal subunits, followed by 50S ribosomal subunits and 70S ribosomes. At equimolar amounts of protein to ribosomes, ΔL432 Yhih ATPase does not appear to be stimulated; however, at higher concentrations, both 70S ribosomes and 50S ribosomal subunits appear to influence ATP hydrolysis, suggesting that ribosome interactions are not completely abolished by deleting the region between L432 and P541, though either this interaction is significantly weaker, or the ATP binding sites are no longer being stimulated upon ribosome binding.

The dissociation constant for 70S ribosomes is an estimate, as the conditions used allow for multiple turnover ATP hydrolysis. Despite stimulating ATP hydrolysis to a greater extent, the affinity of ΔP541 Yhih for 50S ribosomal subunits appears to be significantly lower than the affinity for 70S ribosomes.

5.4 Dissociation rate of ATP from ΔP541 Yhih

The dissociation rate constant of ATP from ΔP541 Yhih, as determined by mant fluorescence change, is 0.0037 s^{-1}. Since the bound mant-ATP is "chased" from the ATP binding sites by unlabelled ATP, this number represents a pseudo-first order rate constant. Based on scheme 2 and equation 5 below, the apparent association rate ($k_{association}$) can be calculated as 1.93 x 10^7 M^{-1}s^{-1}, suggesting that ATP associates readily and remains bound to ΔP541 Yhih. Upon binding to the ribosome, a conformational

change likely occurs that causes the protein to hydrolyze ATP. Based on the "switch" model, ABC transporters stimulate ATP binding upon binding of the substrate to the transmembrane domains (Linton & Higgins, 2007); however, ATP binding has been shown to occur in the absence of ribosomes. The effect of ribosomes or ribosomal subunits on the rate of ATP binding, however, is not known.
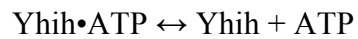
$$Yhih \bullet ATP \leftrightarrow Yhih + ATP \qquad \text{Scheme 1}$$

$$K_D = k_{dissociation} \,/\, k_{association} \qquad (5)$$

5.5 A possible kinetic scheme for Yhih

Based on the gathered experimental evidence and based on the "switch" mechanism of ABC transporters, a partial scheme for the interaction between ΔP541 Yhih and the 70S ribosome can be proposed (Figure 43).
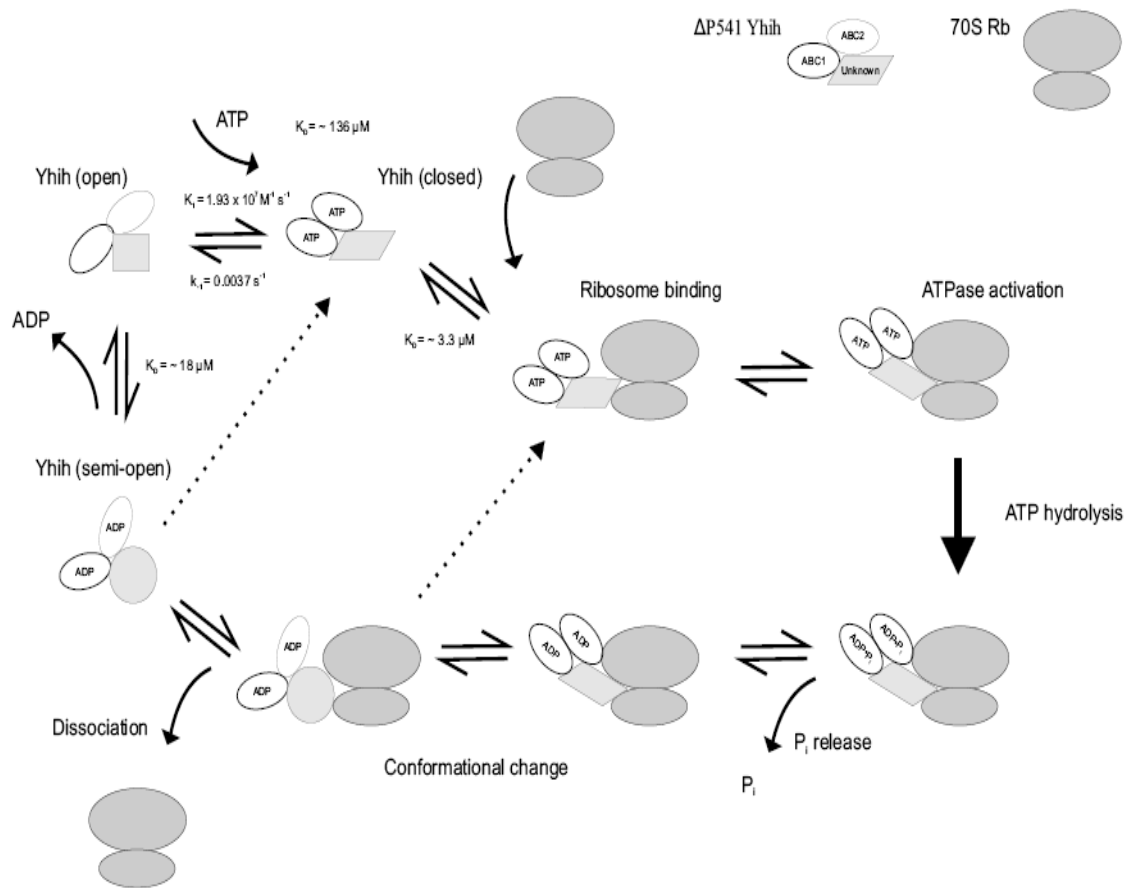
Figure 43: Proposed interaction between ΔP541 Yhih and the 70S ribosome.

This model is described in greater detail below. The schematic representations of the involved factors are shown in the top right of the figure.

ΔP541 Yhih in the "open" state (no nucleotide bound, top left), binds ATP to the ABC domains, inducing a conformational change to the "closed" conformation (observed by intrinsic tryptophan fluorescence in the presence of ATP). This allows the protein to interact with the 70S ribosome, which again causes a conformational change that activates the ATPase activity of ΔP541 Yhih. Upon ATP hydrolysis, P_i is (rapidly) released and the protein adopts a "semi-open" conformation. This "semi-open" conformation dissociates, ADP can be exchanged for ATP, and the cycle can continue.

ADP may be exchanged while Yhih is still bound to the ribosome, but it is more likely that it is rapidly exchanged upon dissociation from the ribosome. As *in vivo* concentrations are in the mM concentration range, the nucleotide-free protein is not likely to be present and nucleotide exchange is likely to be concentration driven rather than facilitated by a nucleotide exchange factor. This model is limited, as it does not take into account other ribosomal factors, or of the presence of tRNA in any of the A, P, or E sites; however, it seems feasible based on the ABC "switch" mechanism. The exact role of Yhih is still not understood, thus this model only represents the protein•ribosome interaction rather than accounting for any other activity.

Chapter 6 – Conclusions

The expression of the recombinant, full length *yhih* gene in *E. coli* blocks bacterial growth. Truncated forms of Yhih (ΔP541 and ΔL432 Yhih respectively) readily express, though as inclusion bodies that can be purified under denaturing conditions. Once purified, the proteins can successfully be refolded. Both truncated forms of Yhih bind adenine nucleotides, and fluorescence studies suggest that at least two conformations exist in solution, depending upon the presence of ATP or ADP. Interestingly, ATP hydrolysis only occurs in the presence of 30S and 50S ribosomal subunits, and 70S ribosomes, in a concentration-dependent manner. The region between L432 and P541 heavily influences this ribosome-stimulated ATPase activity, suggesting the interaction between the protein and the ribosome is related to this domain, which is found in numerous other ABC transporters. Previous experiments by Ganoza and coworkers indicate this protein is a homolog of yeast eEF-3. A possible kinetic scheme for Yhih is proposed, that accounts for the data obtained in this study. However, the exact role of Yhih and its interaction with the ribosome remains to be elucidated.

Chapter 7 – Future Directions

The role of Yhih in protein synthesis is still not well understood. If it has the same role as yeast eEF-3 in facilitating release of deacyl-tRNA from the ribosomal E-site, this must be confirmed. The coupling of ATP hydrolysis to the role of Yhih must be determined. Obtaining a crystal structure of this protein is vital, as this will provide a basis for future experiments to determine the exact role of Yhih. The role of the putative transmembrane domain is also unknown and must be ascertained; thus, expression of the full-length protein must be achieved. The kinetics of the interaction with ADP should be investigated, using a different fluorescent analog; as well, the kinetics of the protein – ribosome interaction will be examined. Though many ABC transporters require ATP hydrolysis by only one nucleotide binding domain to function, it remains unclear if any cross-talk exists between the two ABC domains. In the longer term, as Yhih is a bacterial specific protein, it represents a promising target for development of antibacterial drugs.

The homolog of Yhih, encoded for by the open reading frame *ybhf*, presents an excellent candidate for further research in translational ATPases. Lacking a putative transmembrane domain, this protein may be easier to purify and characterize. Its high degree of similarity to Yhih, while also containing a putative chromodomain also found in eEF-3, suggests this protein may play some role in protein synthesis.

References

Ahmadian MR, Wittinghofer A, Herrmann C. 2002. *GTPase Protocols: The Ras Superfamily*. Totowa, NJ: Humana Press.

Allali-Hassani A, Campbell TL, Ho A, Schertzer JW, Brown ED. 2004. Probing the active site of YjeE: a vital *Escherichia coli* protein of unknown function. *Biochemistry Journal 384*:577-584.

Ambudkar SV, Kim I-W, Xia D, Sauna ZE. 2006. The A-loop, a novel conserved aromatic acid subdomain upstream of the Walker A motif in ABC transporters, is critical for ATP binding. *FEBS Letters 580*:1049-1055.

Amoah LE, Lekostaj JK, Roepe PD. 2007. Heterologous Expression and ATPase Activity of Mutant versus Wid Type PfMDR1 Protein. *Biochemistry 46*:6060-6073.

Anand M, Balar B, Ulloque R, Gross SR, Kinzy TG. 2006. Domain and Nucleotide Dependence of the Interaction between *Saccharomyces cerevisiae* Translation Elongation Factors 3 and 1A. *The Journal of Biological Chemistry 281*:32318-32326.

Andersen CBF, Becker T, Blau M, Anand M, Halic M, Balar B, Mielke T, Boesen T, Pedersen JS, Spahn CMT, Kinzy TG, Andersen GR, Beckman R. 2006. Structure of eEF3 and the mechanism of transfer RNA release from the E-site. *Nature 443*:663-668.

Andersen DS, Leevers SJ. 2007. The Essential *Drosophila* ATP-binding Cassette Domain Protein, Pixie, Binds the 40S Ribosome in an ATP-dependent Manner and Is Required for Translation Initiation. *Journal of Biological Chemistry 282*:14752-14760.

Arakawa T, Ejima D, Tsumoto K, Obeyama N, Tanaka Y, Kita Y, Timasheff SN. 2007. Suppression of protein interactions by arginine: A proposed mechanism of the arginine effects. *Biophysical Chemistry 127*:1-8.

Arakawa T, Tsumoto K, Kita Y, Chang B, Ejima D. 2007. Biotechnology applications of amino acids in protein purification and formulations. *Amino Acids 33*:587-605.

Ario de Marco ED, Axel Mogk, Toshifumi Tomoyasu, and Bernd Bakau. 2007. Chaperone-based procedure to increase yields of soluble recombinant proteins produced in *E. coli*. *BMC Biotechnology 7*:1-9.

Bajorunaite E. SJ, Bumelis V A. 2007. L-Arginine Suppresses Aggregation of Rcombinant Growth Hormones in Refolding Process from *E. coli* Inclusion Bodies. *The Protein Journal 26*:547-555.

Belfield GP, Tuite MF. 1993. Translation elongation factor 3: a fungus-specific translation factor? *Molecular Microbiology 9*:411-418.

Bertram G, Innes S, Minella O, Richardson JP, Stansfield I. 2001. Endless possibilities: translation termination and stop codon recognition. *Microbiology 147*:255-269.

Boriack-Sjodin PA, Margarit SM, Bar-Sagi D, Kuriyan J. 1998. The structural basis of the activation of Ras by Sos. *Nature 394*:337-343.

Brands JGHM, Maassen JA, vanHemert FJ, Amons R, Moeller W. 1986. The primary structure of the alpha subunit of human elongation factor 1. Structural aspects of

guanine-nucleotide-binding sites. *European Journal of Biochemistry 155*:167-171.

Brown ED. 2005. Conserved P-loop GTPases of unknown function in bacteria: an emerging and vital ensemble in bacterial physiology. *Biochemistry and Cell Biology 83*:738-746.

Buche A, Mendez C, Salas JA. 1997. Interaction between ATP, oleandomycin and the OleB ATP-binding cassette transporter of *Streptomyces antibioticus* involved in oleandomycin secretion. *Biochemistry Journal 321*:139-144.

Buskiewicz I, Peske F, Wieden H-J, Gryczynski I, Rodnina MV, Wintermeyer W. 2005. Conformations of the Signal Recognition Particle Ffh from *Escherichia coli* as Determined by FRET. *Journal of Molecular Biology 351*:417-430.

Caldon CE, Yoong P, March PE. 2001. Evolution of a molecular switch: universal bacterial GTPases regulate ribosome function. *Molecular Microbiology 41*:289-297.

Chakraburtty K. 2001. Translational regulation by ABC systems. *Research in Microbiology 152*:391-399.

Chen J, Lu G, Lin J, Davidson AL, Quiocho FA. 2003. A Tweezers-like Motion of the ATP-Binding Cassette Dimer in an ABC Transport Cycle. *Molecular Cell 12*:651-661.

Cohen-Zinder M, Seroussi E, Larkin DM, Loor JJ, Everts-vanderWind A, Lee J-H, Drackley JK, Band MR, Hernandez AG, Shani M, Lewin HA, Weller JI, Ron M. 2005. Identification of a missense mutation in the bovine ABCG2 gene with a major effect on the QTL in chromosome 6 affecting milk yield and composition in Holstein cattle. *Genome Research 15*:936-944.

Dasmahapatra B, Chakraburtty K. 1981. Protein Synthesis in Yeast: Purification and Properties of Elongation Factor 3 from *Saccharomyces cerevisiae. The Journal of Biological Chemistry 256*:9999-10004.

Davidson AL, Laghaeian SS, Mannering DE. 1996. The Maltose Transport System of *Escherichia coli* Displays Positive Cooperativity in ATP Hydrolysis. *Journal of Biological Chemistry 271*:4858-4863.

Daviter T, Wieden H-J, Rodnina MV. 2003. Essential Role of Histidine 84 in Elongation Factor Tu for the Chemical Step of GTP Hydrolysis on the Ribosome. *Journal of Molecular Biology 332*:689-699.

Demeshkina N, Hirokawa G, Kaji A, Kaji H. 2007. Novel activity of eukaryotic translocase, eEF-2: dissociation of the 80S ribosome into subunits with ATP but not with GTP. *Nucleic Acids Research 35*:4597-4607.

El'skaya AV, Ovcharenko GV, Palchevskii SS, Petrushenko ZM, Triana-Alonso FJ, Nierhaus KH. 1997. Three tRNA Binding Sites in Rabbit Liver Ribosomes and Role of the Intrinsic ATPase in 80S Ribosomes from Higher Eukaryotes. *Biochemistry 36*:10492-10497.

Flick K, Ahuja S, Chene A, Bejarano MT, Chen Q. 2004. Optimized expression of *Plasmodium falciparum* erythrocyte membrane protein I domains in *Escherichia coli. Malaria Journal 3*:1-8.

Friedrich Grummt IG, and Volker A. Erdmann. 1974. ATPase and GTPase Activities Isolated from Rat Liver Ribosomes. *European Journal of Biochemistry 43*:343-348.

Ganoza MC, Cunningham C, Green RM. 1985. Isolation and point of action of a factor from *Escherichia coli* required to reconstruct translation. *Proceedings of the National Academy of Sciences of the United States of America 82*:1648-1652.

Ganoza MC, Cunningham C, Green RM. 1995. A New Factor from *Escherichia coli* Affects Translocation of mRNA. *The Journal of Biological Chemistry 270*:26377-26381.

Ganoza MC, Kiel MC. 2001. A Ribosomal ATPase Is a Target for Hygromycin B Inhibition on *Escherichia coli* Ribosomes. *Antimicrobial Agents and Chemotherapy 45*:2813-2819.

Ganoza MC, Kiel MC, Aoki H. 2002. Evolutionary Conservation of Reactions in Translation. *Microbiology and Molecular Biology Reviews 66*:460-485.

Gao H, Zhou Z, Rawat U, Huang C, Bouakaz L, Wang C, Cheng Z, Liu Y, Zavialov A, Gursky R, Sanyal S, Ehrenberg M, Frank J, Song H. 2007. RF3 induces ribosomal conformational changes responsible for dissociation of class I release factors. *Cell 129*:929-941.

Garnier C, Lafitte D, Tsvetkov PO, Barbier P, Leclerc-Devin J, Millot J-M, Briand C, Makarov AA, Catelli MG, Peyrot V. 2006. Binding of ATP to Heat Shock Protein 90. *The Journal of Biological Chemistry 277*:12208-12214.

Gasteiger E, Hoogland C, Gatiker A, Duvaud S, Wilkins MR, Appel RD, Bairoch A. 2005. Protein Identification and Analysis Tools on the ExPASy Server. *The Proteomics Protocols Handbook*:571-607.

Goldberg J. 1998. Structural basis for activation of ARF GTPase: mechanisms of guanine nucleotide exchange and GTP-myristoyl-switching. *Cell 95*:237-248.

Golovanov AP, Hautbergue GM, Wilson SA, Lian L-Y. 2004. A Simple Method for Improving Protein Solubility and Long-Term Stability. *Journal of the American Chemical Society 126*:8933-8939.

Gontarek RR, Li H, Nurse K, Prescott CD. 1998. The N terminus of eukaryotic translation elongation factor 3 interacts with 18S rRNA and 80S ribosomes *Journal of Biological Chemistry 273*:10249-10252.

Green RH, Glick BR, Ganoza MC. 1985. Requirements for the *in vitro* Reconstruction of Protein Synthesis. *Biochemical and Biophysical Research Communications 126*:792-798.

Gromadski KB, Wieden H-J, Rodnina MV. 2002. Kinetic Mechanism of Elongation Factor Ts-Catalyzed Nucleotide Exhange in Elongation Factor Tu. *Biochemistry 41*:162-169.

Grummt F, Grummt I. 1974. Studies on free and 5 S RNA-bound Ribosomal GTPase and ATPase. *FEBS Letters 42*:343-346.

Higgins CF. 2001. ABC transporters: physiology, structure, and mechanism: an overview. *Research in Microbiology 152*:205-210.

Higgins CF, Linton KJ. 2004. The ATP switch model for ABC transporters. *Nature Structural and Molecular Biology 11*:918-926.

Horne JR, Erdmann VA. 1973. ATPase and GTPase Activities Associated with a Specific 5S RNA-Protein Complex. *PNAS 70*:2870-2873.

Hutchison JS, Feinberg B, Rothwell TC, Moldave K. 1984. Monoclonal Antibody Specific for Yeast Elongation Factor 3. *Biochemistry 23*:3055-3063.

Inoue S, Sano H, Ohta M. 2000. Growth Suppression of *Escherichia coli* by Induction of Expression of Mammalian Genes with Transmembrane or ATPase Domains. *Biochemical and Biophysical Research Communications 268*:553-561.

Kamath A, Chakraburtty K. 1986. Protein Synthesis in Yeast. *Journal of Biological Chemistry 261*:12596-12598

Kamath A, Chakraburtty K. 1989. Role of Yeast Elongation Factor 3 in the Elongation Cycle. *Journal of Biological Chemistry 264*:15423-15428.

Kawashima T, Berthet-Colominas C, Wulff M, Cusack S, Leberman R. 1996. The structure of the *Escherichia coli* EF-Tu EF-Ts complex at 2.5 Angstrom resolution. *Nature 379*:511-518.

Keller EB, Zamecnik PC. 1956. The effect of guanosine diphosphate and triphosphate on the incorporation of labeled amino acids into proteins. *Journal of Biological Chemistry 221*:45-60.

Kerr ID. 2002. Structure and association of ATP-binding cassette transporter nucleotide-binding domains. *Biochimica et Biophysica Acta 85536*:1-18.

Kiel MC, Aoki H, Ganoza MC. 1999. Identification of a ribosomal ATPase in *Escherichia coli* cells. *Biochimie 81*:1097-1108.

Kiel MC, Ganoza MC. 2001. Functional interactions of an *Escherichia coli* ribosomal ATPase. *European Journal of Biochemistry 268*:278-286.

Kisselev L, Ehrenberg M, Frolova L. 2003. Termination of translation: interplay of mRNA, rRNAs and release factors. *The EMBO Journal 22*:175-182.

Kisselev LL, Buckingham RH. 2000. Translation termination comes of age. *Trends in Biological Science 25*:561-566

Kit S, Greenberg DM. 1952. Incorporation of isotopic threonine and valine into the protein of rat liver particulates. *Journal of Biological Chemistry 194*:377-381.

Koonin EV. 1993. A Superfamily of ATPases with Diverse Functions Containing Either Classical or Deviant ATP-binding Motif. *Journal of Molecular Biology 229*:1165-1174.

Kothe U, Wieden H-J, Mohr D, Rodnina MV. 2004. Interaction of Helix D of Elongation Factor Tu with Helices 4 and 5 of Protein L7/L12 on the Ribosome. *Journal of Molecular Biology 336*:1011-1021.

Kovalchuke O, Kambampati R, Pladies E, Chakraburtty K. 1998. Competition and cooperation among yeast elongation factors. *European Journal of Biochemistry 258*:986-993.

Kozak M. 1999. Initiation of translation in prokaryotes and eukaryotes. *Gene 234*:187-208.

Laursen BS, Sorensen HP, Mortensen KK, Sperling-Peterson HU. 2005. Initiation of Protein Synthesis in Bacteria. *Microbiology and Molecular Biology Reviews 69*:101-123.

Lee T-H, Blanchard SC, Kim HD, Puglisi JD, Chu S. 2007. The role of fluctutations in tRNA selection by the ribosome. *Proceedings of the National Academy of Science USA 104*:13661-13665.

Leeds NB, Small EC, Hiley SL, Hughes TR, Staley JP. 2006. The Splicing Factor Prp43p, a DEAH Box ATPase, Functions in Ribosome Biogenesis. *Molecular and Cellular Biology 26*:513-522.

Leipe DD, Wolf YI, Koonin EV, Aravind L. 2002. Classification and Evolution of P-loop GTPases and Related ATPases. *Journal of Molecular Biology 317*:41-72.

Linton KJ, Higgins CF. 2007. Structure and function of ABC transporters: the ATP switch provides flexible control. *European Journal of Physiology 453*:555-567.

Lu G, Westbrooks JM, Davidson AL, Chen J. 2005. ATP hydrolysis is required to reset the ATP-binding cassette dimer into the resting-state conformation. *Proceedings of the National Academy of Science 102*:17969-17974.

Maegley KA, Admiraal SJ, Herschlag D. 1996. Ras-catalyzed hydrolysis of GTP: A new perspective from model studies. *Proceedings of the National Academy of Science USA 93*:8160-8166.

Marcotrigiano J, Lomakin IB, Sonenberg N, Pestova TV, Hellen CU, Burley SK. 2001. A conserved HEAT domain within eIF4G directs assembly of the translation initiation machinery *Molecular Cell 7*:193-203.

Michelsen PRJaO. 1992. Carbon and Energy Requirements of *atp* Mutants of *Escherichia coli*. *Journal of Bacteriology 174*:7635-7641.

Miyazaki H, Miyazaki Y, Geber A, Parkinson T, Hitchcock C, Falconer DJ, Ward DJ, Marsden K, Bennett JE. 1998. Fluconazole resistance associated with drug efflux and increased transcription of a drug transporter gene, PDH1, in *Candida glabrata*. *Antimicrobial Agents and Chemotherapy 42*:1695-1701.

Miyazaki M, Kagiyama H. 1990. Soluble Factor Requirements for the *Tetrahymena* Peptide Elongation System and the Ribosomal ATPase and a Counterpart of Yeast Elongation Factor 3 (EF-3). *Journal of Biochemistry 108*:1001-1008.

Moller W, Amons R. 1985. Phosphate binding sequences in nucleotide binding proteins. *FEBS 186*:1-7.

Myers KK, Fonzi WA, Sypherd PS. 1992. Isolation and sequence analysis of the gene for translation elongation factor 3 from *Candida albicans*. *Nucleic Acids Research 20*:1705-1710.

Nagahama M, Hara Y, Seki A, Yamazoe T, Kawate Y, Shinohara T, Hatsuzawa K, Tani K, Tagaya M. 2004. NVL2 Is a Nucleolar AAA-ATPase that Interacts with Ribosomal Protein L5 through Its Nucleolar Localization Sequence. *Molecular Biology of the Cell 15*:5712-5723.

Nathans D, Lipmann F. 1961. Amino acid transfer from aminoacyl-ribonucleic acids to protein on ribosomes of *Escherichia coli*. *PNAS 47*:497-504.

Nikaido H. 2002. How are the ABC transporters energized? *PNAS 99*:9609-9610.

Pasqualato S, Menetrey J, Franco M, Cherfils J. 2001. The structural GDP/GTP cycle of human Arf6. *EMBO Reports 2*:234-238.

Peske F, Matassova NB, Savelsbergh A, Rodnina MV, Wintermeyer W. 2003. Conformationally restricted elongation factor G retains GTPase activity but is inactive in translocation on the ribosome. *Molecular Cell 6*:510-505.

Peterson EA, Greenberg DM. 1952. Characteristics of the amino acid-incorporating system of liver homogenates. *Journal of Biological Chemistry 194*:359-375

Qian F, Wei D, Liu J, Yang S. 2006. Molecular Model and ATPase Activity of Carboxyl-Terminal Nucleotide Binding Domain from Human P-Glycoprotein. *Biochemistry (Moscow) 71*:S18-S24.

Qin S, Xin A, Christina M, Banato M, McLaughlin C. 1990. Sequence analysis of the translational elongation factor 3 from *Sacharomyces cerevisiae*. *Journal of Biological Chemistry 265*:1903-1912.

Qin Y, Polacek N, Vesper O, Staub E, Einfeldt E, Wilson DN, Nierhaus KH. 2006. The highly conserved LepA is a ribosomal elongation factor that back-translocates the ribosome. *Cell 127*:721-733.

Raj VS, Kaji H, Kaji A. 2005. Interaction of RRF and EF-G from E. coli T. thermophilus with ribosomes from both origins-insight into the mechanism of the ribosome recycling step. *RNA 11*:275-284.

Rak A, Pylypenko O, Durek T, Watzke A, Kushnir S, Brunsveld L, Waldmann H, Goody RS, Alexandrov K. 2003. Structure of Rab GDP-dissociation inhibitor in complex with prenylated YPT1 GTPase. *Science 302*:646-650.

Rariy RV, Klibanov AM. 1997. Correct protein folding in glycerol. *Proceeding of the National Academy of Science 94*:13520-13523.

Ren X-Q, Furukawa T, Haraguchi M, Sumizawa T, Aoki S, Kobayashi M, Akiyama S-i. 2004. Function of the ABC Signature Sequences in the Human Multidrug Resistance Protein 1. *Molecular Pharmacology 65*:1536-1542.

Rodnina MV, Gromadski KB, Kothe U, Wieden H-J. 2005. Recognition and selection of tRNA selection in translation. *FEBS Letter 579*:938-942.

Rodnina MV, Serebryanik AI, Ovcharenko GV, El'skaya AV. 1994. ATPase strongly bound to higher eukaryotic ribosomes. *FEBS 225*:305-310.

Rodnina MV, Stark H, Savelsbergh A, Wieden H-J, Mohr D, Matassova NB, Peske F, Daviter T, Gualerzi CO, Wintermeyer W. 2000. GTPase Mechanisms and Functions of Translation Factors on the Ribosome. *Biological Chemistry 381*:377-387.

Sandbaken M LJA, DiDomenico B, Chakraburtty K. 1990. Isolation and characterization of the structural gene encoding elongation factor 3. *Biochimica et Biophysica Acta 1050*:230-234.

Sandbaken MG, Lupisella JA, DiDomenico B, Chakraburtty K. 1990. Structural and Functional Analysis of the Gene Encoding Elongation Factor 3. *The Journal of Biological Chemistry 265*:15838-15844

Schlessinger D. 1964. Requirement for K+ and ATP in Protein Synthesis by *Escherichia coli* Ribosomes. *Biochimica et Biophysica Acta 80*:473-477.

Schneider E, Hunke S. 1998. ATP-binding cassette (ABC) transport systems: Functional and structural aspects of the ATP-hydrolyzing subunits/domains. *FEMS Microbiology Reviews 22*:1-20.

Schneider E, Linde M, Tebbe S. 1995. Functional Purification of a Bacterial ATP binding Cassette Transporter Protein (MalK) from the Cytoplasmc Fraction of an Overproducing Strain. *Protein Expression and Purification 6*:10-14.

Scrima A, Wittinghofer A. 2006. Dimerisation-dependent GTPase reaction of MnmE: how potassium acts as a GTPase-activating element *EMBO Journal 25*:2940-2951.

Siekevitz P. 1952. Uptake of Radioactive Alanine *in vitro* into the Proteins of Rat Liver Fractions. *Journal of Biological Chemistry 195*:549-565.

Skogerson L, Wakatama E. 1976. A ribosome-dependent GTPase from yeast distinct from elongation factor 2. *PNAS 73*:73-76.

Soundararajan M, Yang X, Elkins JM, Sobott F, Doyle DA. 2007. The centaurin γ -1 GTPase-like domain functions as an NTPase. *Journal of Biochemistry 401*:679-688.

Stagg SM, Harvey SC. 2005. Exploring the Flexibility of Ribosome Recycling Factor Using Molecular Dynamics. *Biophysical Journal 89*:2659-2666.

Stark H, Rodnina MV, Wieden H-J, vanHeel M, Wintermeyer W. 2000. Large-Scale Movement of Elongation Factor G and Extensive Conformational Change of the Ribosome during Translocation. *Cell 100*:301-309.

Story RM, Steitz TA. 1992. Structure of the recA protein-ADP complex. *Nature 355*:374-376

Stroupe C, Brunger AT. 2000. Crystal Structure of a Rab protein in its inactive and active conformations. *Journal of Molecular Biology 304*:585-598.

Swietnicki W. 2006. Folding aggregated proteins into functionally active forms. *Current Opinion in Biotechnology 17*:367-372.

Teplyakov A, Obmolova G, Chu SY, Toedt J, Eisenstein E, Howard AJ, Gilliland GL. 2003. Crystal structure of the YchF protein reveals binding sites for GTP and nucleic acid *Journal of Bacteriology 185*:4031-4037.

Triana-Alonso FJ, Chakraburtty K, Nierhaus KH. 1995. The Elongation Factor 3 Unique in Higher Fungi and Essential for Protein Biosynthesis Is an E Site Factor. *The Journal of Biological Chemistry 270*:20473-20478.

Truglio JJ, Croteau DL, Skorvaga M, DellaVecchia MJ, Theis K, Mandavilli BS, VanHouten B, Kisker C. 2004. Interactions between UVRA and UVRB: the role of UVRB's domain 2 in nucleotide excision repair. *The EMBO Journal 1623*:2498-2509.

Uritani M, Miyazaki M. 1988. Characterization of the ATPase and GTPase activities of Elongation Factor 3 (EF-3) Purified from Yeasts. *Journal of Biochemistry 103*:522-530.

Vallejo LF, Rinas U. 2004. Strategies for the recovery of active proteins through refolding of bacterial inclusion body proteins. *Microbial Cell Factories 3*:1-12.

vandenBerg B, Wain R, Dobson CM, Ellis RJ. 2000. Macromolecular crowding perturbs protein refolding kinetics: implications for folding inside the cell. *The EMBO Journal 19*:3870-3875.

vanderBliek AM, Redelmeier TE, Tisdale EJ, Meyerwitz EM, Schmid SL. 1993. Mutations in human dynamin block an intermediate stage in coated vesicle formation. *Journal of Cell Biology 122*:553-563.

Verhoeven EE, Wyman C, Goosen GFMN. 2002. The presence of two UvrB subunits in the UvrAB complex ensures damage detection in both DNA strands. *The EMBO Journal 21*:4196-4205.

Walter C, zuBentrup KH, Schneider E. 1992. Large Scale Purification, Nucleotide Binding Properties, and ATPase activity of the MalK Subunit of *Salmonella typhimurium* Maltose Transport Complex. *The Journal of Biological Chemistry 267*:8863-8869.

Wieden H-J, Gromadski K, Rodnin D, Rodnina MV. 2002. Mechanism of Elongation Factor (EF)-Ts-catalyzed Nucleotide Exchange in EF-Tu. *The Journal of Biological Chemistry 277*:6032-6036.

Wiese C, Hinz JM, Tebbs RS, Nham PB, Urbin SS, Collins DW, Thompson LH, Schild D. 2006. Disparate requirements for the Walker A and B ATPase motifs of human RAD51 in homologous recombination. *Nucleic Acids Research 34*:2833-2843.

Winnick T. 1950. Studies on the mechanism of protein synthesis in embryonic and tumor tissues. II. Inactivation of fetal rat liver homogenates by dialysis and reactivation by the adenylic acid system. *Archives of Biochemistry and Biophysics 28*:338.

Wittinghofer A, Pai EF. 1991. The structure of Ras protein: a model for a universal molecular switch. *Trends in Biological Sciences 16*:382-387.

Xu J, Kiel MC, Golshani A, Aoki H, Ganoza MC. 2006. Molecular localization of a ribosome-dependent ATPase on *Escherichia coli* ribosomes. *Nucleic Acids Research 34*:1158-1165.

Yang C, Hua Q, Baba T, Mori H, Shimizu K. 2003. Analysis of *Escherichia coli* Anaplerotic Metabolism and Its Regulation Mechanisms From the Metabolic Responses to Altered Dilution Rates and Phosphoenolpyruvate Carboxykinase Knockout. *Biotechnology and Bioengineering 84*:129-144.

Yang H, Hamada K, Terashima H, Izuta M, Yamaguchi-Sihta E, Kondoh O, Satoh H, Miyazaki M, Arisawa M, Miyamoto C, Kitada K. 1996. A point mutation in each of two ATP-bindin motifs inactivates the functions of elongation factor 3. *Biochimica et Biophysica Acta 1310*:303-308.

Youngman EE, Green R. 2007. Ribosomal Translocation: LepA does it backwards. *Current Biology 17*:R136-R139.

Zamecnik PC, Keller EB. 1954. Relation between Phosphate Energy Donors and Incorporation of Labeled Amino Acids into Proteins. *Journal of Biological Chemistry 209*:337-354.